CHEMIA

CUPRINS – CONTENT – SOMMAIRE – INHALT

Studia Universitatis Babes-Bolyai Chemia has been selected for coverage in Thomson Reuters products and custom information services. Beginning with V. 53 (1) 2008, this publication will be indexed and abstracted in the following:

- Science Citation Index Expanded (also known as SciSearch®)
- Chemistry Citation Index®
- Journal Citation Reports/Science Edition

SYNTHESIS OF NEW POTENTIAL DENDRITIC CORES: (4-OXOPIPERIDIN-1-YL)-*s*-TRIAZINES

FLAVIA POPA[a], ILIOARA SIMIOANCA[a], MONICA PINTEA[a], MARIJANA FAZEKAS[a], LUCILLE GRATECAP[b], CAMELIA BERGHIAN[a], CARMEN BÂTIU[a], MIRCEA DARABANTU[a*]

ABSTRACT. Starting from 4-piperidone monohydrate hydrochloride or the hydrochloride of its ethylene ketal, the synthesis of new (4-oxopiperidin-1-yl)-*s*-triazine derivatives (potential C_2, C_3 symmetric dendritic cores) based on amination of cyanuric chloride is for the first time reported.

Keywords: *s-triazine, 4-piperidone monohydrate hydrochloride, 1,4-dioxa-8-azaspiro[4.5]decane hydrochloride, amination, dendritic cores*

INTRODUCTION

Following our recent findings in *s*-triazine chemistry [1], particularly in dendrimers [2] and dendrons [3] based on *N*-substituted 2,4,6-triamino-*s*-triazines (*melamines*), we were recently interested in testing the nucleofilicity of 4-piperidone as nucleophile in reaction with cyanuric chloride.

The instability, as free base, of 4-piperidone against autocondensation is well-known as early as 1949 [4]; hence, its monohydrate hydrochloride **1a** and its ethylene ketal (free base **1b** or hydrochloride **1c**), are commercially available (Scheme 1).
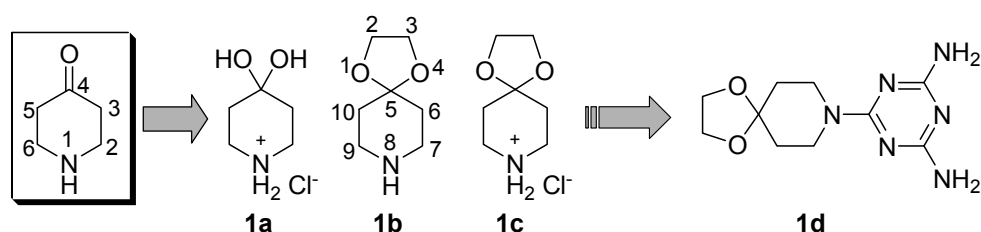
Scheme 1

[a] *"Babes-Bolyai" University, Department of Organic Chemistry, 11 Arany Janos str., 400028, Cluj-Napoca, Romania. darab@chem.ubbcluj.ro*
[b] *Université de Rouen, I.U.T. de Rouen, 76821 Mont Saint-Aignan Cedex, France*

On the other hand, there is nowadays a noticeably highlighting interest in nucleophilic substitution of the reminder chlorine in chlorodiamino-*s*-triazines carried out with 4-piperidone derivatives, providing pharmaceutical compositions for treating pathological states which arise from or are exacerbated by angiogenesis [5] (*e.g.* compound **1d**, Scheme 1).

The aim of this communication is to account on the first synthesis of a melamine built entirely from 4-piperidone, namely 2,4,6-tris(4-oxopiperidin-1-yl)-*s*-triazine, together with some of its useful precursors.

RESULTS AND DISCUSSION

Firstly, our attempts were dedicated to direct amination of cyanuric chloride by using 4-piperidone monohydrate hydrochloride **1a** (Scheme 1) as source of nucleophile in the presence of potassium carbonate as proton scavenger (Scheme 2, **Route A**, Table 1, Entries 1 - 4).
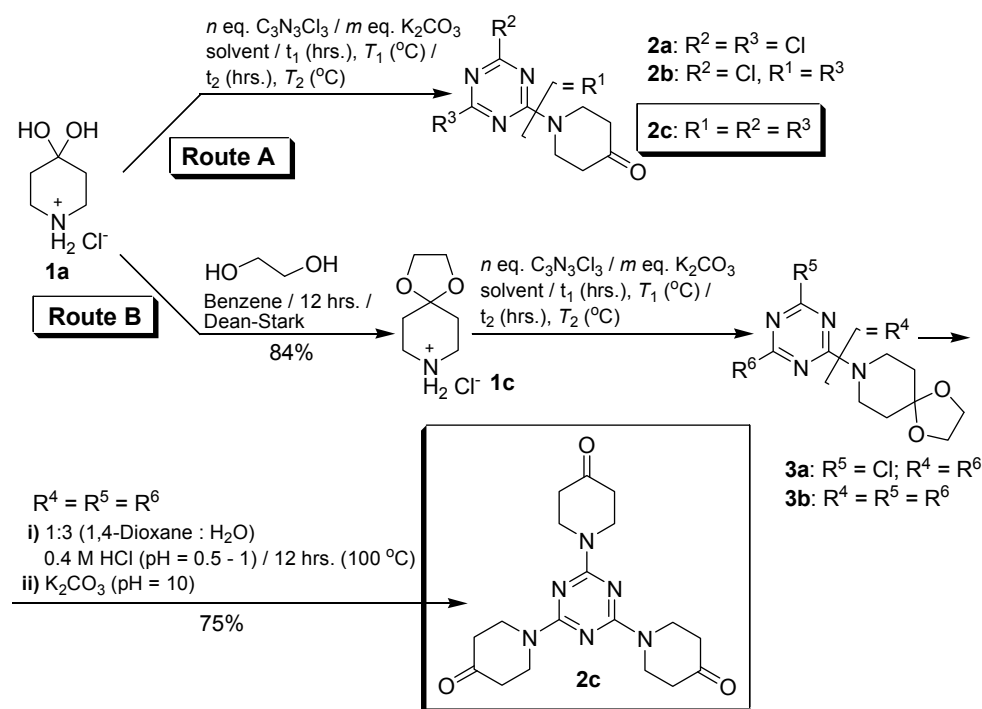
Scheme 2

As shown by the partial conversions of cyanuric chloride, preliminary results in **Route A** (Scheme 2) were not promising at all (Table 1, Entries 1 – 3): its maximum global conversion was about 26% only. Selectivity of chlorine replacement was also poor.

Table 1. Quantitative and qualitative results of amination of cyanuric chloride starting from 4-piperidone hydrochloride **1a** (Scheme 2, **Route A**) or its ethylene ketal hydrochloride **1c** (Scheme 2, **Route B**)

Entry	Molar ratios		Conditions			(Partial) conversions
Route	*n* eq. $C_3N_3Cl_3$	*m* eq. K_2CO_3	Solvent	t_1 (hrs.) t_2 (hrs.)	T_1 (^{o}C) T_2 (^{o}C)	of cyanuric chloride (%)
1 **A**	0.98	1.97	THF	72 -	r.t. -	16 (**2a**); 9 (**2b**); 1(**2c**)*
2 **A**	0.33	1.97	THF	24 29	r.t. reflux	11(**2b**); 4(**2c**)*
3 **A**	0.33	1.97	CHCl$_3$	48 -	reflux -	12(**2b**); 7(**2c**)*
4 **A**	0.50	2.00	THF + 10% H$_2$O	12 24	-10 r.t.	68(**2b**)**
5 **B**	0.50	2.00	THF + 10% H$_2$O	10 24	-10 r.t.	62(**3a**)**
6 **B**	0.32	2.00	DMF	24 12	0 → r.t. reflux	63(**3b**)**

*calculated based on effective amounts isolated by flash column chromatography; **isolated yields

Indeed, 4-piperidone monohydrate hydrochloride **1a** exhibited a very reduced solubility in solvents usually recommended for amination of cyanuric chloride (THF, 1,4-dioxane, chloroform and dichloromethane). Combined with the insolubility of the proton scavenger (K_2CO_3) in the same solvents, at room temperature, 4-piperidone was too slowly generated from **1a**. Upon heating (Table 1, Entries 2, 3), the poorer results obtained inferred us that decomposition of the nucleophile rather occurred instead ofthe desired S_N2Ar process.

A pivotal improvement of our strategy in **Route A** consisted of the use of aqueous THF (10% water) as solvent (Table 1, Entry 4), able to ensure a rapid acid-base interchange between potassium carbonate and 4-piperidone monohydrate hydrochloride **1a**. Thus, in very mild and carefully controlled conditions, the highly selective double replacement of chlorine in cyanuric chloride by two 4-oxopiperidin-1-yl units was achieved, affording the bis(ketone) **2b** with an satisfactory yield. We note that conditions in Table 1 (Entry 4) were appropriate only for the double substitution of chlorine (spot to spot TLC monitoring). They also demonstrated the high reactivity as nucleophile of 4-piperidone in the depicted methodology.

7

Therefore, the exploitation as nucleophile of the freshly prepared ethylene ketal of 4-piperidone **1b** (Scheme 1) was straightforward. Surprisingly, in our hands, **1b** was very volatile during the usual work-up of its hydrochloride **1c**. Consequently, we had to opt for the direct use of **1c** (Scheme 2, **Route B**) and the *in situ* generation of **1b** [6].

Furthermore, our methodology was classic and resumed to three steps: protection by acetalisation of **1a** (→ **1c**), selective aminations (→ **3a**, **3b**) and deprotection of **3b** (→ **2c**).

Protection of the masked carbonyl group of **1a** as ethylene ketal **1c** occurred in 84% yield. Thus, **1c** was routinely prepared. As **1a**, **1c** was also highly insoluble in THF and 1,4-dioxane.

Accordingly, the selectivity as twofold amination of cyanuric chloride by the free base **1b** generated *in situ* from **1c** was achieved (Scheme 2, **Route B**, Table 1, Entry 5) only in similar conditions as in the case of 4 piperidone (Scheme 2, **Route A**, Table 1, Entry 4).

Next, DMF was the suitable solvent for **1c** in order to perform the complete substitution of chlorine in cyanuric chloride in one-pot synthesis (Scheme 2, **Route B**, Table 1, Entry 6) in 63% yield. That is, the generation *in situ* of the nucleophile **1b** from **1c** in the presence of potassium carbonate also occurred in DMF. No problem we encountered during isolation of the triple spirane **3b** as pure analytical sample by simple crystallisation.

In contrast, deprotection of **3b**, carried out in refluxing aqueous 1,4-dioxane at pH = 0.5 – 1.0, required an unexpected long time, about 12 hrs, as indicated by its spot to spot evolution in TLC monitoring. The desired tris(ketone) **2c** was also isolated simply, by direct crystallisation.

CONCLUSIONS

The synthesis of the first melamine based entirely on 4-piperidone and of some of its precursors was realised in three steps by using a classical chemistry in an overall 40% global yield. The study of compound **3b** as dendritic core is in advanced progress.

EXPERIMENTAL SECTION

General. Melting points are uncorrected; they were carried out on ELECTROTHERMAL® instrument. Conventional NMR spectra were recorded on a Bruker® AM 300 instrument operating at 300 and 75 MHz for ^{1}H and ^{13}C nuclei respectively (a Bruker® DMX500 instrument was also used in the case of compound **2b**). All NMR spectra were measured in anhydrous commercially available deuteriated solvents. No $SiMe_4$ was added; chemical shifts were measured against the solvent peak. All chemical shifts (δ values) are given throughout in ppm; all coupling patterns ($^nJ_{H,H}$ values) are given throughout

in Hz.TLC was performed by using aluminium sheets with silica gel 60 F_{254} (Merck®); flash column chromatography was conducted on Silica gel Si 60 (40–63 μm, Merck®). IR spectra were performed on a Perkin-Elmer® Paragom FT-IR spectrometer. Only relevant absorptions are listed [throughout in cm^{-1}: weak (w), medium (m) or (s) strong]. Microanalyses were performed on a Carlo Erba® CHNOS 1160 apparatus. Mass spectra (MS) were recorded a Bruker® Esquire Instrument.

*Preparation of compounds **2a – c** (Scheme 2, **Route A**, Table 1, Entry 1)*

Cyanuric chloride (1.673 g, 9.07 mmol) and anh. K_2CO_3 (2.502 g 18.10 mmol) in dry THF (80 mL) were stirred at room temperature meanwhile 4-piperidone monohydrate hydrochloride **1a** (1.462 g, 9.524 mmol) was added portionwise within 5 hrs. with vigorous stirring. The reaction mixture was kept at room temperature for additional 72 hrs. until no more evolution was observed by TLC monitoring. The resulted suspension was filtered off and solids were well washed with dry THF (100 mL). The THF filtrate was evaporated under reduced pressure to yield 2.300 g crude solid material which was separated by column chromatography (eluent ligroin: acetone 3.8:1 v/v) yielding the title compounds as follows: **2a** (0.363 g, as the first fraction, 16 % conversion of cyanuric chloride), **2b** (0.251 g, as the second fraction, 9 % conversion of cyanuric chloride) and **2c** (0.030 g, as the third fraction, 1 % conversion of cyanuric chloride).

*Alternative preparation of compound **2b** (Scheme 2, **Route A**, Table 1, Entry 4)*

To a 10 % v/v aq. in THF suspension (100 mL) containing cyanuric chloride (0.922 g, 5 mmol) and anh. K_2CO_3 (2.762 g, 20 mmol), cooled at – 15 °C, solid piperidone monohydrate hydrochloride **1a** (1.536 g, 10 mmol) was added slowly and portionwise within 12 hrs with vigorous stirring and keeping temperature to not exceed –10 °C. The reaction mixture was then allowed to reach very slowly room temperature and was kept as such for additional 24 hrs. until TLC monitoring showed completion of reaction (eluent ligroin : acetone 1.5:1 v/v, single spot, R_f = 0.70). The reaction mixture was filtered off, minerals were well washed with dichloromethane (50 mL) then dichloromethane (75 mL) was added to the filtrate with stirring. The organic layer was separated, and then washed several times with water (× 50 mL) to neutrality. After drying over anh. Na_2SO_4, and filtering off, the organic solution was evaporated to dryness under vacuum. The solid residue was crystallised from dry ether (5 mL) at –20 °C to yield 1.053 g pure **2b** (68 % yield).

*In a similar procedure, compound **3a** was prepared (Scheme 2, **Route B**, Table 1, Entry 5).*

9

2,4-Dichloro-6-(4-oxopiperidin-1-yl)-*s*-triazine (2a) (16%) white crystalline powder, mp 219.1 - 220.2 °C (flash column chromatography, eluent ligroin : acetone 3.8:1 v/v). [Found: C, 38.55; H, 3.55; N, 23.05; $C_8H_8Cl_2N_4O$ (246.01) requires: C, 38.89; H, 3.26; N, 22.68%]. R_f 0.50 (80% ligroin/acetone). IR ν_{max} (KBr) = 1726 (s), 1591 (s), 1479 (s), 1366 (s), 1356 (s), 1229 (s), 1176 (s), 1155 (s), 1053 (s), 980 (s), 846 (s), 785 (m) cm^{-1}. ^{1}H NMR (300 MHz, CDCl$_3$) δ_H = 4.14 (4 H, t, $^3J_{H,H}$ = 6.4 Hz, H-2, -6, -a, -e), 2.56 (4 H, t, $^3J_{H,H}$ = 6.4 Hz, H-3, -5, -a, -e) ppm; ^{13}C NMR (75 MHz, CDCl$_3$) δ_C = 205.9 (1 C, C-4, 4-piperidone), 171.1 (2 C, C-2, -4, *s*-triazine), 164.7 (1 C, C-6, *s*-triazine), 43.2 (2 C, C-2, -6, 4-piperidone), 40.6 (2 C, C-3, -5, 4-piperidone) ppm. ^{1}H NMR (300 MHz, [D$_8$]THF) δ_H = 4.12 (4 H, t, $^3J_{H,H}$ = 6.4 Hz, H-2, -6, -a, -e), 2.50 (4 H, t, $^3J_{H,H}$ = 6.4 Hz, H-3, -5, -a, -e) ppm; ^{13}C NMR (75 MHz, [D$_8$]THF) δ_C = 202.4 (1 C, C-4, 4-piperidone), 168.7 (2 C, C-2, -4, *s*-triazine), 162.9 (1 C, C-6, *s*-triazine), 41.0 (2 C, C-2, -6, 4-piperidone), 37.9 (2 C, C-3, -5, 4-piperidone) ppm. MS (EI, 70 eV), m/z (rel. int. %) 246.01 (100) [M$^+$].

2-Chloro-4,6-bis(4-oxopiperidin-1-yl)-*s*-triazine (2b) (9%) white crystalline powder, mp 188.1–189.0 °C (flash column chromatography, eluent ligroin : acetone 3.8:1 v/v). [Found: C, 50.79; H, 4.90; N, 22.71; $C_{13}H_{16}ClN_5O_2$ (309.10) requires: C, 50.41; H, 5.21; N, 22.61%]. R_f 0.35 (80% ligroin/ acetone) R_f 0.70 (60% ligroin/acetone). IR ν_{max} (KBr) = 3007 (w), 2974 (w), 2900 (w), 1714 (s), 1592 (s), 1492 (s), 1450 (s), 1367 (m), 1331 (m), 1231 (s), 1211 (s), 1016 (m), 982 (m), 967 (m), 827 (m), 793 (m), 753 (w), 685 (w), 556 (w), 497 (w) cm^{-1}. ^{1}H NMR (500 MHz, [D$_8$]THF, 303 K) δ_H = 4.10 (8 H, t, $^3J_{H,H}$ = 6.5 Hz, H-2', -2", -6', -6", -a, -e), 2.45 [4 H, bt, H-5'(3'), -5"(3"), -a, -e], 2.44 [4 H, bt, H-3'(5'), -3"(5"), -a, -e] ppm; ^{1}H NMR (500 MHz, [D$_8$]THF, 263 K) δ_H = 4.08 [4 H, t, $^3J_{H,H}$ = 5.8 Hz, H-6'(2'), -6"(2"), -a, -e], 4.07 [4 H, t, $^3J_{H,H}$ = 5.8 Hz, H-2'(6'), -2"(6"), -a, -e], 2.43 [4 H, t, $^3J_{H,H}$ = 6.3 Hz, H-5'(3'), H-5"(3"), -a, -e], 2.41 [4 H, t, $^3J_{H,H}$ = 6.3 Hz, H-3'(5'), -3"(5"), -a, -e] ppm; QC NMR (125 MHz, [D$_8$]THF, 303 K) δ_C = 205.1 (2 C, C-4', -4"), 170.3 (1 C, C-2, *s*-triazine), 165.2 (2 C, C-4, -6, *s*-triazine), 42.7, 42.6 (4 C, C-2', -2", -6', -6"), 40.6, 40.3 (4 C, C-3', -3", -5', -5") ppm; ^{1}H NMR (500 MHz, [D$_6$]DMSO, 343 K) δ_H = 4.03 (8 H, t, $^3J_{H,H}$ = 6.3 Hz, H-2', -2", -6', -6", -a, -e), 2.48 (8 H, t, $^3J_{H,H}$ = 6.3 Hz, H-3', -3", -5', -5", -a, -e) ppm. MS (EI, 70 eV): *m/z* (%) = 309 [M$^+$] (100), 281 (58), 253 (78), 240 (70), 225 (40), 197 (33), 184 (29), 70 (37).

2,4,6-Tris(4-oxopiperidin-1-yl)-*s*-triazine (2c) (1%) yellowish crystalline powder, mp 234.2 °C (dec.) (flash column chromatography, eluent ligroin : acetone 3.8:1 v/v). [Found: C, 57.75; H, 6.88; N, 22.71; $C_{18}H_{24}N_6O_3$ (372.19) requires: C, 58.05; H, 6.50; N, 22.57%]. R_f 0.20 (80% ligroin/acetone). IR ν_{max} (KBr) = 2958 (w), 2862 (w), 1709 (s), 1530 (s), 1490 (s), 1455 (s), 1371 (m), 1316 (m), 1231 (s), 1068 (m), 991 (m), 967 (m), 806 (m), 762 cm^{-1}. ^{1}H NMR

(300 MHz, CDCl$_3$) δ_H = 4.08 (12 H, t, $^3J_{H,H}$ = 6.0 Hz, H-2', -2", -2''', -6', -6", -6''', -a, -e), 2.47 (12 H, t, $^3J_{H,H}$ = 6.0 Hz, H-3', -3", -3''', -5', -5", -5''', -a, -e) ppm; ^{13}C NMR (75 MHz, CDCl$_3$) δ_C = 208.9 (3 C, C-4', -4", -4'''), 165.8 (3 C, C-2, -4, -6, *s*-triazine), 43.0 (6 C, C-2', -2", -2''', -6', -6", -6'''), 41.5 (6 C, C-3', -3", -3''', -5', -5", -5''') ppm. MS (EI, 70 eV): *m/z* (%) = 372 [M$^+$] (100), 344 (20), 329 (18), 316 (58), 303 (75), 288 (47), 275 (45), 260 (50), 247 (60), 232 (25), 219 (28), 203 (26), 177 (25), 163 (21), 122 (33), 94 (32), 80 (46), 68 (28).

Preparation of compound 1c (Scheme 2, Route B)

4-Piperidone monohydrate hydrochloride **1a** (4.70 g, 30.06 mmol) and ethyleneglicol (3.94 g, 60.12 mmol, 3.54 mL) in benzene (125 mL) were refluxed with vigorous stirring and azeotropic removal of water in a Dean-Stark trap until no more water separated (about 12 hrs.). The resulted brownish suspension was cooled at room temperature with stirring then crude **1c** was filtered off and well washed with dry ether ($\times$ 25 mL) to complete removal of benzene. Crude **1c** was taken with isopropanol : ether 1:1 v/v (24 mL), stirred 1 hr. at room temperature then the suspension was cooled at -20 ^{o}C for 12 hrs. After filtering off, washing with cooled isopropanol : ether 1:1 v/v (20 mL) and dry ether (2 $\times$ 25 mL) pure **1c** was obtained (4.62 g, 84% yield with respect to **1a**).

1,4-Dioxa-8-azaspiro[4.5]decane hydrochloride (1c) (84%) yellowish crystalline powder, mp 192.5 – 192.9 ^{o}C (Compd. No. 94532 Fluka mp193 - 197 °C and mp 193 - 198 °C see also CAS Number 42899-11-6 Beilstein Registry Number 7304914). [Found: C, 47.11; H, 7.77; N 8.19; C$_7$H$_{14}$ClNO$_2$ (179.07) requires: C, 46.80; H, 7.86; N, 7.80%]. IR ν_{max} (KBr) = 3394 (s), 2948 (s), 2788 (s), 2616 (s), 2465 (s), 1586 (s), 1474 (m), 1449 (s), 1428 (m), 1376 (s), 1347 (m), 1309 (s), 1228 (m), 1189 (s), 1178 (s), 1110 (s), 1045 (s), 1028 (s), 942 (s), 888 (s), 834 (m), 656 (m) cm^{-1}. ^{1}H NMR (300 MHz, [D$_6$]DMSO) δ_H = 9.30 (2 H, bs, NH$_2^+$), 3.90 (4 H, s, 2 $\times$ H-2, 2 $\times$ H-3), 3.05 (4 H, s, H-7, -9, -a, -e), 1.84 (4 H, t, $^3J_{H,H}$ = 5.6 Hz, H-6, -10, -a, -e) ppm; ^{13}C NMR (75 MHz, [D$_6$]DMSO) δ_C = 104.5 (1 C, C-5), 64.4 (2 C, C-2, -3), 42.2 (2 C, C-7, -9), 31.6 (2 C, C-6, -10) ppm. MS (EI, 70 eV), m/z (rel. int. %) 143 [M$^+$ - HCl] (40), 112 (10), 98 (78), 87 (100), 82 (28), 80 (8), 73 (5), 71 (14), 68 (8).

2-Chloro-4,6-bis(1,4-dioxa-8-azaspiro[4.5]decan-8-yl)-*s*-triazine (3a) (62%) yellowish crystalline powder, mp 143 – 145 ^{o}C (Et$_2$O). [Found: C, 50.98; H, 5.88; N 17.31; C$_{17}$H$_{24}$ClN$_5$O$_4$ (397.15) requires: C, 51.32; H, 6.08; N, 17.60%]. IR ν_{max} (KBr) = 2964 (m), 2932 (m), 2870 (m), 1655 (m), 1571 (s), 1492 (s), 1458 (s), 1364 (m), 1310 (m), 1230 (s), 1146 (m), 1116 (s), 1078 (s), 1034 (m), 979 (m), 944 (m), 908 (m), 796 (m), 660 (w) cm^{-1}. ^{1}H NMR (300 MHz, [D$_6$]DMSO) δ_H = 3.95 (8 H, s, H-2', -2", -3', -3"), 3.79 (8 H, bs, H-7', -7" -9', -9", -a, -e), 1.66 (8 H, bs, H-6', -6", -10', -10", -a, -e) ppm; ^{1}H NMR

(300 MHz, CDCl$_3$) δ_H = 3.97 (8 H, s, H-2', -2", -3', -3"), 3.85 (8 H, bs, H-7', -7" -9', -9", -a, -e), 1.66 (8 H, t, $^3J_{H,H}$ = 5.3 Hz, H-6', -6", -10', -10", -a, -e) ppm; ^{13}C NMR (75 MHz, [D$_6$]DMSO) δ_C = 169.2 (1 C, C-2, s-triazine), 163.9 (2 C, C-4, -6, s-triazine), 106.7 (2 C, C-5', -5"), 64.2 (4 C, C-2', -2", -3', -3"), 41.5 (4 C, C-7', -7", -9', -9"), 34.6 (4 C, C-6', -6", -10', -10") ppm; ^{13}C NMR (75 MHz, CDCl$_3$) δ_C = 170.1 (1 C, C-2, s-triazine), 164.5 (2 C, C-4, -6, s-triazine), 107.5 (2 C, C-5', -5"), 64.8 (4 C, C-2', -2", -3', -3"), 41.8 (4 C, C-7', -7", -9', -9"), 35.2 (4 C, C-6', -6", -10', -10") ppm. MS (EI, 70 eV), m/z (rel. int. %) 397 [M$^+$] (100), 354 (30), 325 (25), 310 (10), 297 (50), 284 (70), 252 (10), 225 (20), 212 (15), 197 (10), 184 (20), 170 (15), 158 (5), 142 (8), 127 (5), 99 (65), 86 (13), 70 (18).

*Preparation of compound 3b (Scheme 2, **Route B**, Table 1, Entry 6)*
1,4-Dioxa-8-azaspiro[4.5]decane hydrochloride **1c** (3.60 g, 20 mmol) was dissolved in dry and freshly distilled DMF (125 mL), then anh. K$_2$CO$_3$ (5.60 g, 40 mmol) was added. The resulted suspension was cooled at 0 ^{o}C when solid cyanuric chloride (1.18 g, 6.35 mmol) was rapidly introduced with vigorous stirring. The reaction mixture was let very gently to reach room temperature (about 24 hrs.) then heated at reflux until TLC monitoring (eluent ligroin : acetone 1.5 : 1 v/v) indicated no more evolution of the reaction and the crude product **3b** as a main spot (about 12 hrs.). The reaction mixture was poured on water (100 mL) then extracted with chloroform (100 ml). After separation, the organic layer was well washed with water (7 × 100 mL) to complete removal of DMF, then dried over anh. Na$_2$SO$_4$. After filtering off and washing minerals with chloroform, the organic solution was evaporated under reduced presure to dryness yielding the crude product which was taken with dry ether (5 mL) with stirring. The resulted suspension was cooled at -20 ^{o}C for 12 hrs. then filtered off and washed with dry and cooled ether to yield the title compound **3b** (2.00 g, 63% yield with respect to cyanuric chloride).

2,4,6-Tris(1,4-dioxa-8-azaspiro[4.5]decan-8-yl)-s-triazine **(3b)**
(63%) yellowish crystalline powder, mp 259 – 263 ^{o}C (Et$_2$O). [Found: C, 56.98; H, 7.33; N 17.01; C$_{24}$H$_{36}$N$_6$O$_6$ (504.27) requires: C, 57.13; H, 7.19; N, 16.66%]. IR ν_{max} (KBr) = 2954 (w), 2927 (w), 2875 (w), 1684 (w), 1539 (s), 1493 (s), 1450 (s), 1360 (w), 1333 (w), 1309 (w), 1234 (m), 1120 (m), 1080 (s), 1038 (w), 947 (m), 908 (m), 804 (w), 661 (w) cm^{-1}. ^{1}H NMR (300 MHz, CDCl$_3$) δ_H = 4.00 [12 H, s, 2 × (H-2', -2", -2'''), 2 × (H-3', -3", -3''')], 3.86 [12 H, t, $^3J_{H,H}$ = 5.2 Hz, H-7', -7", -7''', -9', -9", -9''', -a, -e), 1.70 (12 H, t, $^3J_{H,H}$ = 5.2 Hz, H-6', -6", -6''', -10', -10", -10''', -a, -e) ppm; ^{13}C NMR (75 MHz, CDCl$_3$) δ_C = 165.3 (3 C, C-2, -4, -6, s-triazine), 107.8 (3 C, C-5', -5", -5'''), 64.3 (6 C, C-2', -2", -2''', -3', -3", -3'''), 41.1 (6 C, C-7', -7", -7''', -9', -9", -9'''), 34.8 (6 C, C-6', -6", -6''', -10', -10", -10''') ppm.

*Alternativ preparation of compound 2c (Scheme 2, **Route B**)*

To 2,4,6-tris(1,4-dioxa-8-azaspiro[4.5]decan-8-yl)-*s*-triazine **3b** (1.446 g, 2.86 mmol) suspended in aqueous 1,4-dioxane (water 21 mL + 1,4-dioxane 7 mL), concd. aq. hydrochloric acid (1.00 mL, 1.18 g soln. 37%, 12 mmol HCl) was added and the reaction mixture, having the pH = 0.5 – 1.0, was heated at reflux for 12 hrs. The reaction was monitored spot to spot by TLC (eluent ligroin : acetone 1.5:1 v/v) and stopped when no more evolution was observed and the desired **2c** as largely major spot. The reaction mixture was cooled at room temperature and made alkaline (pH = 10) with solid K_2CO_3 when crude **2c** precipitated abundantly. After filtering off, washing with water to neutrality and drying, pure **2c** (0.800 g, 75 % yield) was obtained after crystallisation from ether at -20 ^{o}C. The pure analytical sample obtained by the above methodology was identical with that obtained in **Route A** (Table 1, Entries 1 – 3).

ACKNOWLEDGMENTS

REFERENCES

1. C. Berghian, P. Lameiras, L. Toupet, E. Condamine, N. Plé, A. Turck, C. Maiereanu, M. Darabantu, *Tetrahedron*, **2006**, *62*(31), 7319.

2. M. Darabantu, M. Pintea, M. Fazekas, P. Lameiras, C. Berghian, I. Delhom, I. Silaghi-Dumitrescu, N. Plé, A. Turck, *Letters in Organic Chemistry*, **2006**, *3*(12), 905.

3. M. Fazekas, M. Pintea, P. Lameiras, A. Lesur, C. Berghian, I. Silaghi-Dumitrescu, N. Plé, M. Darabantu, *Eur. J. Org. Chem.*, **2008**, 2473.

4. S. M. Mc Elvain, R. Mc. Mahon, *J. Am. Chem. Soc.*, **1949**, *71*, 901.

5. *see for example*: a) J. Henkin, D. Davidson, U.S. Pat. 6150362 (**2000**); b) J. Henkin, D. Davidson, G. Sheppard, K. W. Woods, R. W. McCroskey, U.S. Pat. 6288228 (**2001**); d) J. Henkin, D. Davidson, G. Sheppard, K. W. Woods, R. W. McCroskey, Eur. Pat. EP1037886 (**2003**).

6. K. Stach, M. Thiel, F. Bickelhaupt, *Monatshefte fuer Chemie*, **1962**, *93*(5), 1090.

SYNTHESIS AND STRUCTURAL ANALYSIS OF SOME NEW SATURATED SIX-MEMBERED RING HETEROCYLIC COMPOUNDS OBTAINED FROM TERPENOIDS

DANIELA PRODAN, BIANCA MOLDOVAN, LUMINIȚA DAVID[*], ION GROSU

ABSTRACT. The synthesis, structural analysis and the stereochemistry of some new six-membered ring heterocyclic derivatives obtained by the ketalisation reaction of some mono- and bicycloterpenoids are reported. The structural analysis of the compounds was carried out using NMR investigations and the anancomeric structure of the compounds and the influence of the chirality introduced in the molecule by the terpenoidic structure were revealed.

Keywords: spiro-1,3-dioxanes, terpenoids, structural analysis, chirality

INTRODUCTION

Many spiro and polispiro compounds with saturated six-membered rings were studied in connection with their structural behavior.[1-10] The investigations of these compounds revealed the helical chirality of the spirane skeleton and the anancomeric or flipping conformational behavior of the compounds in correlation with the nature of the substituents located in positions 2 and 4 of the spirane skeleton.[1-4,10] Many spiro 1,3-dioxane derivatives were synthesized for various applications in material sciences,[11] as chiral reagents,[12] and drugs[13].

In this context we considered of interest to investigate new spiro 1,3-dioxanes obtained starting from terpenoids.

RESULTS AND DISCUSSIONS

New six membered heterocyclic compounds were synthesized by the condensation reaction of some terpenoids with 1,3-diols (when 1,3-dioxanes were obtained) (Scheme 1). The acetalization reaction being of equilibrium leads to the more stable structure in which the substituents located at the heterocycle exhibit an equatorial orientation.

---

[*] Babeş-Bolyai" University, Organic Chemistry Department and CCOCCAN, 11 Arany Janos str., 400028, Cluj-Napoca, Romania

(-)-Menthone

$R^1 = CH_3, R^2 = H$ **1**
$R^1 = H, R^2 = CH_3$ **2**

α-Thujone

$R^1 = CH_3, R^2 = H$ **3**
$R^1 = H, R^2 = CH_3$ **4**

Scheme 1

Trying to use (-)-carvone for the ketalisation reaction in the same conditions (acidic catalysis) instead of the 1,3-dioxane compound, the characteristic side reaction[14] to carvacrol took place as main process (Scheme 2). Also the ketalisation reaction of (*1S*)-camphor or (*1R*)-verbenone did not worked in the typical procedures and the corresponding 1,3-dioxane derivatives could not be obtained.

(-)-Carvone   Carvacrol

Scheme 2

The structural analysis of **1-4** was carried out using NMR investigations. The spectra of compounds **1-3** exhibit different signals for the axial and equatorial protons of the 1,3-dioxane rings (Table 1) and prove the anancomeric structure of these compounds. On the other side for compounds **1** and **3**,

16

positions 2 and 4 are diastereotopic as a consequence of the chirality of the molecules (helical chirality of the spirane unit and chiral centers of the terpenoid moiety).

Table 1. NMR data (300 MHz, C_6D_6, δ ppm) for compounds **1-3***

Compound	2(2')-H		4(4')-H	
	ax.	eq.	ax.	eq.
1	3.40	3.95	3.17	3.70
2	2.81	-	3.76	3.52
3	3.22	3.57	3.19	3.57

*The NMR spectrum of **4** exhibit overlapping of the investigated signals and their assignment could not be carried out properly.

For compounds **1** and **3** two diastereoisomers are possible (**D₁** and **D₂**, Scheme 3). In **D₁** (exhibiting the *M* configuration of the spirane skeleton) the *i*-Pr group is oriented "inside" referred to the 1,3-dioxane unit. This orientation determines an important hindrance and it is instable. In **D₂** (with *P* configuration of the spirane skeleton) the *i*-Pr group is oriented "outside" relatively to the 1,3-dioxane unit, the steric hindrance is diminished and this conformer is considerably more stable. The synthesis of **1** and **3** is running under thermodynamic control so the reaction leads mainly to the **D₂** isomer.
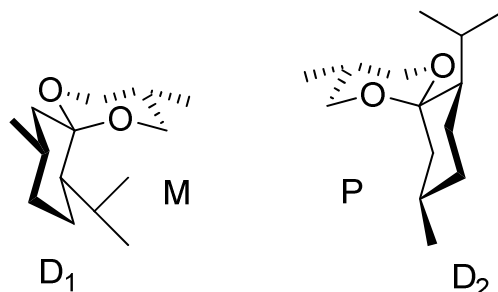
Scheme 3

The methyl group at position 3 of the spirane exhibits an equatorial preference in agreement with the high conformational enthalpy of the methyl substituents located at position 5 of the 1,3-dioxane rings[15-17].

In the case of compound **2** and **4**, the methyl group located in position 4 also prefers the equatorial orientation, the possible equilibrium run during the acetalization reaction being totally shifted towards this isomer. On the other hand as in the previously shown case (for 1 and 3), for compounds 2 and 4 two diastereoisomers are possible. In this case too, the major (representative) diastereoisomer exhibits the methyl group of position 4 oriented "outside" the 1,3-dioxane ring.

17

CONCLUSIONS

New spiro compounds were obtained starting from terpenoids and substituted 1,3-propanediols. The NMR investigations revealed the preference for the formation of the less hindered diastereoisomers and the anancomeric conformational behavior of these ones.

EXPERIMENTAL

^{1}H-NMR (300 MHz) spectra were recorded at *rt* in C_6D_6 on a Bruker 300 MHz / 400MHz spectrometer, using the solvent line as reference.

Chemicals were purchased from Aldrich or Acros and were used without further purification.

General procedure for the synthesis of compounds 1-4

0.1 mol of 1,3-diol and the corresponding quantities of terpenoids (0,1 mol) with catalytic amounts of *p*-toluenesulphonic acid (0.1 g) were solved in 200 mL benzene. The mixture was refluxed and the water produced in the reaction removed using a Dean-Stark trap. When 80 % of the water had been separated, the mixture was cooled to room temperature and the catalyst was neutralized (under stirring 0.5 h) with sodium acetate powder in excess (0.2 g), then washed with water (2 x 100 mL) and dried on anhydrous Na_2SO_4 After filtration, the solvent was removed and the crude products were purified by vacuum distillation (0.5 -1 mmHg).

3,10-dimethyl-7-isopropyl-1,5-dioxaspiro[5.5]undecane 1

Liquid, b.p.=112-114°C (2 mmHg), yield 60 %. $C_{14}H_{26}O_2$ (226.35), calc. 74.28 C, 11.58 H, found 73.97 C, 11.79 H. **^{1}H-NMR** (300 MHz, C_6D_6, δ ppm): 3.95 (1H, dd, J = 11.3 Hz, J = 2.7 Hz, 2-H_{eq}), 3.70 (1H, dd, J = 11.3 Hz, J = 2.7 Hz, 4-H_{eq}), 3.40 (1H, m, 2-H_{ax}), 3.17 (1H, m, 4-H_{ax}), 2.83 (1H, m, 3-H), 2.63 (2H, m, 11-H), 1.20 (3H, d, J = 6.9 Hz, 10-CH_3), 1.09 (3H, d, J = 6.9 Hz, 3-CH_3), 0.87 (6H, d, J = 6.6 Hz, 7-$CH(CH_3)_2$), 0.60-1.80 [7 H, overlapped peaks, 7-H, 8-H_2, 9-H_2, 10 H, 7-$CH(CH_3)_2$]

2,10-dimethyl-7-isopropyl-1,5-dioxaspiro[5.5]undecane 2

Liquid, b.p.=118-120°C (2 mmHg), yield 58 %. $C_{14}H_{26}O_2$ (226.35), calc. 74.28 C, 11.58 H, found 74.70 C, 11.90 H. **^{1}H-NMR** (300 MHz, C_6D_6, δ ppm): 3.76 (1H, m, 4-H_{ax}), 3.52 (1H, m, 4-H_{eq}), 2.81 (1H, m, 2-H), 2.79 (1H, m, 11-H_{eq}), 2.56 (1H, d, J = 13.3 Hz, 11-H_{ax}), 2.24 (2H, m, 3-H), 1.17 (3H, d, J = 6.7 Hz, 2-CH_3), 1.05 (3H, d, J = 6.9 Hz, 10-CH_3), 0.88 (6H, d, J = 6.7 Hz, 7-$CH(CH_3)_2$), 0.70-1.10 [7 H, overlapped peaks, 7-H, 8-H_2, 9-H_2, 10 H, 7-$CH(CH_3)_2$]

3,3-(3'-methyl-1',5'-dioxapentan-1',5'-diyl)-1-isopropyl-4-methyl-byciclo[3.1.0]hexane 3

Liquid, b.p.=108-110°C (1,4 mmHg), yield 56 %. $C_{14}H_{24}O_2$ (224.17), calc. 74.95 C, 10.78 H, found 74.60 C, 11.05 H. **^{1}H-NMR** (300 MHz, C_6D_6, δ ppm): 3.57 (2H, overlapped peaks, 2'-H_{eq} 4'-H_{eq}), 3.22 (1H, d, $J = 11.7$ Hz 2'-H_{ax}), 3.19 (1H, d, $J = 11.7$ Hz 4'-H_{ax}), 2.56 (1H, m, 3'-H_{ax}) 2.39 (1H, d, $J = 13.3$ Hz, 2-H_{eq}), 1.79 (1H, d, $J = 13.3$ Hz, 2-H_{ax}), 1.37 (3H, d, $J = 6.7$ Hz, 3'-CH_3), 1.20 (3H, d, $J = 6.9$ Hz, 4-CH_3), 0.90 [6H, d, $J = 6.7$ Hz, 1-$CH(CH_3)_2$], 0.70-1.10 (5 H, overlapped peaks, 6-H_2, 5-H, 4 H, 1-$CH(CH_3)_2$]

3,3-(2'-methyl-1',5'-dioxapentan-1',5'-diyl)-1-isopropyl-4-methyl-byciclo[3.1.0]hexane 4

Liquid, b.p.=106-107°C (1,4 mmHg), yield 42 %. $C_{14}H_{24}O_2$ (224.17), calc. 74,95 C, 10,78 H, found 74,60 C, 11,05 H. **^{1}H-NMR** (300 MHz, C_6D_6, δ ppm): 3.70-3.60 (2H, overlapped peaks, 4'-H_{eq} 4'-H_{ax}), 2.92 (1H, m, 2'-H_{ax}), 2.49 (1H, d, $J = 12.5$ Hz, 2-H_{eq}), 2.24 (2H, m, 3-H), 1.99 (1H, d, $J = 12.5$ Hz, 2-H_{ax}), 1.37 (3H, d, $J = 6.8$ Hz, 2'-CH_3), 1.20 (3H, d, $J = 6.9$ Hz, 4-CH_3), 0.94 [6H, d, $J = 6.7$ Hz, 1-$CH(CH_3)_2$], 0.70-1.10 (5 H, overlapped peaks, 6-H_2, 5-H, 4 H, 1-$CH(CH_3)_2$]

REFERENCES

1. Grosu I., Mager S., Plé G., Horn M., *J. Chem. Soc. Chem. Commun.* **1995**, 167.

2. Grosu I., Mager S., Plé G., *J. Chem. Soc. Perkin Trans. 2*, **1995**, 1351.

3. Grosu I., Mager S., Plé G., Mesaroş E., Gegö C., Dulău A., *Rev. Roum. Chim.*, **1999**, *44*, 467.

4. Grosu I., Mager S., Plé G., Mesaros E., *Tetrahedron* **1996**, *52*, 12783.

5. Grosu I., Plé G., Mager S., Martinez R., Mesaros C., Camacho B., *Tetrahedron* **1997**, *53*, 6215.

6. Grosu I., Mager S., Plé G., Turos I., Mesaros E., Schirger I., *Monatsh. Chem.*, **1998**, *129*, 59.

7. Opris D., Grosu I., Toupet L., Plé G., Terec A., Mager S., Muntean L., *J. Chem. Soc. Perkin Trans. 1*, **2001**, 2413.

8. Grosu I., Bogdan E., Plé G., Toupet L., Ramondenc Y., Condamine E., Peulon-Agasse V., Balog M., *Eur. J. Org. Chem.* **2003**, 3153.

9. Balog, M., Grosu, I., Plé, G., Ramondenc Y., Toupet, L., Condamine, E., Lange, C., Loutelier, C., Peulon-Agasse, V., Bogdan, E., *Tetrahedron* **2004**, *60*, 4789.

10. Cismaş, C., Terec, A, Mager, S., Grosu, I., *Curr. Org. Chem.* **2005**, *9*, 1287.

11. Lemcoff, N. G., Fuchs, B., *Org. Lett.*, **2002**, *4*, 731.

12. Böhm, U., Voss, G., Möller, G., Gerlach, H., *Tetrahedron*: *Asymmetry*, **1994**, *5*, 1281.

13. Séller, J., Barr, J., Ng, S. Y., Shen, H. -R., Schwach-Abdellaoui, K., Gurny, R., Vivien-Castioni, N., Loup, P. J., Baehni, P., Mombelli, A., *Biomaterials*, **2002**, *23,* 4397.

14. Raner, K. D., Strauss C. R., Vyskoc F., Mokbel L., *J. Org. Chem.* **1993**, *58*, 950.

15. Anteunis M.J.O., Tavernier D., Borremans F., *Heterocycles* **1976**, *4*, 293.

16. Kleinpeter E., *Adv. Heterocycl. Chem.*, **1998**, *69*, 217.

17. Kleinpeter E., *Adv. Heterocycl. Chem.*, **2004**, *86*, 41.

NOVEL SERINOLIC MELAMINES AS POTENTIAL PERIPHERAL GROUPS IN DENDRITIC CHEMISTRY

MIRCEA DARABANTU[a], LUCAS BOULITREAU[b], IOANA OLOSUTEAN[a], PEDRO LAMEIRAS[b], CARMEN BÂTIU[a]

ABSTRACT. A rapid access to elaborated *N*-substituted 2,4,6-triamino-*s*-triazines (*melamines*), seen as potential non-symmetric peripheral groups in dendritic chemistry, is reported. It consists of the highly selective amination of cyanuric chloride by some *C*-substituted 2-aminopropane-1,3-diols (*serinols* as *"open chain serinolic unit"*), their cyclic acetals (*O,O*-protected forms as amino-1,3-dioxanes, *"closed chain serinolic unit"*) and piperazine as linker. All results are fully supported by IR, DNMR and MS data.

Keywords: s-triazine, serinols, amination, restricted rotation

INTRODUCTION

Subsequent to our recent findings in the synthesis [1-5], structure [1-5] and use [6-8] of elaborated *N*-substituted 2,4,6-triamino-*s*-triazines (*melamines*) based on the versatile nucleophilicity of *C*-substituted 2-aminopropane-1,3-diols (*serinols*) against cyanuric chloride, we now report the preliminary results in a combined new approach, resumed in Scheme 1. Both theoretic [9] and/or synthetic [10] recent advances in dendrimers' chemistry called attention on *non-symmetric peripheral groups, providing different sites for further nanoscale manipulation* of these architectures.

In this context, we considered of interest two new *N*-substituted **TARGET MELAMINES** based on serinols (Scheme 1) possessing:

i) A basic site as *closed chain serinolic unit*, *e.g.* of type enantiomerically pure (4*S*,5*S*)-amino-1,3-dioxane (**1a** and **1b**).

ii) An *open-chain serinolic unit*, *e.g.* of type **TRIS (THAM)**.

iii) An appropriate, non sophisticated and widely used dendritic linker, *e.g.* piperazine, able to connect cores [10, 11], generations [12] or both [13].

---

[a] *"Babes-Bolyai" University, Department of Organic Chemistry, 11 Arany Janos str., 400028, Cluj-Napoca, Romania. darab@chem.ubbcluj.ro*

[b] *Université de Rouen, I.R.C.O.F. (Institut de Recherche en Chimie Organique Fine) and I.U.T. (Institut Universitaire de Technologie) de Rouen, 76821 Mont Saint-Aignan Cedex, France*
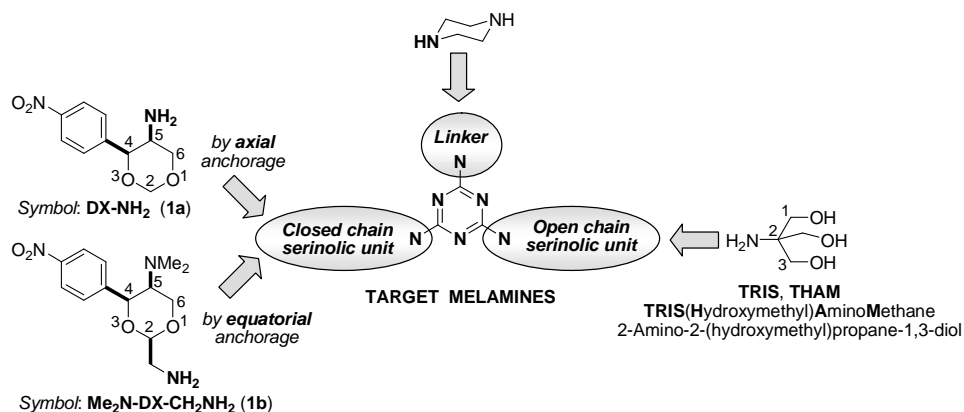
Scheme 1

RESULTS AND DISCUSSION

The chemistry we have developed is depicted in Scheme 2 while reaction conditions are listed in Table 1. Compounds **3a**, **3b**, **4a** and **4b** are new ones.
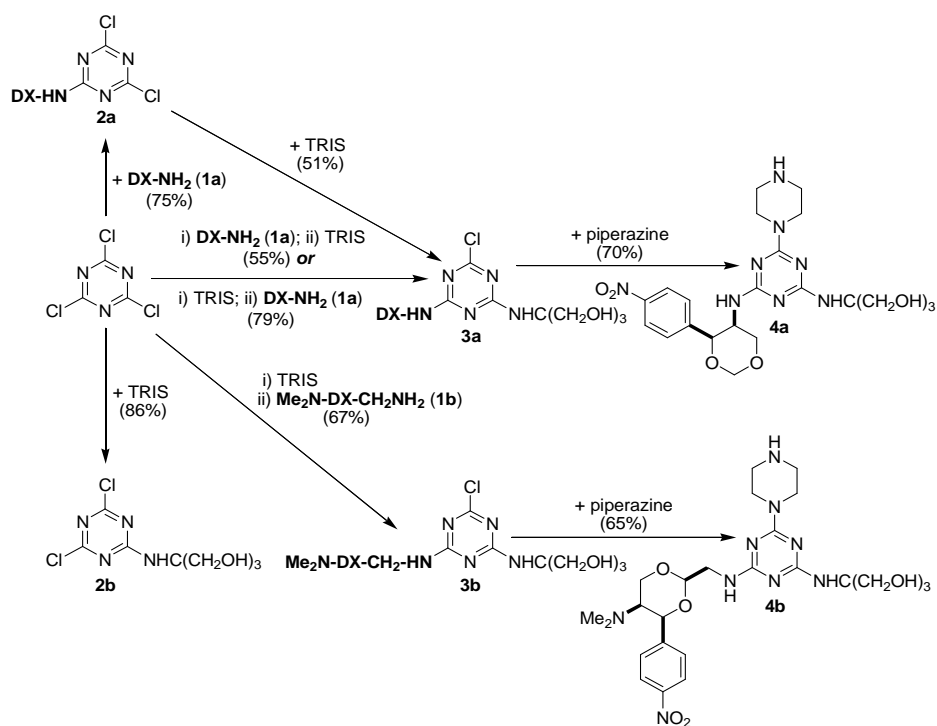
Scheme 2

Table 1. Reaction conditions for the synthesis of compounds **2b**, **3a**, **3b**, **4a** and **4b**

No.	Conditions			
	Molar ratios	Solvent	Time (hrs.)	*T* (^{o}C)
2a	1.03 (**1a**) : 1.03 (Base)* : 1.00 (C.C.)**	THF	24	0 → r.t.
2b	1.00 (TRIS) : 1.00 (Base) : 1.00 (C.C.)	THF	24	-15 → r.t.
3a	1.00 (TRIS) : 1.00 (Base) : 1.00 (**2a**)	THF	17	reflux
3a	1.03 (**1a**) : 1.03 (Base) : 1.00 (C.C.) ⇻	THF	24	0 → r.t.
	⇻1.00 (TRIS) : 1.00 (Base) : 1.00 (*2a*)***	THF	15	reflux
3a	1.00 (TRIS) : 1.00 (Base) : 1.00 (C.C.) ⇻	THF	24	-15 → r.t.
	⇻ 1.00 (**1a**) : 1.00 (Base) : 1.00 (*2b*)	THF	9	reflux
3b	1.00 (TRIS) : 1.00 (Base) : 1.00 (C.C.) ⇻	THF	24	-15 → r.t.
	⇻ 1.00 (**1b**) : 1.00 (Base) : 1.00 (*2b*)	THF	96	r.t.
4a	4.00 (piperazine) : 1.00 (Base) : 1.00 (**3a**)	1,4-dioxane	9	reflux
4b	4.00 (piperazine) : 1.00 (Base) : 1.00 (**3b**)	1,4-dioxane	9	reflux

*Throughout anh. K_2CO_3; **C. C.: Cyanuric Chloride ****Italicised*: intermediates not isolated in the one-pot (⇻) procedure (Scheme 2)

The synthesis and stereochemistry of the starting amino-1,3-dioxanes **1a** and **1b** (Scheme 1) we discussed in detail previously [1, 14]. They were used as pure enantiomeric (4*S*,5*S*-**1a**), (2*R*,4*S*,5*S*-**1b**) forms.

Monoamination of cyanuric chloride by TRIS occurred slowly with high selectivity. In fact, the yield obtained in the case of the resulted **2b** refers rather to its direct isolation by simple crystallisation than to the very clean reaction revealed by the TLC monitoring.

The same clear evolution was observed during the preparation of the dichloroamino-*s*-triazine **2a** whose synthesis and stereochemistry we described elsewhere [1]. Treatment of the isolated **2a** with TRIS required 17 hrs. in refluxing THF in order to afford compound **3a** in 51% yield after flash column chromatography, hence a 38% overall yield with respect to cyanuric chloride.

Two alternative one-pot protocols were envisaged for the preparation of **3a**, account being taken on the expected lower nucleofilicity of TRIS, more solvated in THF, in comparison with the amino-1,3-dioxane **1a**:

a) Amination of cyanuric chloride with **1a** then with TRIS (15 hrs. in refluxing THF) was performed without isolation of the intermediate **2a**. Chlorodiamino-*s*-triazine **3a** was obtained with a higher overall yield (55%, after flash column chromatography).

b) Amination of cyanuric chloride was firstly carried out with TRIS followed by **1a**, without isolation, this time, of the intermediate **2b**. **3a** was prepared in 79% yield and isolated by simple crystallisation.

Besides obvious benefits when one-pot synthesis was applied, the above results observed in the case of **3a** confirmed our anticipations that TRIS should be, like it or not, the first nucleophile in this chemistry.

We also note that, despite the presence of three hydroxymethyl groups *vs.* but one amino in TRIS, we detected no product of a competitive alkoxylation *vs.* amination in the depicted conditions when accessing compounds **2b** or **3a** [15].

We next used this know-how in the preparation of the chlorodiamino-*s*-triazine **3b**.

Previous findings of us evidenced the non-selective interaction between equimolar amounts of cyanuric chloride and the amino-1,3-dioxane **1b** as oligomerisations and *N*-demethylation [1]. Therefore, the single option we had consisted of the use, again, of TRIS as the first nucleophile with respect to cyanuric chloride, followed by **1b**, in a one-pot procedure. **3b** was obtained simply, in 67% overall yield, in much milder conditions than **3a**.

Particularly, one must observe that amino-1,3-dioxanes **1a**, **1b** were both anancomeric structures because of their overwhelmingly one-sided conformational equilibriums due to *p*-nitrophenyl ring located at C-4 in equatorial position (A value ≈ 11.93 kJ/mol) [16]. It was by far greater than A values of C-5 amino (5.15 – 7.10 kJ/mol) in **1a** or C-5 dimethylamino (6.40 – 8.80 kJ/mol) group in **1b** [16].

On the other hand, the expected equatorial linkage of the C-2 aminomethyl group in **1b** (A value up to 7.50 kJ/mol) *vs.* the rigid C-5 axial amino one in **1a** crucially discriminated the nucleofilicity as of **1b** greater than that of **1a** in amination conditions.

Finally, the target melamines **4a**, **4b** were prepared according to our standard procedure [2]: it consisted of adding portionwise the clorodiamino-*s*-triazines **3a**, **3b** to an excess of piperazine dissolved in a refluxing 1,4-dioxanic K_2CO_3 suspension. As expected, due to their basicity and polarity, melamines **4a**, **4b** could not be eluted on silica gel. Thus, after complete removal of 1,4-dioxane, they were isolated by direct crystallisation from cooled water which completely discarded the excess of piperazine. Subsequent crystallisations from appropriate solvents provided pure analytical samples of **4a** and **4b**. Nevertheless, we were suspicious that the quantitative results in the synthesis of melamines **4a** and **4b** disclosed rather their partial solubility in water than the yield of aminations which occurred quantitatively with regard to the complete disappearance of the starting **3a**, **3b** (TLC monitoring).

Except **2b**, total NMR assignment of new compounds **3a**, **3b**, **4a** and **4b** took into account their complex four terms diastereomerism, occurring at room temperature, promoted by the restricted rotation about the C(*s*-triazine)-N(exocyclic) bonds following the normal lpN→π(*s*-triazine) conjugation (Scheme 3) [17]. A typical example is given in Figure 1.

24
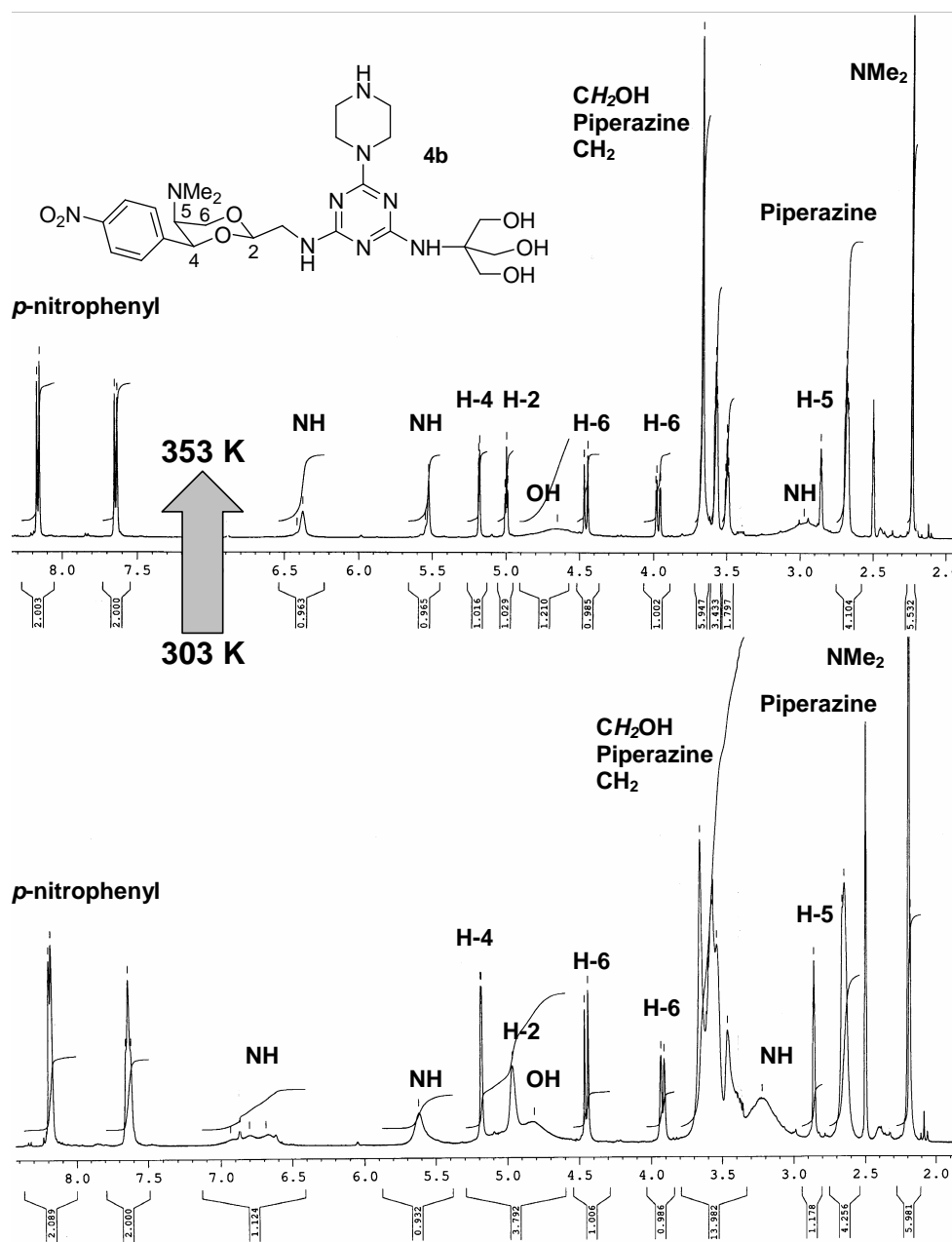
Figure 1. ^{1}H DNMR evolution of compound **4b** on 500 MHz timescale ([D$_6$]-DMSO)

R^1 = Cl: R^2 = **DX** (**3a**), **Me$_2$N-DX-CH$_2$** (**3b**)
R^1 = piperazin-1-yl: R^2 = **DX** (**4a**), **Me$_2$N-DX-CH$_2$** (**4b**)
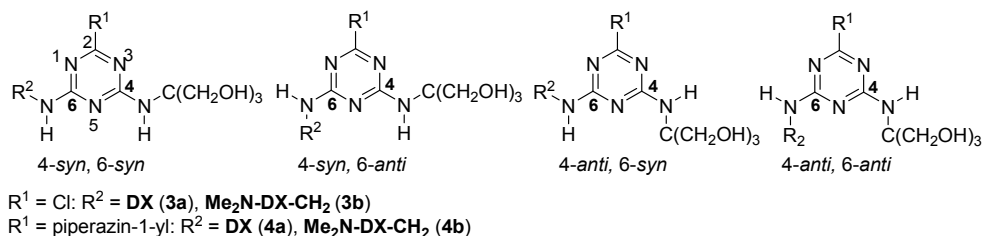
Scheme 3

For the present discussion, introducing for the first time rotational phenomena in *N*-substituted amino-*s*-triazines as a competition between an *open-chain unit* (*e.g.* TRIS) and a *closed chain unit* (Scheme 1), we will limit it to some preliminary remarks only:

a) As shown in Figure 1, upon heating, at 353 K melamine **4b** reached complete flexibility with respect to the bonds C(*s*-triazine)-N(exocyclic). It involved both serinolic units, the *open-chain* (TRIS) and the *closed chain* one (**Me$_2$N-DX-CH$_2$NH**).

b) In the same ^{1}H DNMR conditions, melamine **4a** displayed some residual decoalescence of the signals assigned to protons *p*-nitrophenyl and H-5-e (see **EXPERIMENTAL PART**). It was but almost completely deblocked at 353 K. This nuanced difference between ^{1}H DNMR behaviours of the two serinolic melamines we rationalised recently as steric hindrance in the transition state of the rotational phenomena: it was less crowded in the case of the equatorial anchorage of the amino-1,3-dioxane **1b** on **4b** than the axial one of **1a** on **4a** [1].

c) If the *s*-triazine ring was more π-defficient, *e.g.* due to the presence of the electro-withdrawing chlorine atom linked at C-2 (precursors **3a**, **3b**), the bond order C(*s*-triazine)-N(exocyclic) obviously increased. Hence, the frozen rotamerism about these connections was better exhibited by the chlorodiamino-*s*-triazines **3a** and **3b** (Scheme 3, Figure 2). At 353 K, **3b** was a completely freely rotating structure meanwhile for **3a** one can appreciate two different speed rotational motions:

- the *open-chain serinolic unit* as a freely rotating fragment about the bond C(*s*-triazine)-N(TRIS).

- the *closed chain serinolic unit* in a slow exchange status with respect to rotation regarding the bond C(*s*-triazine)-N(axial-**DX**), mediating unequal populations of rotamers.

26
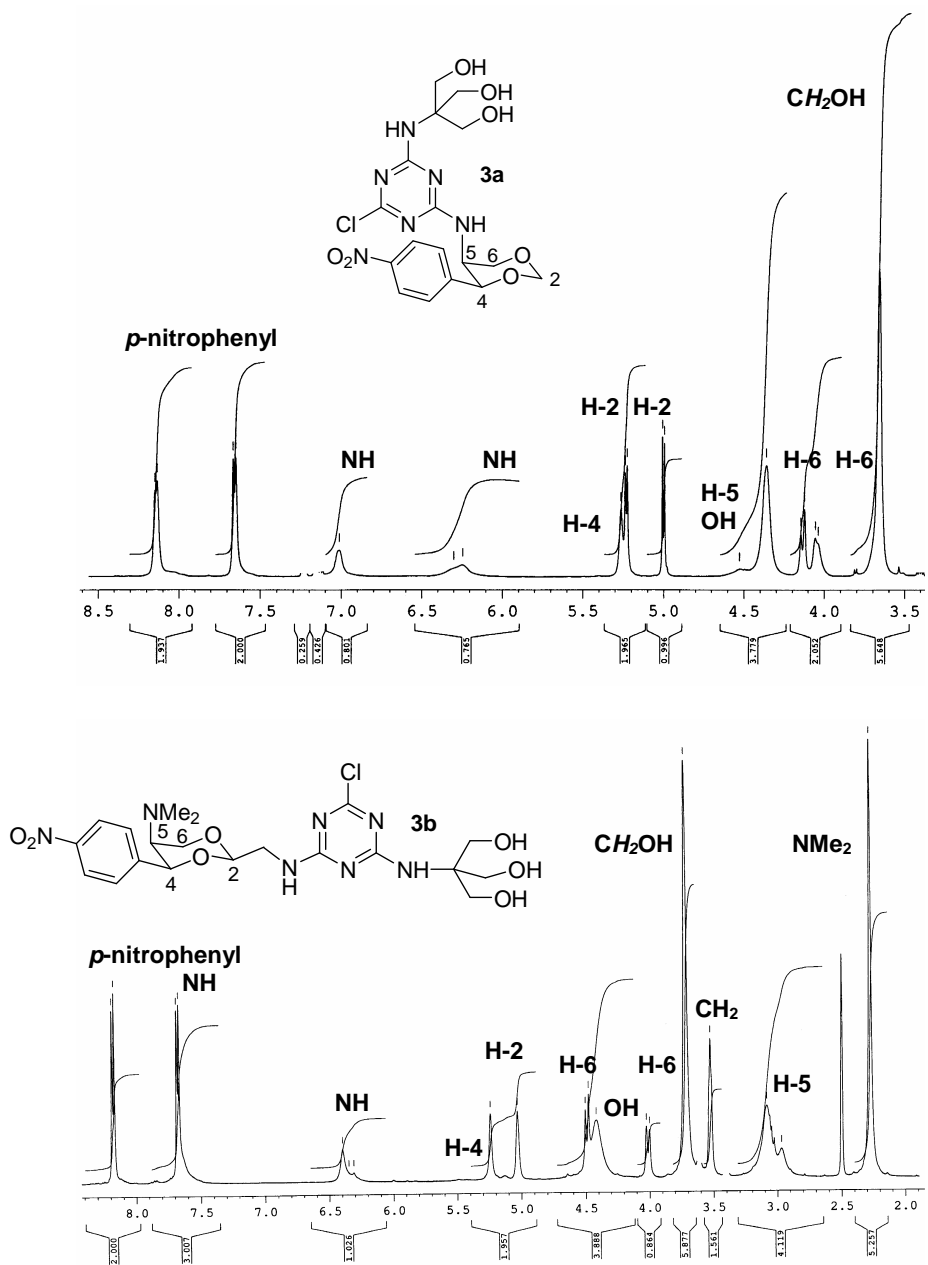
Figure 2. ^{1}H NMR spectra ok compounds 3a and 3b **(**353 K, 500 MHz, [D$_6$]DMSO)

27

CONCLUSIONS

Elaborated *N*-substituted melamines with *open-chain* vs. *closed chain serinolic units* together with a piperazin-1-yl fragment were available rapidly by applying one-pot procedures on cyanuric chloride. The first nucleophile replacing the *s*-triazine chlorine should be to most solvated one, hence the less reactive. The existence of a piperazin-1yl group recommends our compounds as attractive building-blocks in iterativesynthesis directed to dendritic structures. Restricted rotations about the partial double bonds C(*s*-triazine)-N(exocyclic) were encountered. They can be modulated by i) the *open vs. closed chain* nature of the two serinolic fragments substituting amino functionality in melamines and ii) axial vs. equatorial anchorage of the *closed chain serinolic unit* on the *s*-triazine skeleton. The full report on the observed phenomena and other representative examples are in progress.

EXPERIMENTAL SECTION

General. Melting points are uncorrected; they were carried out on ELECTROTHERMAL® instrument. Conventional NMR spectra were recorded on a Brucker® AM 300 instrument operating at 300 and 75 MHz for ^{1}H and ^{13}C nuclei respectively. A Brucker® DMX500 instrument was used for ^{1}H DNMR Experiments. All NMR spectra were measured in anhydrous commercially available deuterated solvents. No SiMe$_4$ was added; chemical shifts were measured against the solvent peak. All chemical shifts (δ values) are given throughout in ppm; all coupling patterns ($^nJ_{H,H}$ values) are given throughout in Hz.TLC was performed by using aluminium sheets with silica gel 60 F$_{254}$ (Merck®); flash column chromatography was conducted on Silica gel Si 60 (40–63 μm, Merck®). IR spectra were performed on a Perkin-Elmer® Paragom FT-IR spectrometer. Only relevant absorptions are listed [throughout in cm^{-1}: weak (w), medium (m) or (s) strong]. Microanalyses were performed on a Carlo Erba® CHNOS 1160 apparatus. Mass spectra (MS) were recorded on a Brucker® Esquire Instrument. Specific rotations were measured on a Polamat A® Karl Zeiss Jena Instrument.

Note 1

Specific abbreviations used in description of NMR spectra: *p*-NPh (*p*-nitrophenyl), DX (1,3-dioxane ring of type **DX-NH$_2$** or **Me$_2$N-DX-CH$_2$NH$_2$**), pip. (piperazin-1-yl), *s*-T (*s*-triazine).

Note 2

The NMR description of compounds exhibiting frozen rotamers at room temperature was made by considering them as one global structure. Multiple values as chemical shifts and coupling constants for the same labelled

^{1}H or ^{13}C position means mixture of rotamers, as described in Scheme 3. Some specific abbreviations were used: bd (broad doublet) and bm (broad multiplet).

2,4-Dichloro-6-{[(1,3-dihydroxy-2-(hydroxymethyl)prop-2-yl]amino}-*s*-triazine (2b) (86%) white crystalline powder, mp 164–165 ^{o}C (direct trituration from Et$_2$O). [Found C 30.89, H 4.12, N 20.66; C$_7$Cl$_2$H$_{10}$N$_4$O$_3$ (269.09) requires C 31.24, H 3.75, N 20.82%). R_f (50% ligroin/acetone) = 0.80. IR (KBr): ν = 3372 (s), 3094 (s), 2957 (m), 2899 (m), 1751 (w), 1690 (w), 1563 (s), 1413 (s), 1332 (m), 1232 (m), 1161 (m), 1075 (m), 1051 (m), 1016 (m), 958 (m), 858 (m), 797 (m), 638 (w), 605 (w) cm^{-1}. ^{1}H NMR (300 MHz, [D$_6$]DMSO) δ_H = 8.05 (s, 1 H, NH), 4.60 (bs, 3 H, CH$_2$O*H*) 3.62 (s, 6 H, C*H*$_2$OH) ppm. ^{13}C NMR (75 MHz, [D$_6$]DMSO) δ_C = 168.8, 168.2 (2 C, C-2, -4, *s*-T), 165.3 (1 C, C-6, *s*-T), 64.0 (1 C, C-2, TRIS), 58.3 (3 C, CH$_2$OH, TRIS) ppm. MS (DCI, +200 eV, NH$_3$): *m/z* (%) = 269 (100) [M$^+$], 210 (12),192 (20), 140 (25), 122 (33), 104 (62), 88 (90).

*Typical procedure for the synthesis of compounds **3a** and **3b** in a one-pot procedure. Preparation of compound **3a**.*
To anh. K$_2$CO$_3$ (1.38 g, 100%, 10 mmol) suspended in anh. THF (100 mL), TRIS (1.21 g 100%, 10 mmol) was added with vigorous stirring. The resulted suspension was cooled at -15 ^{o}C when cyanuric chloride (1.84 g, 100%, 10 mmol) as clear anh. THF (25 mL) solution was rapidly injected. The reaction mixture was let gently to reach room temperature and was kept as such for additional 24 hrs. with stirring. After this period, TLC monitoring indicated the intermediate 2,4-dichloro-6-{[1,3-dihydroxy-2-(hydroxymethyl)prop-2-yl]amino}-*s*-triazine **2b** as a single spot (eluent acetone: ligroin 2:1, R_f = 0.80). Freshly prepared (4*S*,5*S*)-4-(4- nitrophenyl)-1,3-dioxane (**1a**) (2.24 g 100%, 10 mmol and anh. K$_2$CO$_3$ (1.38 g, 100%, 10 mmol) were added and the reaction mixture was heated at reflux (65 ^{o}C) for 9 hrs (TLC monitoring, eluent toluene : isopropanol 2:1 v/v, R_f = 0.75). When **1a** and **2b** were detected in small traces only, the reaction mixture was cooled at room temperature. Minerals were filtered off and well washed with anh. THF. The organic filtrate was evaporated under reduced pressure to dryness and the resulted oil was twice crystallised from THF/Et$_2$O at -20 ^{o}C affording 3.61 g **3a** (79% yield with respect to cyanuric chloride). Optional purification of **3a**: column chromatography, eluent toluene : isopropanol 2:1 v/v.

2-Chloro-4-{[1,3-dihydroxy-2-(hydroxymethyl)prop-2-yl]amino}-6-{[(4*S*, 5*S*)-4-(4-nitrophenyl)-1,3-dioxan-5-yl]amino}-*s*-triazine (3a) (79%) white crystalline powder, mp 109.0 – 110.2 ^{o}C (flash column chromatography, eluent toluene: *i*-PrOH 2:1 v/v R_f = 0.70 or ligroin : acetone 1.5:2 v/v R_f = 0.60). [Found: C, 45.04; H, 4.55; N, 18.18; C$_{17}$H$_{21}$ClN$_6$O$_7$ (456.116) requires: C, 44.69;

H, 4.63; N, 18.40%]. IR ν_{max} (KBr) = 3369 (s), 2950 (m), 2865 (m), 1586 (s), 1519 (s), 1418 (m), 1387 (m), 1347 (s), 1243 (m), 1175 (s), 1096 (s), 1026 (s), 967 (m), 852 (w), 804 (m), 743 (m), 711 (m), 593 (w) cm^{-1}. ^{1}H NMR (500 MHz, [D$_6$]DMSO, 303 K) δ_H = 8.18, 8.14 (2 H, 2 × d, $^3J_{H,H}$ = 8.5, 9.5 Hz resp., H-3, -5, p-NPh), 7.67, 7.64 (2 H, 2 × d, $^3J_{H,H}$ = 8.5, 9.0 Hz resp., H-2, -6, p-NPh), 7.52, 7.50 (1 H, 2 × d, $^3J_{H,H}$ = 9.5, 9.5 Hz resp., DX-NH), 6.57, 6.50, 6.27, 6.21 (1 H, 4 × bs, TRIS-NH), 5.29, 5.25 (1 H, 2 × s, H-4-a, DX), 5.22 (1 H, d, $^2J_{H,H}$ = 6.0 Hz, H-2-e, DX), 4.98, 4.95 (1 H, d, s resp., $^2J_{H,H}$ = 6.0 Hz, H-2-a, DX), 4.66, 4.50 – 4.46 (3 H, t, m resp., $^3J_{H,H}$ = 5.5 Hz, CH$_2$OH), 4.36, 4.34, 4.32, 4.30 (1 H, 4 × d, $^3J_{H,H}$ = 10.0, 10.5, 10.5, 9.0 Hz resp., H-5-e, DX), 4.13 – 3.94 (2 H, m, H-6-e, -a, DX), 3.68 – 3.58 (6 H, m, CH_2OH) ppm ; ^{1}H NMR (500 MHz, [D$_6$]DMSO, 353 K) δ_H = 8.14 (2 H, bd, $^3J_{H,H}$ = 7.5 Hz, H-3, -5, p-NPh), 7.65 (2 H, d, $^3J_{H,H}$ = 7.5 Hz, H-2, -6, p-NPh), 7.01(1 H, bs, DX-NH), 6.30, 6.24 (1 H, 2 × bs, TRIS-NH), 5.27 (1 H, bs, H-4-a, DX), 5.23 (1 H, d, $^2J_{H,H}$ = 6.0 Hz, H-2-e, DX), 5.00, 4.95 (1 H, d, $^2J_{H,H}$ = 6.0 Hz, H-2-a, DX), 4.53, 4.36 (3 H, 2 × bs, CH$_2$OH), 4.36 (1 H, bs, H-5-e, DX), 4.14 (1 H, d, $^2J_{H,H}$ = 11.5 Hz, H-6-e, DX), 4.05 (1 H, bd, $^2J_{H,H}$ = 9.5 Hz, H-6-a, DX), 3.66 (6 H, bs, CH_2OH) ppm ; ^{13}C NMR (75 MHz, [D$_6$]DMSO, 298 K) δ_C = 167.8, 167.6 (1 C, C-2, s-T), 165.4, 165.2, 165.0, 164.9 (2 C, C-4, -6, s-T), 147.1 (1 C, C-4, p-NPh), 146.6 (1 C, C-1, p-NPh), 127.7, 127.6, 127.4 (2 C, C-3, -5, p-NPh), 123.4, 123.2 (2 C, C-2, -6, p-NPh), 93.8 (1 C, C-2, DX), 78.6, 78.1, 78.0 (1 C, C-4, DX), 70.3, 69.9 (1 C, C-6, DX), 62.4, 62.3, 62.1 (3 C, CH$_2$OH), 60.1, 59.6, 59.4 (1 C, C-2, TRIS), 49.7, 49.3, 49.2 (1 C, C-5, DX) ppm. MS (DCI positive, 200 eV, isobutane), m/z (rel. int. %): 513[M$^+$ + HC(CH$_3$)$_3$ − 2 H] (20), 495 [M$^+$] (< 10), 457 (100), 421 (< 10), 225 (< 10), 140 (10), 104 (< 10), 93 (< 10). $[\alpha]_D^{20}$ = -31.0 (0.5% THF).

2-Chloro-4-{[1,3-dihydroxy-2-(hydroxymethyl)prop-2-yl]amino}-6-{[(2R, 4S,5S)-5-(dimethylamino)-4-(4-nitrophenyl)-1,3-dioxan-2-yl]methylami-no}-s-triazine (3b) (67%) yellow crystalline powder, mp 138.0 – 140.5 ^{o}C (flash column chromatography, eluent ligroin : acetone 1:2.5 v/v, R_f = 0.50). [Found: C, 47.04; H, 5.15; N, 18.89; C$_{20}$H$_{28}$ClN$_7$O$_7$ (513.174) requires: C, 46.74; H, 5.49; N, 19.08%]. IR ν_{max} (KBr) = 3369 (s), 2945 (m), 2876 (m), 1583 (s), 1520 (s), 1460 (m), 1412 (m),1348 (s), 1154 (m), 1113 (m), 1054 (s), 1014 (m), 852 (w), 804 (m), 710 (m), 570 (w) cm^{-1}. ^{1}H NMR (500 MHz, [D$_6$]DMSO, 303 K) δ_H = 8.20 (2 H, d, $^3J_{H,H}$ = 7.8 Hz, H-3, -5, p-NPh), 8.00, 7.94, 7.92 (1 H, 3 × t, $^3J_{H,H}$ = 4.8, 6.0, 6.0 Hz resp., DX-NH), 7.67 (2 H, d, $^3J_{H,H}$ = 7.5 Hz, H-2, -6, p-NPh), 6.64, 6.60, 6.56, 6.28 (1 H, 4 × s, TRIS-NH), 5.25, 5.23 (1 H, 2 × bs, H-4-a, DX), 5.02 – 4.98 (1 H, m, H-2-a, DX), 4.68 (1 H, t, $^3J_{H,H}$ = 5,5 Hz, CH$_2$OH), 4.57 – 4.48 (2 H, m, CH$_2$OH), 4.57 – 4.48 (1 H, m, H-6-e, DX), 3.97, 3.95 (1 H, 2 × bs, H-6-a, DX), 3.68 – 3.65, 3.61 – 3.58 (6 H,

$2 \times$ m, CH_2OH), 3.49 – 3.46 (2 H, m, CH_2NH), 2.93 (1 H, bs, H-5-e, DX), 2.23 (6 H, bs, NMe$_2$) ppm ; ^{1}H NMR (500 MHz, [D$_6$]DMSO, 353 K) δ_H = 8.18 (2 H, d, $^3J_{H,H}$ = 8.5 Hz, H-3, -5, p-NPh), 7.68 (2 H, d, $^3J_{H,H}$ = 8.5 Hz, H-2, -6, p-NPh), 7.68 (1 H, bs, DX-NH), 6.39 (1 H, bs, TRIS-NH), 5.24 (1 H, bs, H-4-a, DX), 5.03 (1 H, bs, H-2-a, DX), 4.49 (1 H, d, $^2J_{H,H}$ = 12.0 Hz, H-6-e, DX), 4.42 (3 H, bs, CH$_2$OH), 4.01 (1 H, d, $^2J_{H,H}$ = 12.0 Hz, H-6-a, DX), 3.72 (6 H, s, CH_2OH), 3.53 (2 H, s, CH_2NH), 2.97 (1 H, s, H-5-e, DX), 2.27 (6 H, s, NMe$_2$) ppm ; ^{13}C NMR (75 MHz, [D$_6$]DMSO, 298 K) δ_C = 168.2, 167.7 (1 C, C-2, s-T), 165.7, 165.2 (2 C, C-4, -6, s-T), 146.7 (2 C, C-1, -4, p-NPh),126.9 (2 C, C-3, -5, p-NPh), 123.2 (2 C, C-2, -6, p-NPh), 99.2 (1 C, C-2, DX), 80.5 (1 C, C-4, DX), 67.4, 65.3, 64.4 (1 C, C-6, DX), 62.5, 62.4, 59.6 (3 C, CH$_2$OH), 60.2, 60.0 (1 C, C-2, TRIS), 58.5 (1 C, C-5, DX), 44.6, 44.2 (1 C, CH$_2$NH), 43.7 (2 C, NMe$_2$) ppm. MS (DCI positive, 200 eV, isobutane), m/z (rel. int. %): 514 [M$^+$ + 1] (25), 310 (< 5), 292 (< 5), 278 (5), 241 (< 5), 178 (100), 166 (<5), 140 (20), 116 (11), 104 (20), 87 (18), 73 (<5). [α]$_D^{25}$ = +137.8 (0.5% THF).

Typical procedure for the synthesis of compounds **4a** *and* **4b**. *Preparation of compound* **4a**.

Anh. piperazine (1.137 g, 13.2 mmol) was dissolved in anh. 1,4-dioxane (75 mL) then anh. K$_2$CO$_3$ (0.455 g, 3.29 mmol) was added. The resulted suspension was heated at reflux (102 ^{o}C) with vigorous stirring. At this temperature, 2-chloro-4-{[1,3-dihydroxy-2-(hydroxymethyl)prop-2-yl]amino}-6-{[(4S,5S)-4-(4-nitrophenyl)-1,3-dioxan-5-yl]amino}-s-triazine **3a** (1.500 g, 3.29 mmol) as anh. 1,4-dioxane (25 mL) solution was added portionwise as 5 mL each 2 hrs. After the addition of each portion, within 2 hrs., TLC monitoring indicated the complete absence of the starting **3a** (eluent toluene : isopropanol 2:1 v/v). The reaction mixture was cooled at room temperature when minerals were filtered off and well washed with anh. 1,4-dioxane (optionally, anh. THF). The organic filtrate was evaporated to dryness under reduced pressure to yield an oily residue (2.158 g). This was taken with cooled water (20 mL) with vigorous stirring to provide a yellowish suspension. The solid was filtered off, well washed with cooled water then dried at room temperature. Supplementary crystallisation from ether at -20 ^{o}C provided the pure product **4a** (1.170 g, 70% yield with respect to **3a**).

1-{4-{[1,3-dihydroxy-2-(hydroxymethyl)prop-2-yl]amino}-6-{[(4S,5S)-4-(4-nitrophenyl)-1,3-dioxan-5-yl]amino}-s-triazin-2-yl}piperazine (4a) (70%) yellowish crystalline powder, mp 119 – 124 ^{o}C (Et$_2$O). [Found: C, 50.03; H, 5.88; N, 21.95; C$_{21}$H$_{30}$N$_8$O$_7$ (506.22) requires: C, 49.80; H, 5.97; N, 22.12%]. IR ν_{max} (KBr) = 3392 (m), 2493 (m), 2856 (m), 1549 (s), 1504 (s), 1446 (m), 1346 (s), 1273 (m) 1174 (m), 1105 (m), 1025 (m), 872 (w), 852 (w), 809 (m), 744 (w), 711 (w), 584 (w) cm^{-1}. ^{1}H NMR (500 MHz, [D$_6$]DMSO, 303 K) δ_H = 8.18, 8.12 (2 H, $2 \times$ bd, $^3J_{H,H}$ = 7.0, 5.5 Hz resp., H-3, -5, p-NPh), 7.64, 7.62 (2 H,

2 × d, $^3J_{H,H}$ = 9.0, 9.0 Hz resp., H-2, -6, *p*-NPh), 5.92, 5.81 (1 H, bs, d, $^3J_{H,H}$ = 6.5 Hz, DX-N*H*), 5.57, 5.49 (1 H, 2 × bs, TRIS-N*H*), 5.28 - 5.21 (2 H, m, H-2-e, H-4-a, DX), 4.96 (1 H, d, $^2J_{H,H}$ = 6.0 Hz, H-2-a, DX), 4.43 - 4.24 (1 H, bm, H-5-e, DX), 4.09 – 3.97 (2 H, bm, H-6-e, -a, DX), 3.59 (6 H, bm, C*H₂*OH), 3.45 (7 H, bs, CH₂O*H*, H-2, -6, pip.), 2.64 – 2.60 (5 H, bm, H-3, -5, NH, pip.) ppm ; ^{1}H NMR (500 MHz, [D₆]DMSO, 353 K) δ_H = 8.12 (2 H, d, $^3J_{H,H}$ = 8.5 Hz, H-3, -5, *p*-NPh), 7.63 (2 H, d, $^3J_{H,H}$ = 8.5 Hz, H-2, -6, *p*-NPh), 5.61 (1 H, d, $^3J_{H,H}$ = 9.5 Hz, DX-N*H*), 5.43 (1 H, s, TRIS-N*H*), 5.23 (2 H, s, d, $^2J_{H,H}$ = 5.8 Hz, H-4-a, H-2-e, DX), 5.00 (1 H, d, $^2J_{H,H}$ = 5.8 Hz, H-2-a, DX), 4.40 (1 H, bd, $^3J_{H,H}$ = 9.5 Hz, H-5-e, DX), 4.11 (1 H, d, $^2J_{H,H}$ = 11.0 Hz, H-6-e, DX), 4.02 (1 H, d, $^2J_{H,H}$ = 11.0 Hz, H-6-a, DX), 3.62 (6 H, s, C*H₂*OH), 3.46 (4 H, t, $^3J_{H,H}$ = 5.0 Hz, H-2, -6, pip.), 3.30 (3 H, bs, CH₂O*H*), 2.65 (5 H, s, t, $^3J_{H,H}$ = 5.0 Hz, H-3, -5, NH, pip.) ppm; ^{13}QC NMR (75 MHz, [D₆]DMSO, 298 K) δ_C = 165.5, 165.4, 165.2, 165.0 (2 C, C-4, -6, *s*-T), 164.2 (1 C, C-2, *s*-T), 146.9 (2 C, C-1, -4, *p*-NPh), 127.4, 127.1 (2 C, C-3, -5, *p*-NPh), 123.3, 123.1 (2 C, C-2, -6, *p*-NPh), 93.9 (1 C, C-2, DX), 78.8, 78.4 (1 C, C-4, DX), 70.7, 70.5 (1 C, C-6, DX), 61.3, 61.0 (4 C, C-2, CH₂OH, TRIS), 48.8 (1 C, C-5, DX), 45.4 (2 C, C-2, -6, pip.), 43.9 (2 C, C-3, -5, pip.) ppm. MS (DCI positive, 200 eV, isobutane), m/z (rel. int. %): 563 [M$^+$ + HC(CH₃)₃ - 2] (< 10), 507 [M$^+$ + 1] (100), 489 (10), 477 (10), 404 (10), 282 (15), 225 (10), 208 (35), 178 (25), 165 (12), 115 (< 10), 104 (20), 87 (75). $[\alpha]_D^{20}$ = -16.0 (0.5% THF).

1-{4-{[1,3-dihydroxy-2-(hydroxymethyl)prop-2-yl]amino}-6-{[(2*R*,4*S*,5*S*) -5-(dimethylamino)-4-(4-nitrophenyl)-1,3-dioxan-2-yl]methylamino}-*s*-triazin-2-yl}piperazine (4b) (65%) yellow crystalline powder, mp 145 – 147 ºC (Et₂O) [Found: C, 50.97; H, 6.88; N, 22.05; C₂₄H₃₇N₉O₇ (563.282) requires: C, 51.15; H, 6.62; N, 22.37%]. IR ν_{max} (KBr) = 3298 (m), 2940 (m), 2858 (m), 1551 (s), 1515 (s), 1446 (s),1347 (s), 1297 (m), 1151 (m), 1112 (m), 1054 (m), 1015 (m), 852 (m), 809 (m), 710 (w), 578 (w) cm^{-1}. ^{1}H NMR (500 MHz, [D₆]DMSO, 303 K) δ_H = 8.18 (2 H, d, $^3J_{H,H}$ = 7.5 Hz, H-3, -5, *p*-NPh), 7.64, 7.63 (2 H, 2 × d, $^3J_{H,H}$ = 9.0 Hz, H-2, -6, *p*-NPh), 6.93, 6.80, 6.69 (1 H, 3 × bs, DX-N*H*), 5.62 (1 H, bs, TRIS-N*H*), 5.19 (1 H, d, $^3J_{H,H}$ = 2.5 Hz, H-4-a, DX), 4.97 (1 H, bs, H-2-a, DX), 4.81 (3 H, bs, CH₂O*H*), 4.45 (1 H, d, $^2J_{H,H}$ = 11.3 Hz, H-6-e, DX), 3.92 (1 H, d, $^2J_{H,H}$ = 11.3 Hz, H-6-a, DX), 3.66 - 3.54 (10 H, bm, C*H₂*OH, H-2, -6, pip.), 3.40 (2 H, bs, C*H₂*NH), 3.22 (1 H, bs, NH, pip.), 2.86 (1 H, dd, $^3J_{H,H}$ = 2.5 Hz, H-5-e, DX), 2.66 (4 H, m, H-3, -5, pip.), 2.20, 2.18 (6 H, m, NMe₂) ppm ; ^{1}H NMR (500 MHz, [D₆]DMSO, 353 K) δ_H = 8.17 (2 H, d, $^3J_{H,H}$ = 8.5 Hz, H-3, -5, *p*-NPh), 7.64 (2 H, d, $^3J_{H,H}$ = 8.5 Hz, H-2, -6, *p*-NPh), 6.41 (1 H, bs, DX-N*H*), 5.53 (1 H, bs, TRIS-N*H*), 5.19 (1 H, d, $^3J_{H,H}$ = 3.0 Hz, H-4-a, DX), 5.00 (1 H, dd, $^3J_{H,H}$ = 4.5 Hz, H-2-a, DX), 4.65 (3 H, bs, CH₂O*H*), 4.46 (1 H, d, $^2J_{H,H}$ = 12.5 Hz, H-6-e, DX), 3.97 (1 H, dd, $^2J_{H,H}$ = 12.5 Hz, $^3J_{H,H}$ = 3.0 Hz, H-6-a, DX), 3.66 (6 H, s, C*H₂*OH), 3.57 (4 H, t, $^3J_{H,H}$ = 4.3 Hz, H-2, -6,

pip.), 3.50 (2 H, dd, $^3J_{H,H}$ = 4.5 Hz, CH_2NH), 2.97 (1 H, bs, NH, pip.), 2.86 (1 H, dd, $^3J_{H,H}$ = 2.8 Hz, H-5-e, DX), 2.68 (4 H, m, H-3, -5, pip.), 2.23 (6 H, s, NMe$_2$) ppm ; ^{13}C NMR (75 MHz, [D$_6$]DMSO, 298 K) δ_C = 165.8 (1 C, C-4, -6, s-T), 164.4 (1 C, C-2, s-T), 148.8 (1 C, C-4, p-NPh), 146.5 (1 C, C-1, p-NPh), 126.9, 125.3, 123.1 (4 C, C-2, -3, -5, -6, p-NPh), 99.6 (1 C, C-2, DX), 80.0 (1 C, C-4, DX), 65.3, (1 C, C-6, DX), 64.3 (3 C, CH$_2$OH), 61.4, 61.3 (1 C, C-2, TRIS), 58.4 (1 C, C-5, DX), 46.3, 46.1 (2 C, C-2, -6, pip.), 45.8 (2 C, C-3, -5, pip.), 44.3 (1 C, CH$_2$NH), 43.7 (2 C, NMe$_2$) ppm. MS (DCI positive, 200 eV, isobutane), m/z (rel. int. %): 620 [M$^+$ + HC(CH$_3$)$_3$ - 2] (< 10), 564 [M$^+$ + 1] (65), 449 (28), 380 (55), 300 (10), 282 (15), 221 (< 10), 178 (100), 165 (25), 148 (10), 104 (45), 87 (35). [α]$_D^{25}$ = +140.8 (0.5% THF).

ACKNOWLEDGMENTS

REFERENCES

1. M. Fazekas, M. Pintea, P. Lameiras, A. Lesur, C. Berghian, I. Silaghi-Dumitrescu, N. Plé, M. Darabantu, *Eur. J. Org. Chem.*, **2008**, 2473.

2. M. Darabantu, M. Pintea, M. Fazekas, P. Lameiras, C. Berghian, I. Delhom, I. Silaghi-Dumitrescu, N. Plé, A. Turck, *Letters in Organic Chemistry*, **2006**, *3*(12), 905.

3. C. Berghian, P. Lameiras, L. Toupet, E. Condamine, N. Plé, A. Turck, C. Maiereanu, M. Darabantu, *Tetrahedron*, **2006**, *62*(31), 7319.

4. M. Fazekas, M. Darabantu, M. Pintea, P. Lameiras, C. Bele, C. Berghian, N. Plé*, Heterocyclic Commun.*, **2006**, *12*(2), 151.

5. M. Pintea, M. Darabantu, M. Fazekas, P. Lameiras, C. Berghian, I. Delhom, C. Bele, N.Plé, *Heterocyclic Commun.*, **2006**, *12*(2), 135.

6. V. Lates, D. Gligor, M. Darabantu, L. M. Muresan, *J. Appl. Electrochem.*, **2007**, *37*(5), 631.

7. C. Bele, M. Darabantu, C. T. Matea, M. Pintea, M. Fazekas, C. Berghian, *Buletin USAMV-CN*, **2005**, *61*, 194.

8. C. Bele, M. Darabantu, E. Muntean, M. Pintea, M. Fazekas, C. Berghian, D. Lazar, *Buletin USAMV-CN* **2004**, *60*, 35-38, ISSN 1454.

9. D. A. Tomalia, *Aldrichimica Acta*, **2004**, *37*(2), 39.

10. M. B. Steffensen, E. E. Simanek, *Angew. Chem. Int. Ed.*, **2004**, *43*, 5178.

11. a) W. Zhang, D. T. Nowlan, L. M. Thomson, M. W. Lackowski, E. E. Simanek, *J. Am. Chem. Soc.*, **2001**, *123*, 8914; b) J. Lim, E. E. Simanek, *Molecular Pharmaceutics*, **2005**, *2*(4), 273; c) G. R. Newcome, J. Gross, C. N. Moorefield, B. D. Woosley, *Chem. Commun.*, **1997**, 515.

12. a) A. P. Umali, E. E. Simanek, *Org. Lett.*, **2003**, *5*(8), 1245; b) H. T. Chen, M. F. Neerman, A. R. Parrish, E. E. Simanek, *J. Am. Chem. Soc.*, **2004**, *126*, 10044. c) L. –L. Lai, L. –Y. Wang, C-H. Lee, C. Y. Lin, K. –L. Cheng, *Org. Lett.*, **2006**, *8*(8), 1541; d) E. J. Acosta, S. O. Gonzalez, E. E. Simanek, *J. Polym. Sci. Part A.*, **2005**, *43*, 168.

13. a) W. Zhang, S. O. Gonzalez, E. E. Simanek, *Macromolecules*, **2002**, *35*, 9015; b) E. Hollink, E. E. Simanek, *Org. Lett.*, **2006**, *8*(11), 2293; c) M. F. Neerman, W. Zhang, A. R. Parrish, E. E. Simanek, *Int. J. Pharm.*, **2004**, *281*, 129; d) L. –L. Lai, C. –H. Lee, L. –Y. Wang, K. L. Cheng, H. –F. Hsu, *J. Org. Chem.*, **2008**, *73*, 485.

14. M. Darabantu, C. Maiereanu, G. Plé, C. Berghian, E. Condamine and Y. Ramondenc, *Heterocyclic Commun.*, **2001**, *7*(6), 593.

15. a) R. Menicagli, C. Malanga, P. Peluso, *Synth. Commun.*, **1994**, *24*, 2153; b) S. Samaritani, P. Peluso, C. Malanga, R. Menicagli, *Eur. J. Org. Chem.*, **2002**, 1551.

16. a) E. L. Eliel, H. S. Wilen, *Stereochemistry of the Organic Compounds*; John Wiley & Sons, Inc. **1994**; pp. 1191, 696, 697, 21, 466. b) M. J. O. Anteunis, D. Tavernier, F. Borremans, *Heterocycles*, **1976**, *4*, 293.

17. a) I. Willner, J. Rosengaus, Y. Eichen, *J. Phys. Org. Chem.*, **1993**, *6*(1), 29; b) A. R. Katritzky, I. Ghiviriga, D. Oniciu, A. Barkock, *J. Chem. Soc. Perkin Trans. 2*, **1995**, 785; c) A. R. Katritzky, I. Ghiviriga, P. G. Steel, D. C. Oniciu, *J. Chem. Soc. Perkin Trans. 2*, **1996**, 443; d) S. A. Brewer, H. T. Burnell, I. Holpen, G. B. Jones, R. C. Willis, *J. Chem. Soc., Perkin Trans. 2* **1999**, *6*, 1231; e) H. E. Birkett, R. K. Harris, P. Hodgkinson, K. Carr, M. H. Charlton, J. C. Cherryman, A. M. Chippendale, R. P. Glover, *Magn. Reson. Chem.*, **2000**, *38*, 504; f) I. Ghiviriga, D. C. Oniciu, *Chem. Commun.*, **2002**, *22*, 2718; g) H. E. Birkett, J. C. Cherryman, A. M. Chippendale, J. S. O. Evans, R. K. Harris, M. James, I. J. King, G. McPherson, *Magn. Reson. Chem.*, **2003**, *41,* 324.

SONOCHEMICAL SYNTHESIS OF SOME CHALCONETRICARBONYLIRON(0) COMPLEXES

LUIZA GĂINĂ, ANDREEA IFTIMIA, MIHAI SURDUCAN, CASTELIA CRISTEA[*], LUMINIȚA SILAGHI-DUMITRESCU

ABSTRACT. Sonication was applied to provide energy for the chemical reaction between diiron nonacarbonyl and 1,3-di-(hetero)aryl-propenone derivatives. New chalcone tricarbonyliron(0) complexes were obtained and characterized by IR spectroscopy. Advantages of this synthetic method are related to short reaction times and good yields.

Keywords: chalconetricarbonyliron(0), heteroarylchalcone, sonochemistry, IR spectroscopy.

INTRODUCTION

Many applications of organometallic derivatives in synthetic chemistry were developed based on the capacity of steric and electronic properties of the ligands to modify the reactivity of metal complexes and thus to modulate their catalytic activity.

Several organic compounds were proved to form stable tricarbonyliron complexes and among these, a special attention was given to butadiene-tricarbonyliron [1-4] and heterodiene (-C=C-C=Y where Y=O, N) tricarbonyliron complexes [5-8], due to tunable donor/acceptor interactions between these π-ligands and low-valent metal center.

Diaryl-substituted α,β-unsaturated ketones (generic name chalcones) are such π-ligands which were proved to establish strong donor/acceptor interactions with iron(0). The first reported preparation of chalcone tricarbonyliron(0) compounds $(Fe(ch)(CO)_3$ where ch = benzylideneacetone, chalcone, 2'-hydroxychalcone, and 2,6-dibenzylidene-cyclohexanone), was a thermal procedure consisting of heating the enone with enneacarbonyldi-iron in toluene at 70-80 $^{\circ}$C, which afforded the complexes in moderate yields (≈30%), as air-stable crystalline solids. [7]. Several other chalcones, obtained by Claisen Schmitt condensation of acetophenone with various substituted benzaldehides, were also coordinated to iron(0) by heating at

---

[*] *Universitatea Babeş-Bolyai, Facultatea de Chimie şi Inginerie Chimică, Str. Kogălniceanu, Nr. 1, RO-400084 Cluj-Napoca, Romania, castelia@chem.ubbcluj.ro*

reflux with $Fe_2(CO)_9$ in ether solution for 16 h. The complexes were all obtained as orange-red air-stable solids in good to modest yields [9] and extensive structural studies were performed.

Applications of sonochemistry were reported in both homogeneous liquids and in heterogeneous liquid-solid systems. The chemical effect of ultrasound has proved to be extremely useful in the synthesis of a wide range of nanostructured materials [10], preparation of biomaterials (most notably protein microspheres) [11], etc. Even though the chemical effects of ultrasound do not come from a direct interaction with molecular species, the acoustic cavitation (consisting in the formation, growth and implosive collapse of bubbles in a liquid) serves as a mean of concentrating the diffuse energy of sound and thus, chemical reactions which require high energy can be performed in apparently mild conditions [12].

Thermal procedures affording $Fe(ch)(CO)_3$ complexes encouraged us to perform the sonication of diironnonacarbonyl in the presence of some chalcones prepared by the Claisen Schmitt condensation of acetophenone derivatives with (hetero)aromatic carboxaldehydes. In this paper we describe the synthesis of new 1,3-di-(hetero)aryl-propenone-tricarbonyliron(0) complexes by sonication.

RESULTS AND DISCUSSION

The sonochemistry of metal carbonyl compounds dissolved in organic liquids was first reported in 1981, by P. F. Schubert, J. W. Goodale and Suslick who performed the first sonochemistry study of discrete organometallic complexes and demonstrated the effects of ultrasound on metal carbonyls. Sonolysis of $Fe(CO)_5$ in alkane solvents causes the clusterification to $Fe_3(CO)_{12}$ but in the presence of added Lewis bases, sonochemical ligand substitution also occurs. Thermal decomposition of diiron nonacarbonyl appears at 100 ^0C according to scheme 1, but sonolysis of $Fe_2(CO)_9$ in decalin yields $Fe(CO)_5$ and finely divided iron at rates fast compared to $Fe_3(CO)_{12}$ formation [13].

$$Fe_2(CO)_9 \xrightarrow{\quad \Delta \quad} Fe(CO)_5 + Fe(CO)_4$$
$$\xrightarrow{\quad))) \quad} Fe(CO)_5 + Fe + 4CO$$
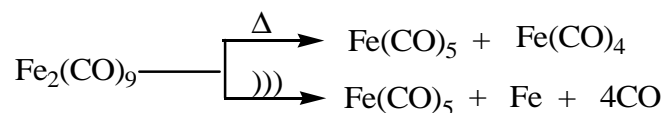
Scheme 1

Sonication of $Fe(CO)_5$ in the presence of ligands (abbreviated L) produces iron carbonyl derivatives $Fe(CO)_{5-n}L_n$ (n=1,2) according to the general mechanism shown in scheme 2 (L = phosphines or phosphates, [14]). The $Fe(CO)_4 L : Fe(CO)_3L_2$ ratio is dependent on ligand and its concentration.

1,3-*Bis*(*p*-methoxiphenyl)-propenone **1** and heteroaromatic chalcones containing phenothiazine units **2** [15] and thiazole units **3** [16] respectively, were subjected to sonication in an ultrasonic bath in the presence of diironnonacarbonyl; new $Fe(ch)(CO)_3$ complexes were thus obtained according to scheme 3.

$$Fe(CO)_5 \xrightarrow{\;)))\;} Fe(CO)_{5-n} + nCO$$

$$Fe(CO)_4 + L \longrightarrow Fe(CO)_4L$$

$$Fe(CO)_3 + L \longrightarrow Fe(CO)_3L$$

$$Fe(CO)_3L + L \longrightarrow Fe(CO)_3L_2$$

$$Fe(CO)_3L + CO \longrightarrow Fe(CO)_4L$$

$$Fe(CO)_4L + L \xrightarrow{\;)))\;} Fe(CO)_3L_2$$
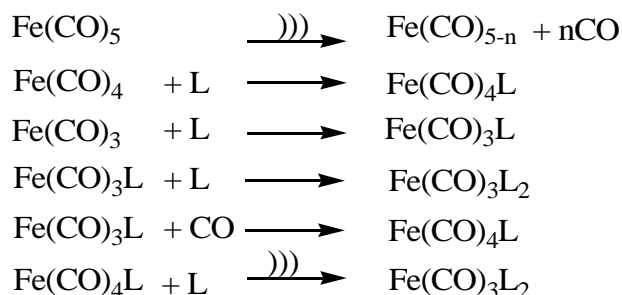
Scheme 2

Short reaction times were required for the preparation of $Fe(ch)(CO)_3$ complexes containing chalcones **1, 2a, 2b, 3**, in excellent to good yields. The sonication of heteroaromatic chalcones containing nitro-substituents in the aromatic rings (**2c, 2d**) was not succesfull in terms of complex preparation and produced the decomposition of the starting material. Table 1 shows the reaction characteristics for the preparation of $Fe(ch)(CO)_3$ complexes.

1 (Het)Ar = Ar = *p*-CH$_3$O-C$_6$H$_4$

2 (Het)Ar =

2a Ar = 2-naphthyl
2b Ar = *p*-CH$_3$O-C$_6$H$_4$
2c Ar = *p*-NO$_2$-C$_6$H$_4$
2d Ar = *m*-NO$_2$-C$_6$H$_4$

3 (Het)Ar = C$_6$H$_5$ Ar = -C$_6$H$_5$
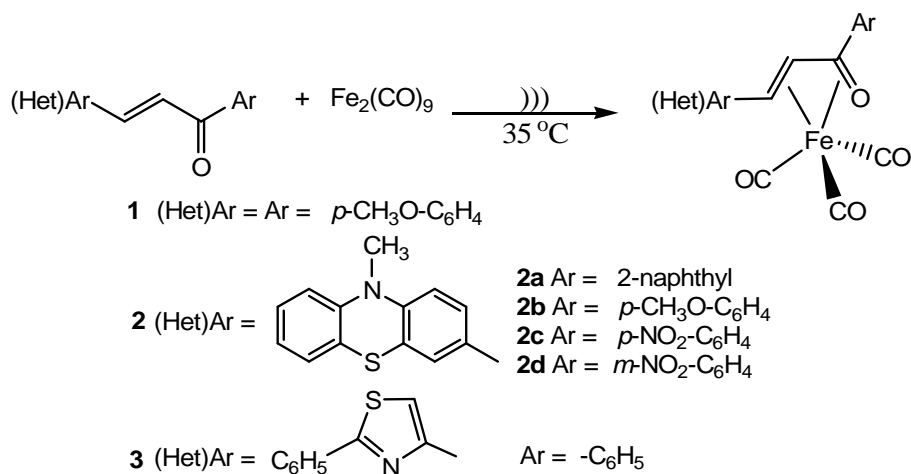
Scheme 3

The major bonding interactions between the α,β-unsaturated carbonyl unit in the chalcone and the iron(0)tricarbonyl fragment were rationalized in terms of the frontier molecular orbitals involved [**9**]. The theoretical calculations by Calhorda and Vichi [17] using the extended Huckel method illustrate that the bonding between the metal and the α,β-unsaturated carbonyl ligand is dominated by donation from filled orbitals π_1 and π_2 to vacant metal-centered orbitals and donation from a filled metal orbital to the vacant π_3-orbital of the ligand, while donation to π_4 is thought to be only a minor component. In solution, the complex is approximating C_{3V}-symmetry due to rapid rotation around the $Fe(CO)_3$ chalcone axis, an effect that was observed in the IR and $^{13}C\{^1H\}$ NMR reported spectra [9].

Table 1. The reaction characteristics for the preparation of $Fe(ch)(CO)_3$ complexes by sonication of chalcones with $Fe_2(CO)_9$

Chalcone	Sonication time [min]	Yields [%]
1	30	70
2a	45	55
2b	45	56
3	30	80
2c	60	0
2d	60	0

The IR spectra of **1-3** complexes were recorded. In agreement with the formulation as iron tricarbonyl derivatives their IR spectra show three strong v(CO) bands in the region 2100-1900 cm^{-l}. Strong bands in the region 1600-1700 cm^{-l} found in the spectra of the free chalcones disappeared on co-ordination. The recorded values for the stretching vibrations of CO units in the prepared $Fe(ch)(CO)_3$ complexes **1-3** are listed in table 2.

The position of the infrared bands due to the CO stretching vibrations in the structure of the $Fe(ch)(CO)_3$ was found to be finely tuned by the structure of the chalcone unit. The amount of electron density available at the metal center that may be donated into the antibonding orbitals of the carbon monoxide ligands may be approximated from the frequency of the infrared bands due to the CO stretching vibrations: thus, aromatic units containing substituents with net electron-withdrawing properties were proved to determine CO stretch bands situated at higher frequencies, whereas net electron-donating substituents result in bands at lower frequencies [9].

Table 2. IR spectroscopic data for the CO stretching bands in Fe(ch)(CO)$_3$ complexes**1-3**

Complex	υ_{co} (cm^{-1})
1	2085; 2022; 1987
2a	2050; 1993; 1964
2b	2049; 1983; 1957
3	2092; 2018; 1977

1-Aryl-3-phenothiazinyl-propenones **2** contain an extended π conjugated system which benefit from the electron-donor effect of the phenothiazine nucleus. As it can be seen from the values listed in table 2, the electron-donor properties of the phenothiazine moiety in complexes **2a, 2b** determines the lowest values for the CO stretching bands, whereas according to this criterion the 2-phenyl-thiazole unit in **3** appears to be less electron-donor.

CONCLUSIONS

An advantageous method for the synthesis of chalconetricarbonyl-iron(0) complexes appears to be the sonochemical π-ligand substitution which occurs when Fe$_2$(CO)$_9$ is treated with chalcones in organic solvents. As compared to previously reported thermal procedures employed for the synthesis of Fe(ch)(CO)$_3$ complexes, ultrasonic irradiation increased the yields and dramatically reduced the reaction time.

IR spectroscopy can be employed for the structural assignment of chalconetricarbonyliron(0)complexes based on the three strong absorption bands due to carbonyl stretching vibrations which appear in the characteristic region 2100-1900 cm^{-1}.

EXPERIMENTAL SECTION

Ultrasonic bath: Elma S15H
FT-IR spectrometer Bruker Vector 22
Merck reagents were used.

General procedure for sonication of chalcone and Fe$_2$(CO)$_9$

In a round-bottomed flask fitted with a condenser and a gas inlet, chalcone (1 mmol) was dissolved in dried dichloromethane and in the stirred solution nitrogen gas was bubbled for aprox. 5 minutes (until saturation was reached). 2.5 mmol Fe$_2$(CO)$_9$ were added carefully maintaining the nitrogen atmosphere. The reaction flask was placed in an ultrasonic bath and sonicated at 35 ^{0}C for several minutes (according to table 1). The product mixture was then filtered through celite using DCM as eluent and the solvent was removed *in vacuo*. The raw product was purified by column chromatography (silica gel; eluent ethyl-ether/petroleum-ether:1/4) and recrystallised from hexane, to give the complex as air relatively stable crystalline material.

η^4-((E)-1,3-di-(4-methoxiphenyl)-2-propen-1-one)-tricarbonyl-iron(0)
0.28 g (yields 70%) orange-yellow crystals m.p.= 90-91 ^{0}C
IR (cm^1): 2085, 2022, 1987, 1628, 1601, 1572, 1512, 1475, 1280, 1230, 1160, 1034, 839.

η^4-((E)-3-(10methyl-phenothiazin-3yl)-1-(2-naphthyl)-2-propen-1-one)-tricarbonyliron(0)
0.3 g (yields 55%) brown-red crystalls, m.p. = 95-96 ^{0}C
IR (cm^1): 2050, 1993, 1964, 1597, 1573, 1469, 1337, 1258, 749.

η^4-((E)-3-(10methyl-phenothiazin-3yl)-1-(4-methoxiphenyl)-2-propen-1-one)-tricarbonyliron(0)
0.28 g (yields 56%) brown-red crystalls, m.p.=149-150 ^{0}C
IR (cm^1): 2049, 1983, 1957, 1600, 1588, 1498, 1454, 1332, 1259, 810, 757, 738.

η^4-((E)-3-(2-phenyl-thiazol-4yl)-1-(4-phenyl)-2-propen-1-one)-tricarbonyl-iron(0)
0.34g (yields 80%) light yellow, m.p.86-88 ^{0}C
IR (cm^1): 2092, 2018, 1977, 1639, 1599, 1468, 1274, 1200, 763, 688.

ACKNOWLEDGMENTS

REFERENCES

1. H. Rheilem, A. Grubl, G. Hessling, O. Pfrengle, *Justus Liebigs Ann. Chem.* **1930**, 482, 161.

2. B.F. Hallam, P.L. Pauson, *J. Chem. Soc.* **1958**, 642.

3. R. Pettit, G.F. Emerson, *Adv. Organomet. Chem.* **1964**, 1, 1.

4. M.R. Churchill, R. Mason, *Adv. Organomet. Chem.* **1967**, 5, 93.

5. S. Otsuka, T. Yoshida, A. Nakanima, *Inorg. Chem.* **1967,** 6, 20.

6. H. tom Dieck, H. Bock, *J. Chem. Soc., Chem. Commun.* **1968**, 678.

7. A.M. Brodie, B.F.G. Johnson, P.L. Josty, J. Lewis, *J. Chem. Soc., Dalton. Trans.* **1972**, 2031.

8. D. Liebfritz, H. tom Dieck, *J. Organomet. Chem.* **1976**, 105, 255.

9. B. E. Moulton, A. K. Duhme-Klair, I. J. S. Fairlamb, J. M. Lynam, and A. C. Whitwood, *Organometallics*, **2007**, 26 (25), 6354.

10. K.S. Suslick in *Kirk-Othmer Encyclopedia of Chemical Technology*; 4th Ed. J. Wiley & Sons: New York, **1998**, vol. 26, 517.

11. K. S. Suslick, M. W. Grinstaff, *J. Am. Chem. Soc.*, **1990**, 112, 780.

12. K. S. Suslick, *Science*, **1990**, 247, 1439.

13. K. S. Suslick, P. F. Schubert and J. W. Goodale, *J. Am Chem. Soc.* **1981**, 103, 7342.

14. K. S. Suslick, J. W. Goodale, P. F. Schubert and H. H. Wang, *J. Am Chem. Soc.* **1983**, 105, 5781.

15. L. Găină, A. Csámpai, G. Túrós, T. Lovász, V. Zsoldos-Mády, I. A. Silberg and P. Sohár, *Org. & Biomol. Chem.* **2006**, 4, 4375.

16. I. Simiti, V. Zaharia, M. Coman, H. Demian, A. Muresan, *Pharmazie,* **1988**, 43(2), 82.

17. M. J. Calhorda, E. J. S. Vichi, *Organometallics* **1990**, *9*, 1060.

CYSTEINOLS: IMPROVED SYNTHESIS OF 2-AMINO-2-(MERCAPTOMETHYL)PROPANE-1,3-DIOL HYDROCHLORIDE

ANDRADA BUT, CARMEN BATIU, DAN PORUMB, MIRCEA DARABANTU*

ABSTRACT. An enhanced know-how preparation of the title compound is described starting from TRIS[®] [2-amino-2-(hydroxymethyl)propane-1,3-diol, *2-(hydroxymethyl)serinol*].

Keywords: cysteinols, 1,3-oxazolines, thionation, TRIS[®]

INTRODUCTION

Cysteinol, 2-amino-3-mercaptopropanol, was seen as the reduced form of cysteine and entitled as such by Broadbent in 1976 [1a], inspired from the pioneering work of Enz and Cecchinato as early as 1961 [1b] *("cysteine synthetic approach"*, Scheme 1).
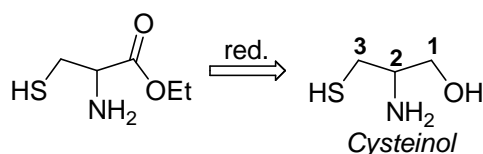
Scheme 1

With minor modifications, *"cysteine synthetic approach"* remained of interest in the next period [2] for the preparation of functionalised heterocyclic saturated systems, 1,3-thiazolidines, 1,3-oxazolidines and fused systems thereof *e.g.* as key intermediates in the total synthesis of *Biotin*,[2b] *Micacocidine* [2c] and *Farnesyl Transferase* [2e]. Regardless the context, the isolation of *cysteinol* as hydrochloride or the trapping *in situ* of its free base with >C=O electrophiles were throughout preferred.

---

* *"Babes-Bolyai" University, Department of Organic Chemistry, 11 Arany Janos str., 400028, Cluj-Napoca, Romania. darab@chem.ubbcluj.ro*

Therefore, our expertise in *C*-substituted-2-aminopropane-1,3-diols' chemistry (*serinols*),[3] seen *mutatis-mutandis* as reduced forms of *C*-substituted serines, prompted us to investigate their conversion into mercapto analogues, for example the well known TRIS®, 2-amino-2-(hydroxymethyl)propane-1,3-diol **Ia** [*2-(hydroxymethyl)serinol*] into 2-amino-2-(mercaptomethyl)propane-1,3-diol **IIa** [*2-(hydroxymethyl)cysteinol*, Scheme 2].

$R = H$

serinol   *cysteinol*

R = CH$_2$OH (**a**), Me (**b**), Et (**c**)
Ia *2-(hydroxymethyl)serinol* → **IIa** *2-(hydroxymethyl)cysteinol*
Ib *2-methylserinol*   →   **IIb** *2-methylcysteinol*
Ic *2-ethylserinol*   →   **IIc** *2-ethylcysteinol*
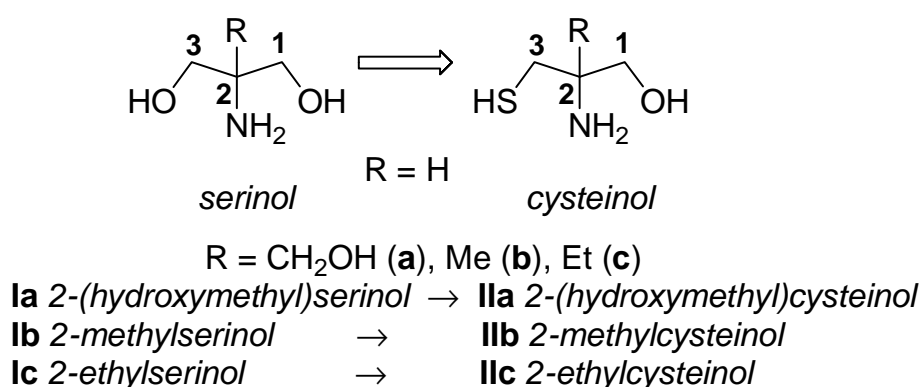
Scheme 2

That is, we explored a *"serinolic synthetic approach"* directed to *cysteinols*.

To the best of our knowledge, there are only two old patents [5] from which one dedicated completely to the preparation of *cysteinols* **IIa-c** (Scheme 2), **IIb** and **IIc** being by far much better documented with respect to **IIa**. However, careful examination of the cited patents inferred us about the instability, as free bases, of all **IIa-c**. They were claimed to be useful in protection of mammalians against radiation (free bases or hydrochlorides). Except elemental analysis, no spectroscopic data of **IIa-c** were reported so far.

Hence, the aim of the present preliminary report consists of the essentially improved synthesis of *cysteinol* **IIa** starting from TRIS® **Ia** (Scheme 2). Indeed, **IIa** appeared to us more attractive due to its additional functionality with respect to **IIb** and **IIc**.

RESULTS AND DISCUSSION

Targeting *cysteinol* **IIa** (Scheme 2), the chemistry we applied, based orientatively on the above two cited patents [5], is resumed in Scheme 3.

Scheme 3
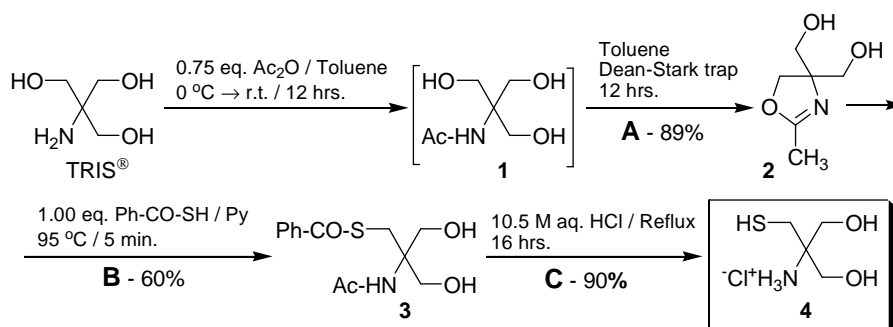
Each step made the object of serious improvements.

In step **A**, one of the three homotopic methylenes of TRIS® was activated by including it into a 1,3-oxazoline ring, **2**. Differently than previously reported,[5] rather than operating in boiling acetic acid with azeotropic removal of water from the reaction mixture followed by fractional distillation of crude **2** under reduced pressure, then recrystallisation from THF (52% yield [5b]), we opted for a more reactive electrophile, acetic anhydride in toluene, according to the below stoichiometry (Eq. 1, 2).

$$H_2NC(CH_2OH)_3 + Ac_2O \longrightarrow \textbf{2} + AcOH + H_2O \quad (1)$$
$$H_2NC(CH_2OH)_3 + AcOH \longrightarrow \textbf{2} + 2\,H_2O \quad (2)$$
$$2\,H_2NC(CH_2OH)_3 + Ac_2O \longrightarrow 2 \times (\textbf{2}) + 3\,H_2O \quad (1+2)$$
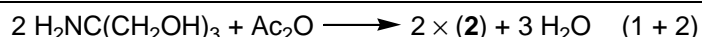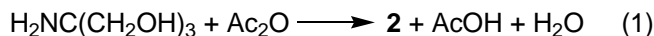
Thus, although 0.5 molar equivalents of acetic anhydride theoretically ensured that all acetyl groups were incorporated in the 1,3-oxazoline **2** with no statistically favoured side *O*-acylation of TRIS®, we anyhow used 0.75 eq. of Ac_2O and removed the resulting water with the use of a Dean-Stark trap.* To our surprise, while the yield of crude freshly isolated **2** was 93% (96 % ^{1}H NMR purity and 4% amide **1**), in our hands, it was an unstable compound. Indeed, in the crude **2**, the content of TRIS' amide **1** increased to 15% within drying 24 hrs. at room temperature to reach 40% after one week of storage.♥ Fortunately, in this case, the mixture **1** + **2** could be resubmitted to the dehydrating cyclisation conditions (**1** → **2** + H_2O, Scheme 3) affording quantitatively, again, the above crude **2** (96% ^{1}H NMR purity, 4% **1**).

---

*In both Patents,[5] the use of 1.5 eq. AcOH is recommended for the synthesis of **2**.

♥It appeared to us that **2** was sensitive to moisture, especially if residual AcOH was present in the crude material.

So, we used oxazoline **2** in the next step of the synthesis (**B**, Scheme 3) with no other purification than a rapid triturating with dry ether, intended to eliminate the residual amounts of acetic acid.

In the key step **B**, we obtained the *S*-, *N*-protected form **3** of the *cysteinol* **IIa** in 60% yield (previously reported, 57% [6a]). Despite the excellent NMR appearance of crude **3** (71% yield), it required two purifications from EtOH, in order to reach the analytical purity.

Both ^{1}H and ^{13}C NMR spectra of crude compound **3** exhibited just a single pair of enantiotopic CH_2O groups located at 60.3 ppm ppm [$\delta(CH_2S)$ = 30.3 ppm] and just one clear AX geminal coupling pattern between their diastereotopic protons [$\Delta\delta$(H-a/H-b) = 0.03 – 0.05 ppm, $^2J_{a-b}$ = 10.3 – 10.6 Hz]. Accordingly, we concluded that thionation of **2** (Scheme 3) was completely chemioselective.

Finally, in step **C**, we *N*-, *S*-deprotected the amidoester **3** in boiling 10.5 M aq. HCl in 90% yield (lit. 68% [5b]) and isolated the *cysteinol* **IIa** as hydrochloride **4** following one of our previous patented protocols [6] (see EXPERIMENTAL SECTION and Figure1).
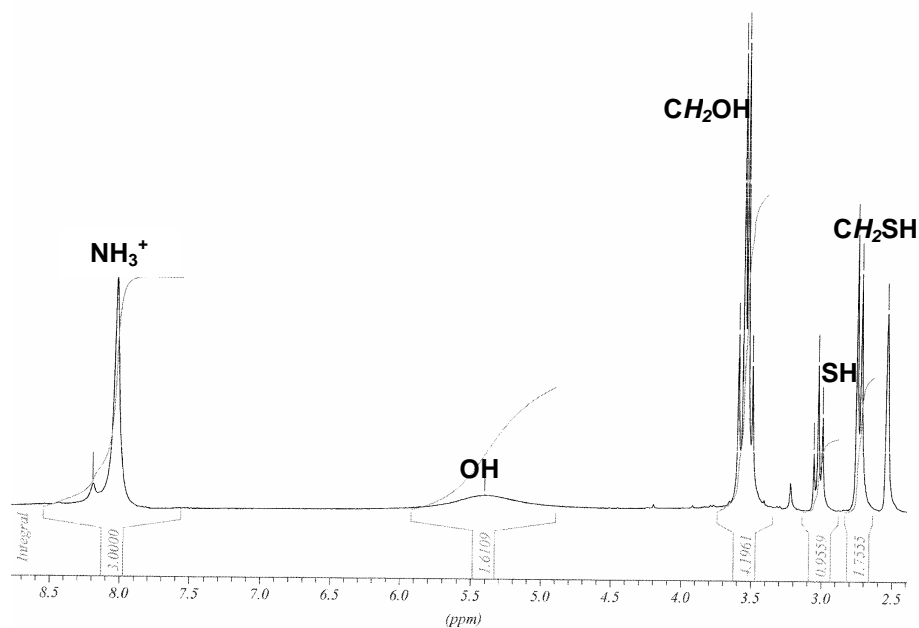
Figure 1. ^{1}H NMR of compound **4** on 300 MHz timescale ([D$_6$]DMSO)

The amount of the resulting side product, benzoic acid (90% yield), was indicative for the very clean reaction observed. Compound **4** was stable on storage indefinitely.

CONCLUSIONS

Starting from TRIS®, an essentially improved three steps synthesis of 2-amino-2-(mercaptomethyl)propane-1,3-diol, [*2-(hydroxymethyl)cystei-nol*], hydrochloride, occurring in 48 % overall yield, was described (lit. 20% [5b]).

EXPERIMENTAL SECTION

General. Melting points are uncorrected; they were carried out on ELECTROTHERMAL® instrument. NMR spectra were recorded on a Brucker® AM 300 instrument operating at 300 and 75 MHz for ^{1}H and ^{13}C nuclei respectively. All NMR spectra were measured in anhydrous commercially available deuteriated solvents. No SiMe$_4$ was added; chemical shifts were measured against the solvent peak. All chemical shifts (δ values) are given throughout in ppm; all coupling patterns ($^n J_{H,H}$ values) are given throughout in Hz.TLC was performed by using aluminium sheets with silica gel 60 F$_{254}$ (Merck®); flash column chromatography was conducted on Silica gel Si 60 (40–63 μm, Merck®). IR spectra were performed on a Perkin-Elmer® Paragom FT-IR spectrometer. Only relevant absorptions are listed [throughout in cm^{-1}: weak (w), medium (m) or (s) strong]. Microanalyses were performed on a Carlo Erba® CHNOS 1160 apparatus. Mass spectra (MS) were recorded on a Brucker® Esquire Instrument.

Preparation of 4,4-bis(hydroxymethyl)-2-methyl-1,3-oxazoline (2).

To TRIS® (8.48 g, 70 mmol) suspended in cooled (0 °C) dry toluene (125 mL), acetic anhydride (5.00 mL, 5.36 g, 52.5 mmol) was rapidly injected under vigorous stirring. The resulted suspension was stirred and let to reach room temperature overnight (12 hrs.) then heated at reflux for additional 12 hrs. with continuous removal of water in a Dean-Stark trap (TLC monitoring, eluent toluene : ethanol 3/1 v/v, visualisation in a I$_2$ bath). The reaction was stopped when no more water was separated and no more evolution was observed on TLC. At this step, starting from refluxing toluene, the reaction mixture, as a fine colourless emulsion, was let very gently to reach room temperature under vigorous stirring in order to ensure successfully the obtention of a fine white suspension. After filtering, well washing with dry ether ($\times$ 25 mL) and drying at room temperature within one hour, 9.45 g of the crude title compound **2** were obtained (yield 89% with respect to TRIS®; ^{1}H NMR purity 96%; 4% compound **1**).

47

2-Acetamido-2-(hydroxymethyl)propane-1,3-diol (1): ^{1}H NMR (300 MHz, [D$_6$]DMSO): δ = 1.73 (s, 3 H, CH$_3$), 3.50 (s, 6 H, C*H$_2$*OH), 4.62 (bs, 3 H, CH$_2$O*H*), 7.22 (bs, 1 H, NH) ppm. ^{13}C NMR (75 MHz, [D$_6$]DMSO): δ = 24.0 (1 C, CH$_3$), 60.0 (1 C, Cq., C-2), 60.8 (3 C, 3 × CH$_2$OH), 175.2 (1 C, >C=O) ppm.

4,4-Bis(hydroxymethyl)-2-methyl-1,3-oxazoline (2): white crystalline powder, m.p. 82–84 °C (Et$_2$O) [lit.[5a] 95 − 97 °C (CHCl$_3$/Et$_2$O/AcOEt); lit. [5b] 88 − 89 °C (THF)]. R_f (75% toluene/EtOH) = 0.45. IR (KBr): ν = 3360 (s), 3271 (s), 3108 (s), 2982 (s), 2941 (s), 2872 (s), 1670 (s), 1629 (m), 1572 (m), 1459 (m), 1384 (s), 1270 (s), 1229 (w), 1187 (w), 1143 (w), 1029 (s), 994 (s), 972 (w), 942 (w), 882 (w), 843 (w), 691 (w), 649 (w), 625 (w), 588 (w), 525 (w) cm^{-1}. ^{1}H NMR (300 MHz, [D$_6$]DMSO): δ = 1.84 (s, 3 H, CH$_3$), 3.29 (d, 2 H, $^2J_{H,H}$ = 11.0 Hz, C*H$_2$*OH), 3.36 (d, 2 H, $^2J_{H,H}$ = 11.0 Hz, C*H$_2$*OH), 4.02 (s, 2 H, H-5), 4.69 (bs, 2 H, CH$_2$O*H*) ppm. ^{13}C NMR (75 MHz, [D$_6$]DMSO): δ = 13.6 (1 C, CH$_3$), 63.9 (2 C, CH$_2$OH), 70.3 (1 C, C-4), 76.4 (1 C, C-5), 163.4 (1 C, C-2) ppm. MS (positive CI, isobutane, 200 eV): *m/z* (%) = 202 (17) [M+*i*-BuH-2]$^+$, 188 (7) [M+42]$^+$, 164 (15) [M+18]$^+$, 146 (100) [M+1]$^+$, 114 (6), 73 (< 5); C$_6$H$_{11}$NO$_3$ (145.07).

Preparation of 2-acetamido-2-(benzoylthiomethyl)propane-1,3-diol (3)
In a vigorously stirred solution prepared from 4,4-bis(hydroxymethyl)-2-methyl-1,3-oxazoline **(2)** (3.68 g, 25.35 mmol) dissolved in dry pyridine (10.00 mL, 10.50 g, 133 mmol), thiobenzoic acid (3.30 mL, 3.50 g 100%, 25.35 mmol) was rapidly injected at room temperature. The resulted yellow solution was heated at 95 °C and kept at this temperature for 5 min. A clear orange-reddish solution was obtained which was cooled at 0 °C for 30 min. then poured on aq. HCl (45.00 mL, 47.70 g, 4 M aq. HCl, 179 mmol). Crude **3** crystallised as a yellow mass (pH = 0.5 - 1) which was cooled for additional 12 hrs. at 0 °C. After filtering, washing with cooled water (3 × 15 mL) and drying at r.t., 6.90 g crude **3** were obtained as a yellow amorphous powder. This was twice recrystallised from boiling ethanol (15 mL) to yield 4.30 g pure **3** as a white crystalline powder (60% yield with respect to **2**).

2-Acetamido-2-(benzoylthiomethyl)propane-1,3-diol (3):white crystalline powder, m.p. 143–145 °C (EtOH) [lit. [5a] 147 − 148 °C (-); lit. [5b] 146 − 147 °C (EtOH)]. C$_{13}$H$_{17}$NO$_4$S (283.09): calcd. C 55.11, H 6.05, N 4.94; found C 54.88, H 5.88, N 5.29. R_f (75% toluene/EtOH) = 0.75. IR (KBr): ν = 3380 (s), 3344 (m), 3153 (m), 2942 (m), 2895 (m), 2837 (m), 1662 (s), 1648 (s), 1557 (s), 1450 (m), 1372 (m), 1323 (w), 1205 (s), 1176 (m), 1079 (m), 1064 (s), 969 (w), 913 (s), 774 (m), 690 (m), 645 (m), 596 (w), 554 (m), 533 (w) cm^{-1}. ^{1}H NMR (300 MHz, [D$_6$]DMSO): δ = 1.86 (s, 3 H, CH$_3$), 3.62 (dd, 2 H, $^2J_{H,H}$ = 10.3 Hz, $^3J_{H,H}$ = 5.7 Hz, C*H$_2$*OH), 3.61 (dd, 2 H, $^2J_{H,H}$ = 10.3 Hz, $^3J_{H,H}$ = 4.6 Hz, C*H$_2$*OH), 4.99 (dd as t, $^3J_{H,H}$ = 5.7 Hz, CH$_2$O*H*), 7.39 (s, 1 H, NH), 7.59 (t, 2 H,

$^3J_{H,H}$ = 7.5 Hz, H-3, Ph), 7.72 (t, 1 H, $^3J_{H,H}$ = 7.4 Hz, H-4, Ph), 7.95 (d, 2 H, $^3J_{H,H}$ = 7.5 Hz, H-2, Ph) ppm. ^{13}C NMR (75 MHz, [D$_6$]DMSO): δ = 23.4 (1 C, CH$_3$), 30.3 (1 C, CH$_2$S), 60.3 (2 C, CH$_2$OH), 61.2 (1 C, C-2), 126.8 (2 C, C-2, -6, Ph), 129.0 (2 C, C-3, -5, Ph), 133.7 (1 C, C-4, Ph), 136.5 (1 C, C-1., Ph), 170.3 [1 C, >C(=O)-NH-), 191.1 [1 C, >C(=O)-S-] ppm. MS (positive CI, isobutane, 200 eV): *m/z* (%) = 340 (< 5) [M+*i*-BuH-1]$^+$, 284 [M+1]$^+$ (48), 266 (8), 252(< 5), 236 (5), 218 (7), 180 (100), 162 (10), 148 (8), 130 (< 5), 123 (10), 116 (< 5), 73 (< 5).

Preparation of 2-amino-2-(mercaptomethyl)propane-1,3-diol hydrochloride **(4)**. 2-Acetamido-2-(benzoylthiomethyl)propane-1,3-diol **(3)** (2.41 g, 8.50 mmol) was suspended in aq. HCl (7.40 mL, 8.57 g, 10.5 M aq. HCl, 77.7 mmol) and the reaction mixture was heated at reflux with stirring for 16 hrs. After cooling at room temperature, benzoic acid crystallised abundantly and was filtered off, washed with aq. HCl (3 × 5 mL, 10.5 M aq. HCl) to yield 0.93g pure by product (90% with respect to the theoretical amount). The combined aqueous filtrate was added to benzene (100 mL) and the resulted mixture was heated with stirring at reflux with azeotropic removal of water (Dean-Stark trap). During anhydrification, compound **4** separated as an oily mass. When no more water separated, the mixture was kept at reflux for additional 2 hrs. in order to eliminate thes excess of hydrochloric acid. After cooling at room temperature, benzene was decanted and crude oily **4** was crystallised at 0 ^{o}C from 10 mL 1:1 v/v isopropanol : ether to yield 1.32 g pure **4** (90% yield).

2-Amino-2-(mercaptomethyl)propane-1,3-diol hydrochloride (4): white crystalline powder, m.p. 102 - 104 ^{o}C (*i*-PrOH/Et$_2$O 1:1 v/v) [lit. [5b] 104 – 105 ^{o}C (*i*-PrOH)]. C$_4$H$_{12}$ClNO$_2$S (173.03): calcd. C 27.66, H 6.96, N 8.07; found C 28.02, H 6.88, N 7.99. IR (KBr): ν = 3344 (s), 3265 (s), 3008 (s), 2554 (m), 1602 (m), 1542 (m), 1514 (s), 1458 (m), 1399 (m), 1277 (m), 1247 (m), 1112 (m), 1062 (s), 918 (m), 671 (m), 546 9w) cm^{-1}. ^{1}H NMR (300 MHz, [D$_6$]DMSO): δ = 2.74 (d, 2 H, $^3J_{H,H}$ = 9.1 Hz, C*H$_2$*SH), 3.03 (d, 1 H, $^3J_{H,H}$ = 9.1 Hz, CH$_2$S*H*), 3.52 (d, 2 H, $^2J_{H,H}$ = 11.6 Hz, C*H$_2$*OH), 3.58 (d, 2 H, $^2J_{H,H}$ = 11.6 Hz, C*H$_2$*OH), 5.40 (bs, 2 H, CH$_2$O*H*), 8.03 (s, 3 H, NH$_3$$^+$) ppm. ^{13}C NMR (75 MHz, [D$_6$]DMSO): δ = 24.5 (1 C, CH$_2$S), 59.7 (1 C, C-2), 61.0 (2 C, CH$_2$OH) ppm. MS (positive CI, isobutane, 200 eV): *m/z* (%) = 176 [M+3]$^+$, 152 (7), 138 (100), 103 (9), 90 (6).

ACKNOWLEDGEMENTS

REFERENCES

1. a) H. S. Broadbent, W. S. Burnham, R. M. Sheely, R. K. Olsen, *J. Heterocyclic Chem.,* **1976**, *13*, 337; b) W. Enz, M. Cecchinato, *Helv. Chim. Acta*, **1961**, *44*(3), 706; c) G. G. Habernel, W. Ecsy, *Heterocycles*, **1977**, *7*(2), 1029 .

2. a) D. Seebach, T. Weber, *Tetrahedron Lett.*, **1983**, *24*(32), 3315; b) A. Gonzales, R. Lavilla, J. F. Piniella, A. Alvarez - Larena, *Tetrahedron*, **1995**, *51*(10), 3015; c) F. D. Deroose, P. J. De Clercq, *J. Org. Chem.*, **1995**, *60*(2), 321; d) A. Ino, Y. Hasegawa, A. Murabayashi, *Tetrahedron Lett.*, **1998**, *39*(21), 3509; e) H. Yang, X. C. Sheng, E. M. Harrington, K. Ackerman, A. M. Garcia, M. D. Lewis, *J. Org. Chem.,* **1999**, *64*(1), 242.

3. for example in context: a) M. Darabantu, G. Plé, C. Maiereanu, I. Silaghi-Dumitrescu, Y. Ramondenc and S. Mager *Tetrahedron*, **2000**, *56*(23), 3799; b) M. Darabantu, C. Maiereanu, I. Silaghi-Dumitrescu, L. Toupet, E. Condamine, Y. Ramondenc, C. Berghian, G. Plé and N. Plé, *Eur. J. Org. Chem.*, **2004**, 2644; c) C. Berghian, P. Lameiras, L. Toupet, E. Condamine, N. Plé, A. Turck, C. Maiereanu, M. Darabantu, *Tetrahedron*, **2006**, *62*(31), 7319.

5. a) J. Nys, J. Libeer (Gevaert Photo-Producten N. V.), U. S. Pat. 2 954 376, Sept. 27, 1960; cf. *Chem. Abstr.*, **1961**, *55,* 36770; b) C. R. Bresson (Phillips Petroleum Co.), U. S. Pat. 3 351 664, Nov. 7, 1967; cf. *Chem. Abstr.* **1968**, *68*, 95331.

6. M. Darabantu, D. Breazu, V. Vasilioni, M. Brodszky, I. Cotora, Z. Pap, Patent RO 91181 (**1987**); cf. *Chem. Abstr.* **1991**, *114*, 121788.

SYNTHESIS OF A G-2 MELAMINE BASED DENDRON HAVING 2-AMINO-2-METHYLPROPANOL UNITS AS PERIPHERAL GROUPS

ANTAL ZOLTÁN, CARMEN BATIU, MIRCEA DARABANTU[*]

ABSTRACT. Starting from 2-amino-2-methylpropanol, a concise five steps iterative synthesis of a title type compound is described.

Keywords: amino alcohols, dendrons, iterative synthesis, melamines

INTRODUCTION

In continuation of our recent findings [1] in the field of *N*-substituted-2,4,6-triaimino-*s*-triazines' (*melamines*) based dendrons and dendrimers by convergent iterative approach starting from *C*-substituted-2-aminopropane-1,3-diols (*serinols*), we report herein the preparation of a G-2 dendron having amino monoalcohol units, namely 2-amino-2-methylpropanol **A**, as peripheral groups (Scheme 1).

Scheme 1

[*] *"Babes-Bolyai" University, Department of Organic Chemistry, 11 Arany Janos st., 400028, Cluj-Napoca, Romania. darab@chem.ubbcluj.ro*

Indeed, we have previously described our failure, involving C-2-substituted serinols (*e.g.* 2-amino-2-methylpropane-1,3-diol, *methylserinol*) [1b], to perform iterative synthesis directed to dendritic melamines. Hence, we considered of interest to simplify our attempt by using an amino *mono*-alcohol (Scheme 1).

On the other hand, despite availability of a large variety of amino alcohols, there is just one patent referring to amination of cyanuric chloride by 2-amino-2-methylpropanol **A** [2], the resulting *N*-substituted-2-chloro-4,6-diamino-*s*-triazine being claimed as rubber-to-metal adhesion promoter.

RESULTS AND DISCUSSION
1. Synthesis

The convergent strategy we applied is resumed in Scheme 2 [3, 4] [*].

$$A \xrightarrow{+\,T} TA_2 \xrightarrow{+\,P} PTA_2 \xrightarrow{+\,T} T(PTA_2)_2 \xrightarrow{+\,P} PT(PTA_2)_2 \xrightarrow{+\,T} T^0[PT^I(PT^{II}A_2)_2]_2$$
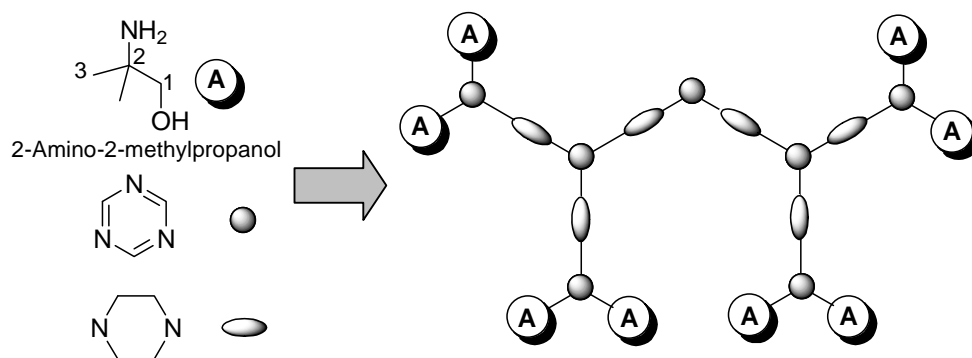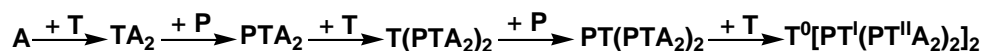
A: 2-**A**mino-2-methylpropanol; **T**: cyanuric chloride (*s*-**T**riazine); **P**: **P**iperazine

Scheme 2

It consisted of five steps selective amination of cyanuric chloride (*s*-triazine as branch cell **T**) carried out firstly with the amino alcohol **A** (peripheral group) as nucleophile then with piperazine (as linker **P**). Reaction conditions and quantitative results are shown in Scheme 3.

The first step, consisting of double amination of cyanuric chloride by 2-amino-2-methylpropanol **A**, reached completion at 45 °C only[*], affording the expected *N*-substituted-chlorodiamino-*s*-triazine **1**. Although compound **1** was contaminated with two side products, presumably the mono- and triaminated *s*-triazines (TLC monitoring), pure analytical samples could be obtained efficiently by simple recrystallisation from boiling ethanol.

We next performed the mono-anchorage of **1** on piperazine, a widely used linker in melamine dendritic chemistry, as connecting cores [4b, 4f, 4h, 5a], generations [4e, 4g, 4i, 5b] or both [4c, 4j, 5c-e]. In our hands, the

---

[*]In the present preliminary report nomenclature and symbols earlier recommended by Tomalia [3] and Simanek [4] are used.

[*]The same synthesis performed with a more solvated nucleophile, 2-amino-2-methylpropane-1,3-diol (*methylserinol*), produced the corresponding *N*-substituted-2-chloro-4,6-diamino-*s*-triazine in refluxing THF (24 hrs. 92% yield) with no noticeably side products (see later discussion, compound **1a**) [1b].
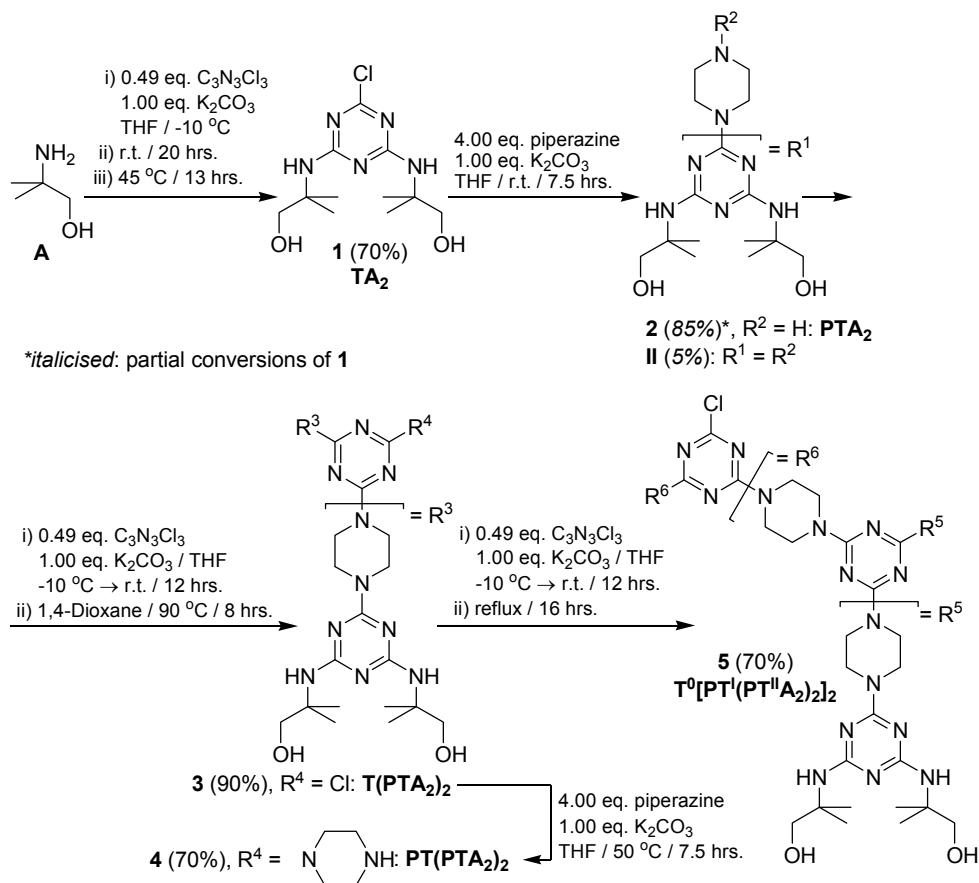
Scheme 3

previously reported direct methodologies [4c, 4e, 4i, 5b] (no protecting-deprotecting step), worked properly just in essentially modified conditions. Thus, selectivity (mono- *vs.* double anchorage) was ensured by adding portionwise chloro-*s*-triazines **1** (0.2 eq. each 90 min.) in THF at room temperature, to 4 equivalents of anhydrous piperazine. After each of these periods, TLC monitoring indicated the complete consumption of the starting **1**, the presence of the desired compound **2** together with significant traces of the symmetrical disubstituted piperazine derivative **II**. To our surprise, the formation of the later was observed even in the first stage of the synthesis when the initial molar ratio **1**: HN< groups was, in fact, 0.2:8. Differently than the corresponding analogous of type **2**, originating from *C*-substituted 2-aminopropane-1,3-diols [1b, 1c], compounds **2** and **II** could be eluted and successfully separated by flash column chromatography but on deactivated silica gel only (see **EXPERIMENTAL SECTION**).

No problem we encountered in the preparation of the G-1 dendron **3** obtainable in high yield. We note the harder conditions required by the complete double amination of cyanuric chloride by **2** in comparison with the synthesis of **1**.

Furthermore, we reiterated the mono anchorage of **3** on piperazine and accessed compound **4** in satisfactory yield. The synthetic protocol we used was similar to the above one in the case of **2**, account being taken on the lower reactivity observed for the chloro-*s*-triazine derivative **3**. No significant side products we detected by TLC monitoring; hence, the G-1 dendron **4** could be purified routinely by flash column chromatography on silica gel or direct crystallisation.

The target G-2 dendron **5** was prepared in a comparable large domain of temperature required by the selective and complete double amination (75 °C) as in the case of the G-1 precursor **3** (100 °C). Compound **5** was purified simply by twice crystallisations from boiling ethanol. The MS spectrum of **5** confirmed the desired structure (Figure 1).
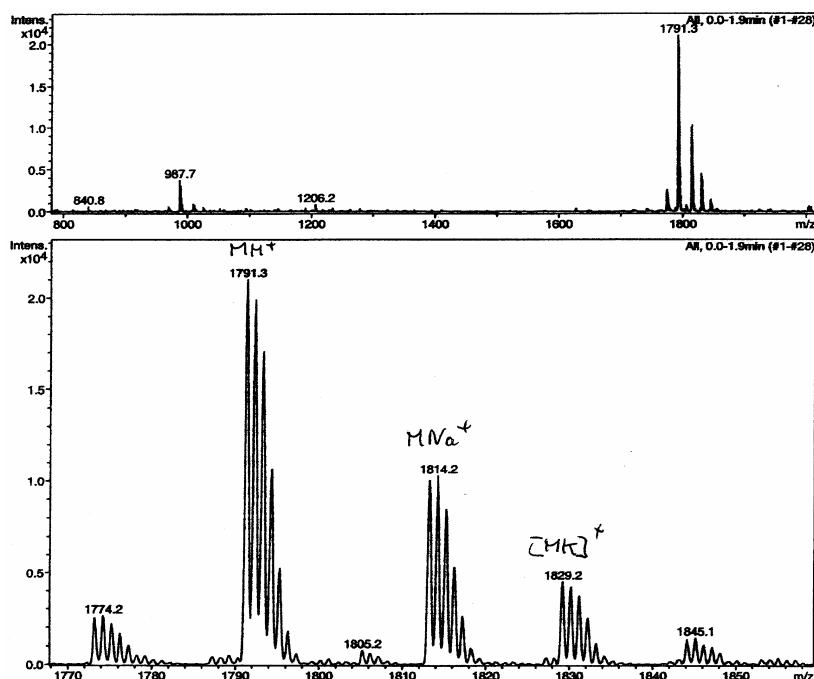
Figure 1: MS Spectrum of compound **5** (ESI+ in acetone-DMSO diluted with ACN) ($C_{77}H_{128}ClN_{41}O_8$ requires 1790.06).

To resume, the G-2 dendron **5** was conveniently obtained in five linear steps in a 26% global yield.

2. Preliminary structural assignments

We will limit the present preliminary discussion to NMR data. Besides fully confirming the identity of all compounds **1-5** (Scheme 3), at room temperature, they exposed the restricted rotation about the C(s-triazine)-N(exocyclic) partial double bonds, caused by the lpN(exocyclic) → π(s-triazine) conjugation. This rotational (pro)diastereomerism [1a, 1b]] is already a well established feature as early as 1993 [6] being supported by molecular mechanics [6a], X-Ray data [6c, 6d, 6f] and DNMR techniques. They all revealed this complex type of rotamerism in *N*-substituted melamines and their chlorodiamino-*s*-triazine precursors. Actual progress in the rotational stereochemistry phenomena of dendritic melamines differentiated their *angular* vs. *linear* construction as well as *internal* vs. *peripheral* location of the involved Ar-N< partial double bonds [1b]. In the same approach, using NMR methods, it was possible, very recently, to probe the "choreography of a dendrimer's dance" following classical concepts of conformational analysis applied to *s*-triazine dendrimers [7].

In our series of compounds, the most relevant rotameric behaviour was observed in the NMR spectra of the first two terms, **1** and **2** (Table 1, Figure 2, 3).

Table 1. ^{1}H NMR data (DMSO-d_6, 300 and 500 MHz) of the rotameric behaviour of compounds **1** and **2** in comparison with the chloro-*s*-triazine derivative **1a** of 2-amino-2-methylpropane-1,3-diol (*methylserinol* [1b])

No.	Indicative protons	Discriminating δ (ppm) values				Content of blocked rotamers (%)**		
		(a-a)*	(a-s) ≡ (s-a)		(s-s)*	(a-a)	(a-s) ≡ (s-a)	(s-s)
1a***	N(')H	6.41	6.66	6.74	6.78	4	46	50
	O(')H	5.19	4.82	4.65	4.65	*Frozen rotamerism*		
1	N(')H	7.13	7.01	6.94	6.61	66	31	3
	O(')H	4.82	4.82, 4.96			*Frozen rotamerism*		
2	N(')H	5.64 (303 K) → 5.45 (353 K)				*Free rotating structure*		
	O(')H	5.00 (303 K) → 4.75 (353 K)						

*substituent R^1 and propan(di)olic chains as references for descriptors *anti* (*a*) and *syn* (*s*) [6g, 7b]; **percentages calculated by using the best separated ^{1}H NMR signals ("indicative protons"): N(')H only (in **1**), averaged values using signals of N(')H, O(')H (in **1a**); ***compound previously reported by us [1b].

1, 1a, 2
anti-anti (a-a)

1, 1a, 2
anti-syn (a-s)

1, 1a, 2
syn-syn (s-s)

1: R^1 = Cl, R^2 = H; **1a**: R^1 = Cl, R^2 = OH; **2**: R^1 = piperazin-1-yl, R^2 = H
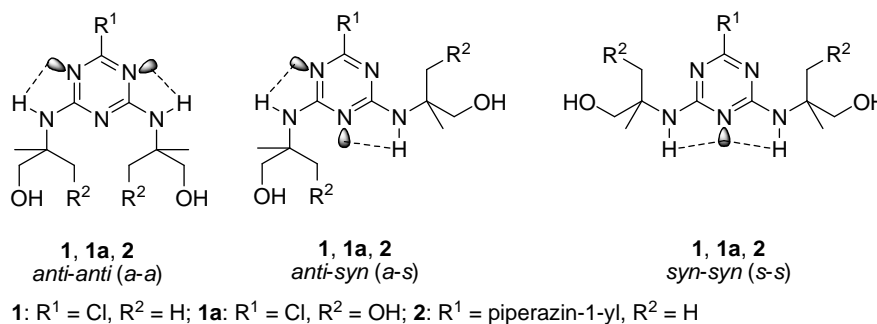
Thus, the withdrawing chlorine substituent in compound **1**, determined the highest π-deficiency of the *s*-triazine ring with respect to all series **1-5**, hence the highest C(*s*-triazine)-N(exocyclic) bond order. Accordingly, at room temperature (Table 1), **1** was clearly detected to be a mixture of three blocked rotamers (four anisochronous sites *anti/syn*, frozen rotamerism, [6g]).
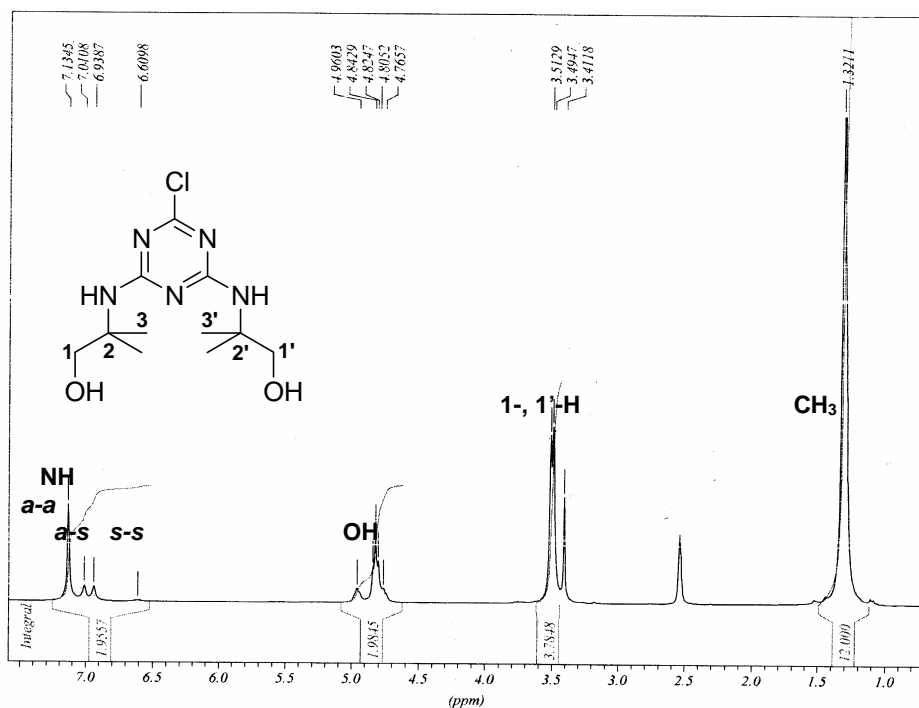
Figure 2. ^{1}H NMR spectrum of compound **1** (DMSO-d_6, 300 MHz, 25 ^{o}C)

56
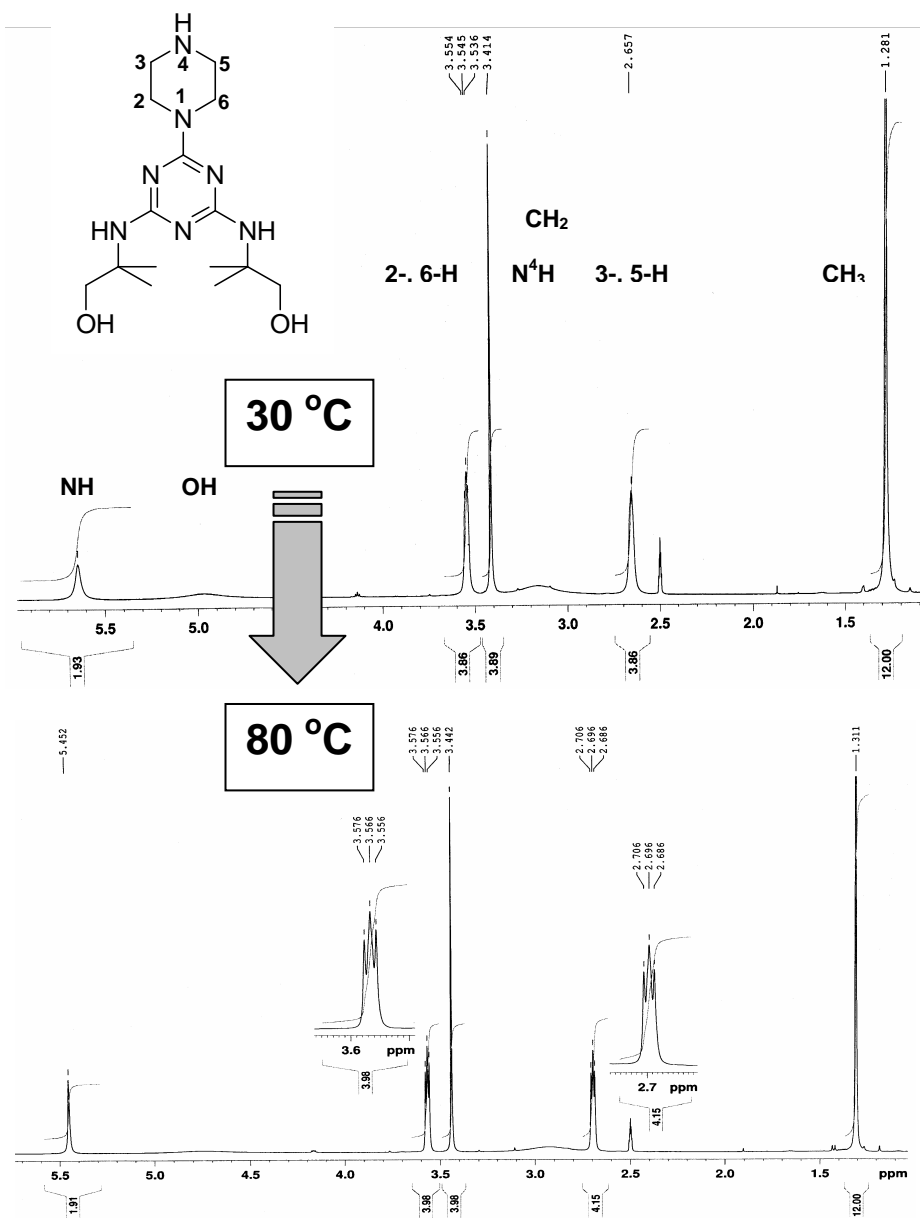
Figure 3. ^{1}H DNMR evolution of compound **2** (DMSO-d_6, 500 MHz)

As in the case of the previously reported by us **1a**, because of the fail in discriminating *directly* by means of NMR the rotamers **1**(*s-s*) *vs.* **1**(*a-a*), we proceeded to an *indirect* assignment.[*] Thus, we ascertained rotamer **1**(*a-a*) as providing the most downfield environment for the isochronous protons N(')H since i) they were positioned towards the close strong dipole moment created by the remainder *s*-triazine chlorine [1a, 4h] and ii) involved in two identically oriented intramolecular hydrogen bonds with the lone pairs of triazine nitrogens N-1, -3; hence, δN(')H(*a-a*) $\approx$ δN(')H($\underline{a}$-*s*) > δN(')H($\underline{s}$-*a*) $\approx$ δN(')(*s-s*) (Figure 2).

This assignment was different in comparison with **1a** (Table 1) where molecular mechanics predicted rotamer **1a**(*s-s*) as being the most stable [1b], and so δN(')H(*s-s*) $\approx$ δN(')H($\underline{s}$-*a*) > δN(')H($\underline{a}$-*s*) $\approx$ δN(')(*a-a*).

There are some additional reasons motivating the above opposite rotameric distribution of **1** vs. **1a** (Table 1):

i) in DMSO-d_6, a hydrogen bond acceptor solvent [6g], *s*-triazine **1a** was by far more solvated than **1**, imposing rotamer **1a**(*s-s*), although the most sterically hindered, to be dominant since it best exposed the four hydroxyl groups to solvent cages. Consequently, protons OH in **1a** were, globally, more deshielded than in **1**. That is, for the tetrahydroxy derivative **1a** the rotameric occurrence was imposed by solvation effects [1b].

ii) solvation was less important for the dihydroxy derivative **1**, able to adopt a different spatial arrangement dictated mainly by steric factors: as a result, rotamer **1**(*a-a*), the less congested, was dominant. Protons N(')H in **1** were throughout located downfield in comparison with **1a** (Table 1) to disclose the stronger deshileding influence of the chlorine atom in **1** vs. **1a**.

If chlorine was replaced by a strong R_2N type donor substituent, as in melamine **2**, its ^{1}H NMR spectrum (Figure 3) was consistent, at room temperature, with a unique mediated structure, hence a free rotating molecule. However, some minor modifications were observed upon heating the NMR sample, consisting of an A_2X_2 type clarification in the vicinal coupling pattern of piperazine methylenes C-3, -5. Since the chair-chair flipping of piperazine ring was better observed at 80 $^{\circ}$C, we were suspicious that, in normal conditions, some residual rotamerism had initially involved the C-2(*s*-triazine)-N-1(piperazine) bond.

On 300 MHz time scale, more elaborated structures (compounds **3-5**) displayed richness of conformational rotamerism giving rise to spectral complexity with respect to signal number, degeneracy, and broad lines, similar to melamine **2**, seen as a *model compound* [1b, 7a] for the whole series.

---

[*]The *indirect* assignment of the rotamerism in *N*-substituted 2-chloro-4,6-diamino-*s*-triazines appeared to us to be in current use approach, for example by comparison with 2-chloro-6-ethyl-4-isopropyl-*s*-triazine (Atrazine[®]) [7].

CONCLUSION

Starting from 2-methyl-2-propanol, we successfully developed a convergent five steps iterative synthesis directed to a G-2 melamine dendron possessing the title amino alcohol as peripheral groups. Rotational diastereomerism about C(*s*-triazine)-N(exocyclic) partial double bonds was typically revealed for the first two model precursors of the G-2 dendron.

EXPERIMENTAL SECTION

General. Melting points are uncorrected; they were carried out on ELECTROTHERMAL® instrument. Conventional NMR spectra were recorded on a Brucker® AM 300 instrument operating at 300 and 75 MHz for ^{1}H and ^{13}C nuclei respectively. A Brucker® DMX500 instrument was used for ^{1}H DNMR Experiments. All NMR spectra were measured in anhydrous commercially available DMSO-d_6. No SiMe$_4$ was added; chemical shifts were measured against the solvent peak. All chemical shifts (δ values) are given throughout in ppm; all coupling patterns ($^nJ_{H,H}$ values) are given throughout in Hz. TLC was performed by using aluminium sheets with silica gel 60 F$_{254}$ (Merck®); flash column chromatography was conducted on Silica gel Si 60 (40–63 μm, Merck®). IR spectra were performed on a Perkin-Elmer® Paragon FT-IR spectrometer. Only relevant absorptions are listed [throughout in cm^{-1}: weak (w), medium (m) or (s) strong]. Microanalyses were performed on a Carlo Erba® CHNOS 1160 apparatus. Mass spectra (MS) were recorded on a Brucker® Esquire Instrument.

Preparation of compound 1

To anhydrous K$_2$CO$_3$ (2.76 g, 20.00 mmol) suspended in dry THF (75 ml), cyanuric chloride (1.80 g, 9.76 mmol) was added with vigorous stirring. The resulted suspension was cooled at -10 ^{o}C when 2-amino-2-methylpropanol (1.78 g, 20.00 mmol) as dry THF (25 ml) solution was injected portionwise (5 mL/portion each hour). The reaction mixture was let to reach room temperature and kept as such for additional 20 hrs. At this stage, TLC monitoring (eluent toluene/isopropanol 2:1) indicated the formation of **1** contaminated with the corresponding intermediate, the *N*-substituted-2,4-dichloro-*s*-triazine. The reaction mixture was heated to 45 ^{o}C for additional 13 hrs. until TLC monitoring revealed completion of the amination, then cooled at room temperature. Minerals were filtered off and well washed with dry THF. The organic filtrate was evaporated under reduced pressure to dryness and the resulted white powder was crystallised from min. boiling ethanol affording 1.97 g **1** (70% yield with respect to cyanuric chloride).

2-Chloro-4,6-bis[(1-hydroxy-2-methylprop-2-yl)amino]-*s*-triazine (1).
White crystalline powder, mp 171.4-172.3 ^{o}C (EtOH). Anal. calcd. for
$C_{11}H_{20}ClN_5O_2$ (289.13): C, 45.60; H, 6.96; N, 24.17. Found: C, 45.77; H,
6.69; N, 23.98. R_f (66% toluene/isopropanol)=0.80. IR (KBr): ν=3370 (s),
3271 (m), 2980 (w), 2839 (w), 1598 (s), 1532 (s), 1474 (m), 1301 (w), 1270 (m),
1196 (m), 1056 (m), 1037 (m), 996 (w), 903 (w), 803 (m), 770 (w), 704 (w),
667 (w), 531 (w), 510 (w) cm^{-1}. ^{1}H NMR (300 MHz, DMSO-d_6, 25 ^{o}C): δ=1.32
(s, 12H, CH$_3$), 3.50 (d, $^3J_{H,H}$=5.5 Hz, 4H, 1-, 1'-H), 4.82, 4.96 (t and bt
respectively, $^3J_{H,H}$=5.6 Hz, 2H, O-, O'-H), 6.61, 6.94, 7.01, 7.13 (4×s, 2H, N-,
N'-H) ppm. ^{13}C NMR (75 MHz, DMSO-d_6, 25 ^{o}C): δ=23.4, 23.5 (4C, CH$_3$),
54.4, 54.5, 54.6 (2C, C-2, -2'), 66.8, 67.1 (2C, C-1, -1'), 164.0, 164.5, 164.8
(2C, C-4, -6, *s*-triazine), 166.8 (1C, C-2, *s*-triazine) ppm. MS (DCI positive,
200 eV, isobutane): m/z (%)=290 (100) [M$^+$+1], 346 (15), 328 (5), 312 (10),
256 (50), 240 (<5), 224 (10), 184 (5), 113 (<5), 85 (<5), 73 (10).

Preparation of compound 2
To anhydrous K$_2$CO$_3$ (0.96 g, 6.90 mmol) suspended in dry THF (50 ml),
anhydrous piperazine (2.37 g, 27.51 mmol) was added with vigorous stirring.
To this suspension, at room temperature, 2-chloro-4,6-bis[(1-hydroxy-2-
methylprop-2-yl)amino]-*s*-triazine **1** (2.00 g, 6.90 mmol) as dry THF (20 mL)
solution was added portionwise. Thus, after each 4 ml of this solution, added
within 90 min., TLC monitoring (eluent toluene/isopropanol 2:1) established
that all starting material **1** was consumed. The use of an alternative TLC
eluent (chloroform/ethanol 1:1) indicated the formation of the desired **2**, as
largely major, together with the corresponding 1,4-disubstituted piperazine
derivative **II** in traces. Minerals were filtered off and thoroughly washed with
dry THF. The organic filtrate was evaporated under reduced pressure to
dryness. The solid residue was separated by column chromatography on
silica gel as follows: the side product **II** was separated as the first fraction
(0.10 g, 5% conversion of **1**, eluent chloroform/ethanol 1:1) then **2** (2.01 g,
86% conversion of **1**, eluent ethanol containing 2.5% ammonia).

**1-{4,6-Bis[(1-hydroxy-2-methylprop-2-yl)amino]-*s*-triazin-2-yl}
piperazine (2).** White crystalline powder, mp 156.5-157.4 ^{o}C (flash column
chromatography, ethanol/2.5% ammonia). Anal. calcd. for $C_{15}H_{29}N_7O_2$ (339.24):
C, 53.08; H, 8.61; N, 28.89. Found: C, 52.88; H, 8.69; N, 29.05. R_f (ethanol/
2.5% ammonia)=0.85. IR (KBr): ν=3275 (s), 2968 (s), 2926 (s), 2858 (m),
1597 (s), 1554 (s), 1504 (s), 1441 (s), 1363 (s), 1275 (s), 1242 (m), 1200 (m),
1125 (w), 1050 (m), 811 (m), 614 (w) cm^{-1}. ^{1}H NMR (500 MHz, DMSO-d_6,
30 ^{o}C): δ=1.28 (s, 12H, CH$_3$), 2.66 (bs, 4H, 3-, 5-H-ax., -eq., piperazine),
3.15 (bs, 1H, NH, piperazine), 3.41 (s, 4H, 1-, 1'-H), 3.55 (t, $^3J_{H,H}$=4.5 Hz,
2H, 2-, 6-H-ax., -eq., piperazine), 5.00 (bs, 2H, O-, O'-H), 5.64 (bs, 2H, N-,
N'-H) ppm; ^{1}H NMR (500 MHz, DMSO-d_6, 80 ^{o}C): δ=1.31 (s, 12H, CH$_3$),

2.70 (t, $^3J_{H,H}$=5.0 Hz, 4H, 3-, 5-H-ax., -eq., piperazine), 2.90 (bs, 1H, NH, piperazine), 3.44 (s, 4H, 1-, 1'-H), 3.57 (t, $^3J_{H,H}$=5.0 Hz, 2H, 2-, 6-H-ax., -eq., piperazine), 4.75 (bs, 2H, O-, O'-H), 5.45 (bs, 2H, N-, N'-H) ppm. ^{13}C NMR (125 MHz, DMSO-d_6, 25 °C): δ=24.4 (4C, CH$_3$), 44.4 (2C, C-3, -5, piperazine), 46.0 (2C, C-2, -6, piperazine), 54.1 (2C, C-2, -2'), 69.0 (2C, C-1, -1'), 164.4 (1C, C-2, s-triazine), 165.6 (2C, C-4, -6, s-triazine) ppm. MS (DCI positive, 200 eV, isobutane): m/z (%)=396 (15) [M$^+$+1+i-BuH], 340 (100) [M$^+$ +1], 324 (<5), 308 (10), 268 (15), 236 (<5), 196 (<5), 169 (<5), 146 (<5), 113 (10), 97 (5), 85 (15), 73 (30), 61 (<10).

Alternative preparation of compound II

To anhydrous K$_2$CO$_3$ (0.56 g, 4.05 mmol) suspended in dry THF (50 ml), anhydrous piperazine (0.17 g, 1.97 mmol) and 2-chloro-4,6-bis[(1-hydroxy-2-methylprop-2-yl)amino]-s-triazine **1** (1.16 g, 4.00 mmol) were added with vigorous stirring. The reaction mixture was heated at reflux for 12 hrs. After this period, TLC monitoring (eluent toluene/isopropanol 2:1) showed the formation of **II** as major component of a mixture containing also the starting **1** and the intermediate **2**. THF was replaced by 1,4-dioxane and refluxing was continued for additional 12 hrs. After this period TLC monitoring revealed the presence of **1** and **2** in small traces only. Minerals were filtered off and thoroughly washed with dry THF. The organic filtrate was evaporated under reduced pressure to dryness. Flash column chromatography (eluent chloroform/ethanol 1:1) afforded pure **II** (0.89 g, 76% yield with respect to piperazine).

1,4-Bis{4,6-bis[(1-hydroxy-2-methylprop-2-yl)amino]-s-triazin-2-yl} piperazine (II). White crystalline powder, mp 230-235 °C (flash column chromatography, eluent chloroform/ethanol 1:1). Anal. calcd. for C$_{26}$H$_{48}$N$_{12}$O$_4$ (592.39): C, 52.68; H, 8.16; N, 28.36. Found: C, 53.02; H, 7.79; N, 28.44. R_f (50% chloroform/ethanol)=0.80. IR (KBr): ν=3502 (s), 3419 (s), 3346 (s), 3168 (s), 2964 (s), 2931 (s), 1563 (s), 1494 (s), 1440 (s), 1360 (s), 1281 (s), 1254 (s), 1199 (m), 1167 (s), 1060 (s), 1048 (s), 1017 (m), 994 (m), 898 (w), 833 (m), 809 (s), 743 (w), 595 (w), 563 (w) cm^{-1}. ^{1}H NMR (300 MHz, DMSO-d_6, 25 °C): δ=1.319, 1.322 (s, 24H, CH$_3$), 3.47 (bs, 8H, piperazine), 3.69 [bs, 8H, 2×(1-, 1'-H)], 5.03 [bs, 4H, 2×(O-, O'-H)], 5.81 [bs, 4H, 2×(N-, N'-H)] ppm. ^{13}C NMR (75 MHz, DMSO-d_6 25 °C): δ=20.8, 20.9 (8C, CH$_3$), 42.0 (4C, piperazine), 53.7 [4C, 2×(C-2, -2')], 68.4 [4C, 2×(C-1, -1')], 164.0 (2C, C-2, -2', s-triazine), 165.0 (4C, C-4, -4', -6, -6', s-triazine) ppm. MS (DCI positive, 200 eV, isobutane): m/z (%)=649 (5) [M$^+$+i-BuH], 593 [M$^+$] (100), 562 (10).

61

Preparation of compound 3

To anhydrous K_2CO_3 (0.44 g, 3.18 mmol) suspended in dry THF (50 ml), cyanuric chloride (0.29 g, 1.57 mmol) was added with vigorous stirring and the resulted suspension was cooled at -10 ^{o}C. At this temperature, 1-{4,6-bis[(1-hydroxy-2-methylprop-2-yl)amino]-*s*-triazin-2-yl}piperazine (**2**) (1.08 g, 3.18 mmol) as dry THF (25 mL) solution was injected very slowly. The reaction mixture was let to warm up to room temperature overnight when TLC monitoring (eluent toluene/isopropanol 2:1) revealed the presence of **3** and the unreacted **2** as well. THF was replaced by 1,4-dioxane and the reaction mixture was heated at 90 ^{o}C for additional 8 hrs. After this period, TLC monitoring confirmed the formation of **3** as largely major in the reaction mixture. At 90 ^{o}C minerals were filtered off and thoroughly washed with anhydrous and hot THF. The organic filtrate was evaporated under reduced pressure to dryness and the resulted crude product was triturated from EtOH/Et$_2$O affording pure **3** (1.12 g, 90% yield with respect to cyanuric chloride).

2-Chloro-4,6-bis{4-{4,6-bis[(1-hydroxy-2-methylprop-2-yl)amino]-*s*-tri-azin-2-yl}piperazin-1-yl}-*s*-triazine (3). White crystalline powder, mp 220-222 ^{o}C (EtOH/Et$_2$O). Anal. calcd. for $C_{33}H_{56}ClN_{17}O_4$ (789.44): C, 50.15; H, 7.14; N, 30.13. Found: C, 50.35; H, 6.88; N, 30.31. R_f (66% toluene/isopropanol)=0.75. IR (KBr): ν=3398 (m), 2967 (m), 2924 (m), 2865 (m), 1566 (s), 1494 (s), 1440 (s), 1361 (s), 1274 (s), 1229 (s), 1169 (m), 1057 (m), 998 (s), 977 (s), 811 (m), 740 (w), 502 (w) cm^{-1}. ^{1}H NMR (300 MHz, DMSO-d_6, 25 ^{o}C): δ=1.34 (bs, 24H, CH$_3$), 3.47 (bs, 8H, 3-, 3'-, 5-, 5'-H-ax., -eq., piperazine), 3.74 [bs, 16H, 2×(1-, 1'-H) 2-, 2'-, 6-, 6'-H-ax., -eq., piperazine), 5.02 [bs, 4H, 2×(O-, O'-H)], 5.85 [bs, 4H, 2×(N-, N'-H)] ppm. ^{13}C NMR (75 MHz, DMSO-d_6, 25 ^{o}C): δ=23.9 (8C, CH$_3$), 42.3, 42.9 (8C, piperazine), 53.7 [4C, 2×(C-2, -2')], 68.4 [4C, 2×(C-1, -1')], 163.8, 164.0, 164.7, 165.1 (8C, C-2', -2", C-4, -4', -4", C-6, -6', -6", *s*-triazine), 168.7 (1C, C-2, *s*-triazine) ppm. MS (ESI+, acetone/DMSO diluted with ACN): m/z (x10^5)=790 [M$^+$ +1] (3.6), 639.5 (0.5), 595.4 (0.6), 551.4 (0.5), 507.4 (0.4), 463.3 (0.2), 413.3 (0.2), 340.2 (<0.1), 276.6 (<0.2), 240.2 (<0.2).

Preparation of compound 4

To anhydrous K_2CO_3 (0.16 g, 1.16 mmol) suspended in dry THF (100 ml), anhydrous piperazine (0.39 g, 4.53 mmol) was added and the suspension was heated at 50 ^{o}C with vigorous stirring. At this temperature, 2-chloro-4,6-bis{4-{4,6-bis[(1-hydroxy-2-methylprop-2-yl)amino]-*s*-triazin-2-yl}pipera-zin-1-yl]-*s*-triazine (**3**) (0.88 g, 1.11 mmol) as dry THF (35 mL) solution was added portionwise, 7 mL/portion each 90 min. Within this period, TLC monitoring (eluent toluene/isopropanol 3:1) established the complete consumption of the starting **3**. The use of an alternative TLC eluent (chloroform/

ethanol 1:1) indicated the formation of the desired **4**, as largely major, together with the corresponding 1,4-disubstituted piperazine derivative in very small traces. At 50 $^{\circ}$C, minerals were filtered off and thoroughly washed with hot and dry THF. The organic filtrate was evaporated under reduced pressure to dryness to provide the crude product which was purified by column chromatography (eluent chloroform/ethanol 3:1) yielding pure **4** (0.65 g, 70% yield with respect to **3**). Optional purification of **4** can be carried out by trituration from EtOH/Et$_2$O (60% yield with respect to **3**).

1-{4,6-Bis{4-{4,6-bis[(1-hydroxy-2-methylprop-2-yl)amino]-*s*-triazin-2-yl}piperazin-1-yl}-*s*-triazin-2-yl}piperazine (4). White crystalline powder, mp 225-230 $^{\circ}$C (flash column chromatography, eluent chloroform/ethanol 3:1). Anal. calcd. for C$_{37}$H$_{65}$N$_{19}$O$_4$ (839.55): C, 52.90; H, 7.80; N, 31.68. Found: C, 53.11; H, 8.09; N, 31.59. R_f (75%chloroform/ethanol)=0.30. IR (KBr): ν=3385 (m), 3330 (m), 2968 (m), 2924 (m), 1543 (s), 1484 (s), 1438 (s), 1359 (m), 1271 (m), 1198 (m), 1054 (w), 999 (m), 809 (m) cm^{-1}. ^{1}H NMR (300 MHz, DMSO-d_6, 25 $^{\circ}$C): δ=1.33 (s, 24H, CH$_3$), 2.84 (bs, 4H, 3-, 5-H-ax., -eq., piperazine), 3.46 (s, 5H, 2-, 6-H-ax., -eq., NH, piperazine), 3.72-3.74 [bd, 24H, 2'-, 2''-, 3'-, 3''-, 5'-, 5''-, 6'-, 6''-H-ax., -eq., piperazine, 2×(1-, 1'-H)], 5.00 [bs, 4H, 2×(O-, O'-H)], 5.80 [bs, 4H, 2×(N-, N'-H)] ppm. ^{13}C NMR (75 MHz, DMSO-d_6, 25 $^{\circ}$C): δ= 24.4 (8C, CH$_3$), 41.4, 43.1, 43.4, 44.9 (12C, piperazine), 54.2 [4C, 2×(C-2, -2')], 68.9 [4C, 2×(C-1, -1')], 164.5, 165.1, 165.2 (9C, C-2, -2', -2'', -4, -4', -4'', -6, -6', -6'', *s*-triazine) ppm. MS (ESI+ MeOH): m/z (x10^6)=862.4 (0.8) [M+Na$^+$], 840.5 (4.8) [M$^+$+1], 809.5 (0.2), 768.4 (0.4), 696.3 (0.5), 624.2 (0.5), 552.2 (0.6), 413.2 (0.3), 276.5 (1.0).

Preparation of compound 5

To anhydrous K$_2$CO$_3$ (0.2034 g, 1.472 mmol) suspended in dry THF (90 ml),1-{4,6-bis{4-{4,6-bis[(1-hydroxy-2-methylprop-2-yl)amino]-*s*-triazin-2-yl}piperazin-1-yl}-*s*-triazin-2-yl}piperazine (**4**) (1.236 g, 1.472 mmol) was added with vigorous stirring and cooled at -20 $^{\circ}$C. At this temperature, cyanuric chloride (0.132 g, 0.716 mmol) as dry THF (10 mL) solution was rapidly injected. The reaction mixture was let gently to reach room temperature and was kept as such for additional 12 hrs. After this period, TLC monitoring (eluent chloroform/ethanol 4:1) still indicated the presence of the starting **4**, therefore the reaction mixture was heated to reflux for additional 16 hours then filtered off. Minerals were thoroughly washed with boiling dry THF. The organic filtrate was evaporated under reduced pressure to dryness. The resulting crude product was twice recrystallised from boiling ethanol to afford pure **5** (0.90 g, 70 % with respect to cyanuric chloride).

2-Chloro-4,6-bis{4-{4,6-bis{4-{4,6-bis[(1-hydroxy-2-methyl-prop-2-yl)-amino]-*s*-triazin-2-yl}piperazin-1-yl}-*s*-triazin-2-yl}piperazin-1-yl}-*s*-triazine (5). White crystalline powder, mp 260-270 $^{\circ}$C (dec.) (EtOH). Anal. calcd. for $C_{77}H_{128}ClN_{41}O_8$ (1790.06): C, 51.62; H, 7.20; N, 32.05. Found: C51.98; H: 6.81; N: 32.39. R_f (80% chloroform/ethanol)=0.75. IR (KBr): ν=3402 (m), 2970 (m), 2927 (m), 2863 (m), 1547 (s), 1484 (s), 1437 (s), 1361 (m), 1265 (m), 1232 (m), 1199 (w), 1177 (w), 1056 (w), 998 (m), 809 (m) cm^{-1}. ^{1}H NMR (300 MHz, DMSO-d_6, 25 $^{\circ}$C): δ=1.33 (bs, 48H, CH$_3$), 3.48 (bs, 24H, piperazine), 3.77 (bs, 24H, piperazine, 16H, C*H*$_2$OH), 5.04 (bs, 8H, CH$_2$O*H*), 5.84 (bs, 8H, NH) ppm. ^{13}C NMR (75 MHz, DMSO-d_6, 25 $^{\circ}$C): δ=23.9 (16C, CH$_3$), 42.6 (24C, piperazine), 53.7 (8C, Cq., C-2), 68.4 (8C, CH$_2$, C-1), 163.9, 164.7, 165.0 [20C, C-N(exocyclic), *s*-triazine], 168.8 (1C, C-Cl, *s*-triazine) ppm. MS (ESI+, acetone-DMSO diluted with ACN): m/z ($\times 10^4$)=1829.2 (0.5) (M+K$^+$), 1814.2 (1.1) (M+Na$^+$), 1791.3 (2.1) (M+H$^+$), 1206.2 (0.1), 987.7 (0.4), 840.8 (0.1).

ACKNOWLEDGEMENTS

REFERENCES

1. a) M. Fazekas, M. Pintea, P. Lameiras, A. Lesur, C. Berghian, I. Silaghi-Dumitrescu, N. Plé, M. Darabantu, *Eur. J. Org. Chem.,* **2008**, 2473; b) M. Pintea, M. Fazekas, P. Lameiras, I. Cadis, C. Berghian, I. Silaghi-Dumitrescu, F. Popa, C. Bele, N. Plé, M. Darabantu, *Tetrahedron*, **2008**, *64*(37), 8851; c) M. Darabantu, M. Pintea, M. Fazekas, P. Lameiras, C. Berghian, I. Delhom, I. Silaghi-Dumitrescu, N. Plé, A. Turck, *Letters in Organic Chemistry*, **2006**, *3*(12), 905.

2. R. F. Seibert, E. L. Wheeler, F. H. Barrows, W. R. True (Uniroyal Chemical Co., Inc., USA), U. S. Pat. 5283274; c.f. *Chem. Abstr.,* **1995**, *122*, P11925.

2. a) J. –L. Chaumette, M. J. Laufersweiler, J. R. Parquette, *J. Org. Chem.,* **1998**, *63*(25), 9399; b) C. Cardona, R. E. Gawley, *J. Org. Chem.,* **2002**, *67*(4), 1411–1413; c) B. Leopoittevin, R. Matmour, R. Francis, D. Taton, Y. Gnanou, *Macromolecules*, **2005**, *38*, 3120; d) M. Ballico, S. Drioli, G. M. Bonora, *Eur. J. Org. Chem.,* **2005**, 2064; e) I. Bury, B. Heinrich, C. Bourgogne, D. Guillon, B. Donnio, *Chem. Eur. J.,* **2006**, *12*, 8396.

3. A. D. Tomalia, *Aldrichimica Acta*, **2004**, *37*(2), 39.

4. a) W. Zhang, E. E. Simanek, *Org. Lett.,* **2000**, *2*(6), 843; b) W. Zhang, D. T. Nowlan, L. M. Thomson, M. W. Lackowski, E. E. Simanek, *J. Am. Chem. Soc.,* **2001**, *123*, 8914; c) W. Zhang, S. O. Gonzalez, E. E. Simanek, *Macromolecules*, **2002**, *35*, 9015; d) W. Zhang, E. S. Tichy, M. L. Pérez, G. C. Maria, P. A. Lindahl, E. E. Simanek, *J. Am. Chem. Soc.*, **2003**, *125*, 5086; e) A. P. Umali, E. E. Simanek, *Org. Lett.*, **2003**, *5*(8), 1245; f) M. B. Steffensen, E. E. Simanek, *Angew. Chem. Int. Ed.,* **2004**, *43*(39), 5178; g) H. T. Chen, M. F. Neerman, A. R. Parrish, E. E. Simanek, *J. Am. Chem. Soc.,* **2004**, *126*, 10044; h) J. Lim, E. E. Simanek, *Molecular Pharmaceutics*, **2005**, *2*(4), 273; i) E. Hollink, E. E. Simanek, *Org. Lett.*, **2006**, *8*(11), 2293; j) M. B. Steffensen, E. Hollink, F. Kuschel, M. Bauer, E. E. Simanek, *J. Polym. Sci.: Part A: Polym. Chem.,* **2006**, *44*, 3411.

5. a) G. R. Newcome, J. Gross, C. N. Moorefield, B. D. Woosley, *Chem. Commun.,* **1997**, 515; b) E. J. Acosta, S. O. Gonzalez, E. E. Simanek, *J. Polym. Sci. Part A.,* **2005**, *43*, 168; c) M. F. Neerman, W. Zhang, A. R. Parrish, E. E. Simanek, *Int. J. Pharm.*, **2004**, *281*, 129; d) L. –L. Lai, C. –H. Lee, L. –Y. Wang, K. L. Cheng, H. –F. Hsu, *J. Org. Chem.,* **2008**, *73*(2), 485; e) L. –L. Lai, L. –Y. Wang, C. -H. Lee, C. Y. Lin, K. –L. Cheng, *Org. Lett.*, **2006**, *8*(8), 1541.

6. a) I. Willner, J. Rosengaus, Y. Eichen, *J. Phys. Org. Chem.*, **1993**, *6*(1), 29; b) A. R. Katritzky, I. Ghiviriga, D. C. Oniciu, A. Barkock, *J. Chem. Soc. Perkin Trans. 2,* **1995**, 785; c) A. R. Katritzky, I. Ghiviriga, P. G. Steel, D. C. Oniciu, *J. Chem. Soc. Perkin Trans. 2,* **1996**, 443; d) M. Amm, N. Platzer, J. Guilhem, J. P. Bouchet, J. P. Volland, *Magn. Reson. Chem.,* **1998**, *36*, 587; e) H. E. Birkett, R. K. Harris, P. Hodgkinson, K. Carr, M. H. Charlton, J. C. Cherryman, A. M. Chippendale, R. P. Glover, *Magn. Reson. Chem.,* **2000**, *38*, 504; f) M. Amm, N. Platzer, J. P. Bouchet, J. P. Volland, *Magn. Reson. Chem.,* **2001**, *39*, 77; g) I. Ghiviriga, D. C. Oniciu, *Chem. Commun.*, **2002**, *22*, 2718; h) H. E. Birkett, J. C. Cherryman, A. M. Chippendale, J. O. S. Evans, R. K. Harris, M. James, I. J. King, G. Mc. Pherson, *Magn. Reson. Chem.*, **2003**, *41*, 324.

7. a) X. K. Moreno, E. E. Simanek, *Macromolecules*, **2008**, *41*(12), 4108; b) in this paper, nomenclature of these rotamers as congested (for a-a), partial congestion (for a-s) and extended (for s-s) has been used together with classical E/Z descriptors by referring to Atrazine®; c) S. S. Mirvish, P. Gannett, D. M. Babcook, D. Williamson, S. C. Chen, D. D. Weisenburger, *J. Agric. Food Chem.*, **1991**, *39*, 1205 and d) G. J. Welhouse, W. F. Bleam, *Environ. Sci. Technol.*, **1992**, *26*, 959.

THIN LAYER CHROMATOGRAPHY SEPARATION OF SOME CAROTENOIDS, RETINOIDS AND TOCOPHEROLS

RODICA DOMNICA BRICIU[a], DORINA CASONI[a], CRISTINA BISCHIN[b]

ABSTRACT. A simple and reliable thin layer chromatography (TLC) method for simultaneous separation of some carotenoids (β-carotene, lycopene, lutein, astaxanthin and zeaxanthin), retinoids (retinol, retinoic acid, 9-*cis*-retinal and all-*trans*-retinal) and tocopherols (α-tocopherol, γ-tocopherol and δ-tocopherol) was described. For a proper separation of all compounds three different mobile phases (Benzene: Petroleum Ether, 10:90, v/v; Methanol: Benzene: Ethyl acetate, 5:75:20, v/v/v; Benzene: Petroleum Ether, 90:10, v/v) were tested, using silica gel F_{254} as stationary phase. The visualization was performed under UV light (254 and 365 nm). The presented method is simple and adequate for the separation and identification of these compounds from different matrices, such as pharmaceuticals and foods.

Keywords: carotenoids, retinoids, tocopherols, thin layer chromatography

INTRODUCTION

The retinoids and tocopherols are known as vitamin A, and E respectively, while carotenoids are vitamin A precursors. The carotenoids are one of the most important groups of natural pigments, because of their wide distribution, structural diversity and numerous functions. Although the classical sources of carotenoids are plants, they are also found in animals and microorganisms [1, 2]. They are classified in two classes, carotenes (i.e. β-carotene and lycopene, Figure 1, 1-2), and xanthophylls (i.e. lutein, astaxanthin and zeaxanthin, Figure 1, 3-5). Nowadays, they are widely associated to retinoids, which are more polar and smaller molecule compounds. Some natural occurring vitamins A are presented in Figures 1, 6-9. Both classes, carotenoids and retinoids, present similar biological activity [3]. On the other part, tocopherols (Figure 1, 10-12) are a series of organic compounds consisting of various methylated phenols. They are biosynthesized by plants. Since animals and humans are unable to biosynthesize

---

[a] *Babeş-Bolyai University of Cluj-Napoca, Faculty of Chemistry and Chemical Engineering, Arany Janos Str, No 11, 400028 Cluj-Napoca Romania, rbriciu@chem.ubbcluj.ro*
[b] *Babeş-Bolyai University of Cluj-Napoca, Faculty of Biology and Geology, Gh. Bilascu Str. No 44, 400015 Cluj-Napoca, Romania*

vitamin E, they have to rely on an external supply of it through their diet. It is well known that some of the tocopherols, the carotenoids and the retinoids are very effective antioxidants and are suspected to reduce the risk of cancer known to be initiated by the production of free radicals [4, 5].
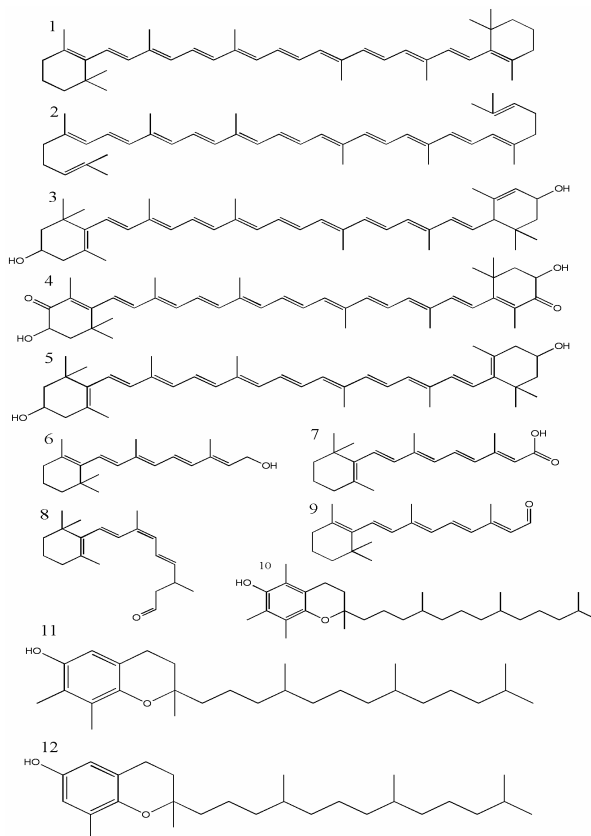
Figure 1. Chemical structure of some carotenoids (1: β-carotene, 2: lycopene, 3: lutein, 4: astaxanthin, 5: zeaxanthin), retinoids (6: retinol, 7: retinoic acid, 8: 9-*cis*-retinal, 9: all-*trans*-retinal), and tocopherols (10: α-tocopherol, 11: γ-tocopherol, 12: δ-tocopherol).

They are found together, often in different pharmaceutical formulations or as food additives, because of their synergic activity [6]. The chromatographic determinations of mixtures of these compounds were intensely studied. The high performance liquid chromatography (HPLC) is, unequivocally the most used chromatographic technique in their determination, because of its sensibility and variability [7-13]. Furthermore, gas chromatography (GC) has extensive applications for tocopherols [14-16] and retinoids [17, 18], while the carotenoid

determinations are more difficult because of compounds physicochemical properties. Other chromatographic techniques, such as sub- and supercritical chromatography are rarely used [19].

Thin layer chromatography methods have been widely employed for the analysis of lipophilic vitamins and their precursors [20, 21]. Normal phases systems based on silica gel and magnesium oxide sorbents and chemically bonded sorbents with largely non-aqueous mobile phases have been most often used for TLC determinations of carotens, while for xanthophylls and retinoids more polar mobile phases are required [22-26]. The tocopherols TLC analysis demands, as well, low polarity mobile phases when silica gel plates are used [27-29]. Moreover, some reverse phase TLC separations were reported [30].

The objective of this work was to develop a proper separation procedure for some carotenoids, retinoids and tocopherols in normal phase chromatography, able to be used for TLC separation from pharmaceutical preparative and foods.

RESULTS AND DISCUSSION

Because of the high variance of analytes polarities the direct separation of compounds by one development was impossible. The polarities of β-carotene and lycopene are lower than of all other compounds. These aspects lead to the using of three different mobile phases. The MP1 had as target the separation of β-carotene and lycopene. A proper separation of these compounds can be observed in Figure 2.

A second elution of the same plate with MP2 can solve the separation of xanthophylls and retinoids. Moreover, the method allows a sufficient separation of all xanthophylls, including the lutein and zeaxanthin isomers. The retinoids are well separated by xanthophylls (Figure 3). The isomers 9-*cis*-retinal and all-*trans*-retinal could not be separated by each other. However, the tocopherols remained at start by using the MP1, while the MP2 moves them in the front. The MP1 and MP2 were not able to offer a proper separation of tocopherols, but the problem was solved by the MP3, which offered a high resolution separation. As can be seen the selectivity of MP1 was modified by changing the solvents ratio, obtaining MP3. The MP3 strength is intermediary between MP1 and MP2. In Figure 4 the sensitive separation of tocopherols can be observed. To create a better estimation of the separation, the R_F values were calculated as a proportion between the migration distance and solvent front of analites. The R_F values were presented in Table 1.
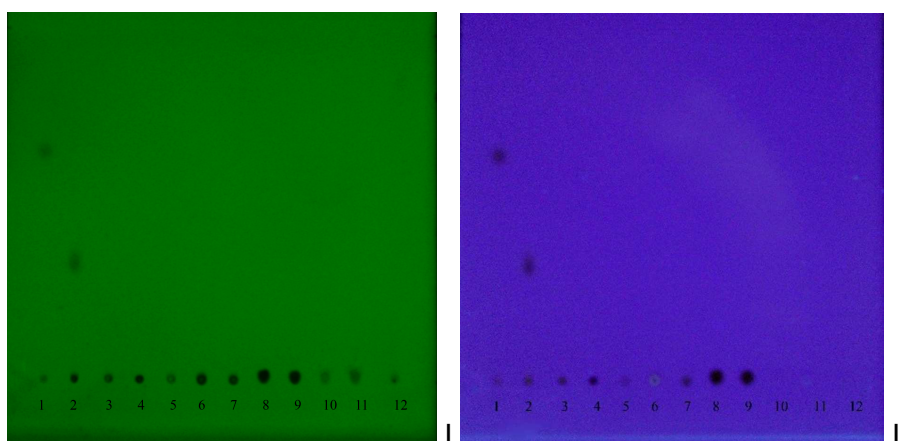
Figure 2. The TLC separation of β-carotene (1) and lycopene (2) by the other compounds (3- lutein, 4- astaxanthin, 5- zeaxanthin, 6- retinol, 7- retinoic acid, 8- 9-*cis*-retinal, 9- all-*trans*-retinal, 10- α-tocopherol, 11- γ-tocopherol, 12- δ-tocopherol) by using the MP1 mobile phase (Benzene: Petroleum Ether; 10:90; v/v) and visualized under UV light at 254 nm (I) and 365 nm (II).
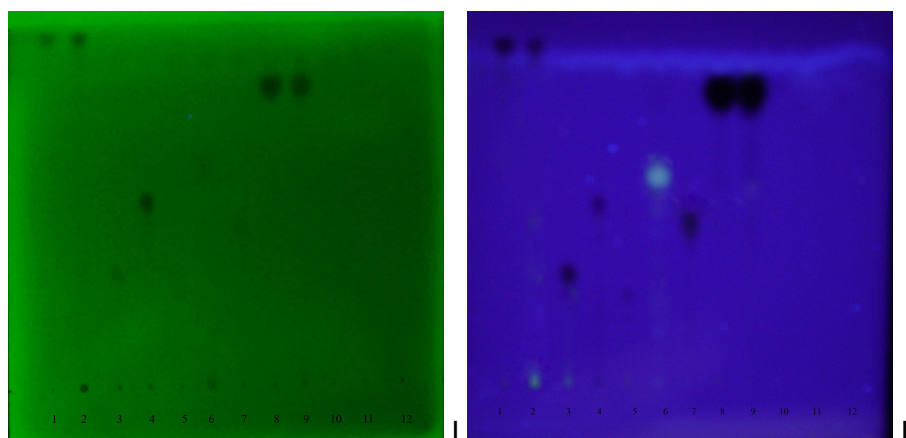
Figure 3. The TLC separation of xanthophylls (3- lutein, 4- astaxanthin, 5- zeaxanthin) and retinoids (6- retinol, 7- retinoic acid, 8- 9-*cis*-retinal, 9- all-*trans*-retinal) by the other compounds (1- β-carotene, 2- lycopene, 10- α-tocopherol, 11- γ-tocopherol, 12- δ-tocopherol) by using the MP2 mobile phase (Methanol: Benzene: Ethyl acetate; 5:75:20; v/v/v) and visualized under UV light at 254 nm (I) and 365 nm (II).
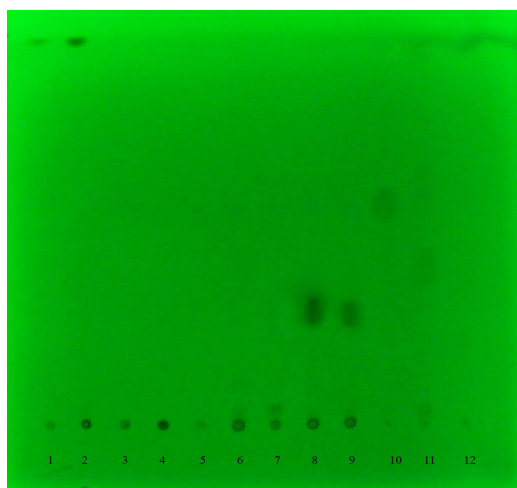
Figure 4. The TLC separation of tocopherols (10- α-tocopherol, 11-γ-tocopherol, 12- δ-tocopherol) by the other compounds (1- β-carotene, 2- lycopene, 3- lutein, 4- astaxanthin, 5- zeaxanthin, 6- retinol, 7- retinoic acid, 8- 9-cis-retinal, 9- all-trans-retinal) by using the MP3 mobile phase (Benzene: Petroleum Ether; 90:10; v/v) and visualized under UV light at 254 nm (A).

Table 1. Rf values of carotenoids, retinoids and tocopherols.

Name	Rf		
	MP1	**MP2**	**MP3**
β-carotene	0.83	1.00	1.00
Lycopene	0.37	1.00	1.00
Lutein	0.00	0.48	0.00
Astaxanthin	0.00	0.71	0.00
Zeaxanthin	0.00	0.45	0.00
Retinol	0.00	0.74	0.00
Retinoic Acid	0.00	0.61	0.00
9-*cis*-retinal	0.00	0.94	0.36
All-*trans*- retinal	0.00	0.94	0.37
α-tocopherol	0.00	1.00	0.44
γ-tocopherol	0.00	1.00	0.31
δ-tocopherol	0.00	1.00	0.24

The method described above was tested on two types of samples, vegetables and pharmaceutical products. Three extracts of carrots, tomatoes and tomato sauce were spotted near by standard solutions of carotenoids and tocopherols. After developing using MP1 a good identification of β-carotene and lycopene was obtained (Figure 5). The rest of carotenoids and tocopherols were not presented in the analyzed extracts.

71

The second test for method ability was performed on an antioxidant pharmaceutical product containing β-carotene, α-tocopherol acetate and ascorbic acid. The β-carotene, tocopherols and ascorbic acid were spotted near by the product solution. The mobile phase chosen for developing was the MP3. A certain identification of β-carotene could be observed (Figure 6). However, the method is not proper for the identification of ascorbic acid, because it was not moved from the start position. The R_F values obtained for standard and identified compounds in both, vegetables and pharmaceutical product, presented in table 2, confirm the identity of extracted compounds.
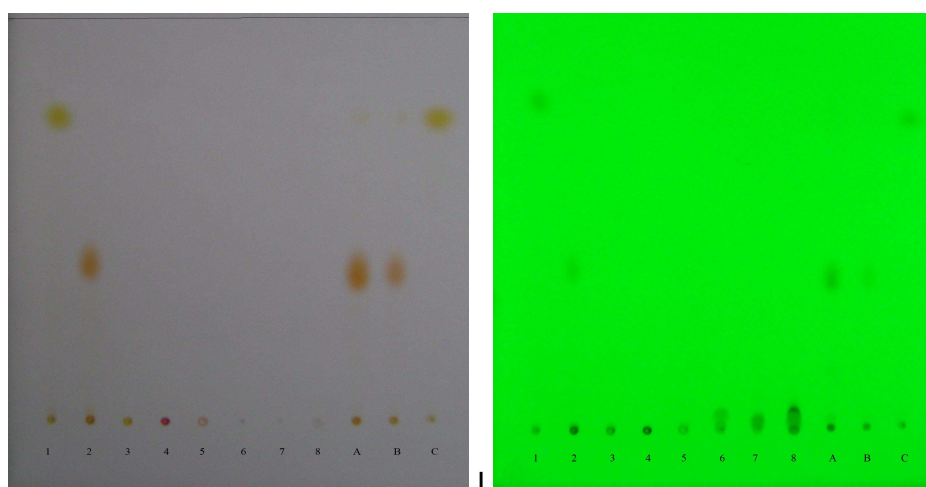
Figure 5. The identification of β-catotene (1) and lycopene (2) in the extracts of tomatoes (A), tomato souce (B) and carrots (C) by using MP1 mobile phase (Benzene: Petroleum Ether; 10:90; v/v) and visualized under visible (I) and UV light (II). The other spotted compounds were lutein (3), astaxanthin (4), zeaxanthin (5), α-tocopherol (6), γ-tocopherol (7), δ-tocopherol (8).

Table 2. The Rf values of identified compounds into different vegetable and pharmaceutical products using the proper mobile phases.

Name	R_F			
	Vegetable Products Extracts (MP1)			Triovit (MP3)
	Tomato souce	Tomatoes	Carrots	
β-carotene	0.84	0.83	0.83	0.84
Lycopene	0.37	0.36	nd	-
Lutein	nd	nd	nd	-
Astaxanthin	nd	nd	nd	-
Zeaxanthin	nd	nd	nd	-
α-tocopherol	nd	nd	nd	nd
γ-tocopherol	nd	nd	nd	nd
δ-tocopherol	nd	nd	nd	nd
Ascorbic Acid	-	-	-	0.00
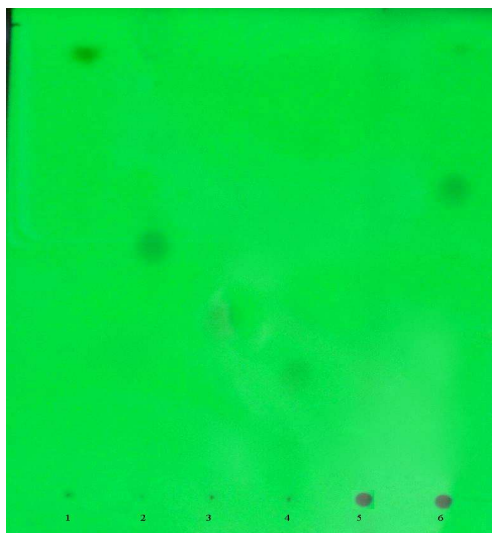
Figure 6. Separation and identification of some vitamins in Triovit capsule unde
UV light (254 nm) with MP3 mobile phase (Benzene: Petroleum Ether; 90:10; v/v).
Spots: 1- β-carotene, 2- α-tocopherol, 3- γ-tocopherol, 4- δ-tocopherol,
5- ascorbic acid, and 6- Triovit capsule.

CONCLUSIONS

The chromatographic separation of some complex mixtures of vitamins
and precursors is difficult because of the variability of compound nature.
The thin layer chromatography is an effective method for the separation of large
groups of substances, especially if more chromatographic systems with different
selectivities are used. The separation of carotenoids, retinoids and tocopherols
on silica gel F_{254} plates with three different mobile phases could be obtained.
Also, the separation of carotenes and tocopherols using benzene: petroleum
ether (10:90 and 90:10 v/v) indicates that, by changing the solvents ratio were
provided different selectivity mobile phase. The obtained results indicate that
the method is suitable to be used for qualitative determination of investigated
compounds into real samples of vegetable and pharmaceutical products.

EXPERIMENTAL SECTION

Materials. The β-carotene, lycopene, lutein, astaxanthin, 9-*cis*-reinal,
all-*trans*-retinal, δ-tocopherol and ascorbic acid standards were obtained
from Sigma, while zeaxanthin, retinol and retinoic acid were Fluka products.
α and γ-tocopherols were purchased from Acros Organics. The solvents used
(petroleum ether, methanol, benzene and ethyl acetate) were obtained from

Chimopar. All the chemicals were analytical degree purity. As stationary phases were used TLC silica gel F_{254} plates 10 x 10 cm from Merck. The spotting was performed using a Hamilton microsyringe of 10 µL.

Samples of carrots, tomatoes, tomato sauce, and pharmaceutical product (Triovit capsule) were obtained commercially. The Triovit is a diet supplement containing β-carotene (10 mg), α-tocopherol acetate (40 mg), ascorbic acid (100 mg), selenium (50 µg) and excipients (magnesium stearate and silicon dioxide anhydrous).

Extraction Procedure. 10 g of each vegetable product were extracted according to Cimpan *et al.* [31]. The pharmaceutical product (1 capsule of Triovit) was dissolved in 5 mL of chloroform followed by a filtration step performed in order to remote the excipients. The obtained extracts could be directly applied on the chromatographic plate.

Chromatography. 2 µL of standard solutions (1 mg mL^{-1}) and extracts were spotted on the TLC plates at 1.5 cm from the bottom edge and at 1 cm from lateral edges. The distance between spots were 0.7 cm. Plates were developed on 8 cm using three different mobile phases:

MP1. Benzene: Petroleum Ether (10:90; v/v);
MP2. Methanol: Benzene: Ethyl acetate (5:75:20; v/v/v);
MP3. Benzene: Petroleum Ether (90:10; v/v).
The visualization was performed under UV light at 254 and 365 nm.

ACKNOWLEDGMENTS

REFERENCES

1. J. Oliver, A. Palou, *J. Chromatogr. A*, **2000**, *881*, 543.
2. M. A. Lila, In K. Davis, "Plant Pigments and Their Manipulation", Blackwell, Oxford, **2004**, *14*, pp. 248.
3. A. B. Barua, H. C. Furr, J. A. Olson, R. B. van Breemen, In A. P. de Leenher, W. E. Lambert, J. F. van Bocxlaer, "Modern Chromatographic Analysis of Vitamins", 3rd Ed, Marcel Dekker, Inc., New York, **2000,** pp. 1.
4. H. J. Nelis, E. D'Haese, K. Vermis, In A. P. de Leenher, W. E. Lambert, J. F. van Bocxlaer, "Modern Chromatographic Analysis of Vitamins", 3rd Ed, Marcel Dekker, Inc., New York, **2000,** pp. 143.
5. W. Stahl, S. Nicolai, K. Briviba, M. Hanusch, G. Broszeit, M. Peters, H.-D. Martin, H. Sies, *Carcinogenesis*, **1997**, *18*, 89.
6. https://oa.doria.fi/bitstream/handle/10024/3305/**effects**o.pdf?sequence=1

7. I. Citova, L. Havlikova, L. Urbanek, D. Solichova, L. Novakova, P. Solich, *Anal. Bioanal. Chem.* **2007**, *388*, 675.

8. M. Bononi, I. Commissati, E. Lubian, A. Fossati, F. Tateo, *Anal. Bioanal. Chem.* **2002**, *372*, 401.

9. R. Mateos, J. A. Garcia-Mesa, *Anal. Bioanal. Chem.*, **2006**, *385*, 1247.

10. C. Kurz, R. Carle, A. Schieber, *Food Chem.*, **2008**, *110*, 522.

11. M. Vilasoa-Martinez, C. Calaza-Ramos, J. Lopez-Hernandez, M. A. Lage-Yusty, P. P. Losada, A. Rodriguez-Bernaldo de Quiros, *Anal. Chim. Acta*, **2008**, *617*, 225.

12. Y. Yang, X. Dong, M. Jin, Q. Ren, *Food Chem.*, **2008**, *110*, 226.

13. L. Barros, D. M. Correia, J. C. F. R. Ferreira, P. Baptista, C. Santos-Buelga, *Food Chem.*, **2008**, *110*, 1046.

14. H.-U. Melchert, D. Pollok, E. Pabel, K. Rubach, H.-J. Stan, *J. Chromatogr. A*, **2002**, *976*, 215.

15. H.-U. Melchert, E. Pabel, *J. Chromatogr. A*, **2000**, *896*, 209.

16. M. S. Beldean-Galea, A. Mocan, C. Sarbu. *Rev. Chim.* **2006**, *57*, 125.

17. E. Brenna, C. Fuganti, G. Fronza, F. G. Gatti, F. Sala, S. Serra, *Tetrahedron*, **2007**, *63*, 2351.

18. M. J. Casas-Catalan, M. T. Domenech-Carbo, *Anal. Bioanal. Chem.*, **2005**, *382*, 259.

19. E. Lesellier, C. West, A. Tchapla, *J. Chromatogr. A*, **2003**, *1018*, 225.

20. A. Pyka, In J. Sherma, B. Fried, "Handbook of Thin Layer Chromatography", 3rd Ed. Marcel Dekker, Inc. New York, **2003**, pp. 671.

21. A. Ramic, M. Medic-Saric, S. Turina, I. Jasprica, *J. Planar Chromatogr.* **2006**, *19*, 27.

22. M. J. Cikalo, S.K. Poole, C. F. Poole, *J. Planar Chromatogr.* **1992**, *5*, 200.

23. J. Deli, *J. Planar Chromatogr.* **1998**, *11*, 311.

24. T. Cserhati, E. Forgacs, J. Hollo, *J. Planar Chromatogr.* **1993**, *6*, 472.

25. J. R. Maldonade, D. B. Rodriguez-Amaya, A. R. P. Scamparini, *Food Chem.* **2008**, *107*, 145.

26. D. Ren, S. Zhang, *Food Chem.* **2008**, *106*, 410.

27. U. Hachula, F. Buhl, *J. Planar Chromatogr.* **1991**, *4*, 416.

28. J. Sliwiok, B. Kocjan, B. Labe, A. Kozera, J. Zalejska, *J. Planar Chromatogr.* **1993**, *6*, 492.

29. T. Hodisan, D. Casoni, M.S. Beldean-Galea, C. Cimpoiu, *J. Planar Chromatogr.* **2008**, *21*, 213.

30. I. Baranowska, A. Kasziolka, *Acta Chromatogr.* **1996**, *6*, 61.

31. G. Cimpan, S. Cobzac, "Metode analitice de separare, manual de lucrari practice", Babes Bolyai University Editure, Cluj-Napoca, **1995**.

THE SEPARATION OF SOME PRESERVATIVES BY THIN LAYER CHROMATOGRAPHY

CASONI DORINA[a], BRICIU RODICA DOMNICA[a], VERES DANIELA[b]

ABSTRACT. Rapid separation of 18 synthetic preservatives on the silica gel chemically modified HPTLC plates (RP-18F$_{254s}$, RP-18wF$_{254s}$, CN F$_{254s}$ and Nano-SIL Diol/UV$_{254}$) has been achieved with methanol-water as mobile phase. The development distance was 8 cm in all cases. Identification of the separated preservatives was performed by UV light at λ=254 nm. Potassium sorbate, sodium benzoate and ascorbic acid were identified in some soft drinks after sample preparation by solid phase extraction on C18 column.

Keywords: chromatographic separation, chemically modified silica gel, TLC, preservatives

INTRODUCTION

Preservatives are substances commonly added to various foods and pharmaceutical products in order to prolong their shelf life. The addition of preservatives to such products is essential for avoiding alteration and degradation by microorganisms during storage. Preservatives are classified into two main classes: *antimicrobial preservatives* and *antioxidants.*

Antimicrobial preservatives are introduced in the preparations to kill or to inhibit the growth of micro-organisms inadvertently introduced during manufacture or use. Antimicrobial preservatives are classified into two main sub-groups: antifungal preservatives and antibacterial preservatives. Antifungal preservatives include compounds such as benzoic and ascorbic acids and their salts, and phenol compounds such as methyl, ethyl, propyl and butyl p-hydroxybenzoate (parabens). Antibacterial preservatives are compounds such as quaternary ammonium salts, alcohols and other phenols.

---

[a] *Universitatea Babeş-Bolyai, Facultatea de Chimie şi Inginerie Chimică, Str. Kogalniceanu, Nr.1, RO-400084 Cluj-Napoca, România, dcasoni@chem.ubbcluj.ro*

[b] *Universitatea Babeş-Bolyai, Facultatea de Biologie şi Geologie, Str. Kogalniceanu, Nr.1, RO-400084 Cluj-Napoca, România*

Antioxidants are added to the pharmaceutical products to prevent deterioration by oxidation. Antioxidants are classified into three groups. The first group is known as true antioxidants, or anti-oxygen and they inhibit oxidation by reacting with free radicals blocking the chain reaction. Examples are alkylgallates butylated hydroxyanisol (BHA), butylated hydroxytoluene (BHT), and tocopherols. The second group consists of reducing agents, substances with lower redox potentials than the drug. Examples are ascorbic acid and potassium and sodium salts of sulphurous acid. The third group consists of antioxidant synergists which usually have little antioxidant effect themselves but probably enhance the action of antioxidants in the first group. Examples of antioxidant synergists are citric acid, editic acid and its salts, lecithin and tartaric acid.

Usually combinations of preservatives are used in pharmaceuticals, cosmetics, biological samples and foods, to prevent alteration and degradation of the product formulations. It is known that most of preservatives may be harmful to the consumers due to their potency to induce allergic contact dermatitis [1, 2]. Allergic reactions to foods represent a prominent, actual and increasing problem in clinical medicine [3].

Preservatives in common use include sorbic acid and its salts, benzoic acid and its salts, p-hydroxybenzoic acid methyl ester (methyl paraben), p-hydroxybenzoic acid ethyl ester (ethyl paraben), p-hydroxybenzoic acid propyl ester (propyl paraben), p-hydroxybenzoic acid butyl ester (butyl paraben) and salicylic acid. The structures of 18 usually preservatives are listed in Figure 1.

A variety of analytical methods for determining preservatives has been reported. However, because the additives can be present in combinations, chromatographic methods are often used for their selective individual or joint determination.

High–performance liquid chromatography (HPLC) is often preferred for the determination of mixture of additives in food, cosmetics, and pharmaceuticals. The simultaneous determination of sweeteners, preservatives and colorings in soft drinks was done by HPLC with UV detection [4]. Also, this chromatographic technique is the most common analytical procedure for detecting and quantifying sorbic and benzoic acids in foods and beverages [5, 6]. In view of the complexity and diversity foodstuffs composition, most of preservatives (benzoic, sorbic and salicylic acid) are usually analysed by RP-HPLC with an appropriate sample preparation procedure [7-9]. A novel ion chromatographic method was a beneficial alternative to conventional HPLC for simultaneous separation and determination of artificial sweeteners (sodium saccharin, aspartame), preservatives (benzoic acid, sorbic acid), caffeine, theobromine and theophylline in food and pharmaceutical preparations [10].

78
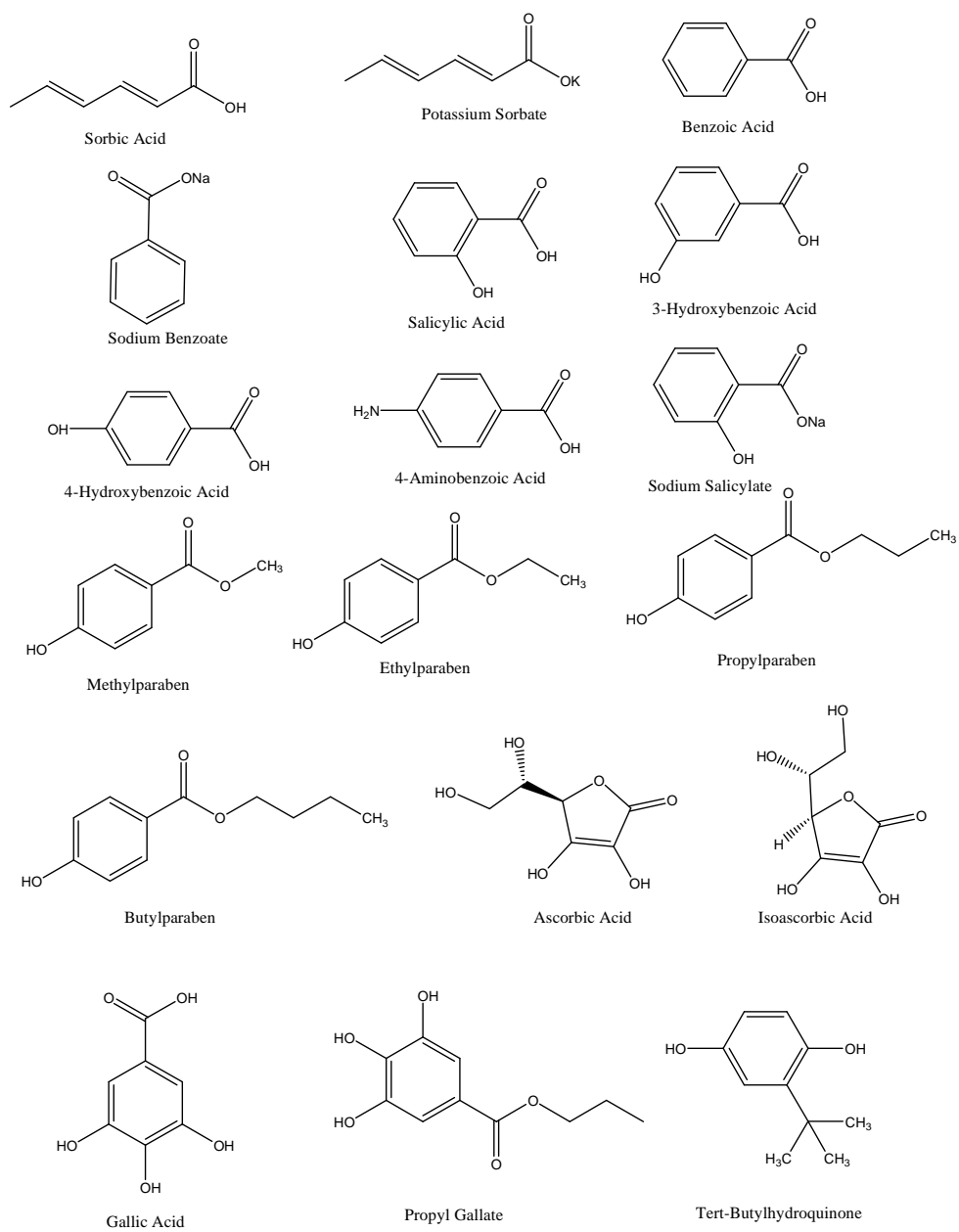
Figure 1. The structures of some usually synthetic preservatives.

Also, HPLC is a reliable method for simultaneous determination of phenolic preservatives such as parahydroxybenzoic acid, methyl, ethyl, propyl, butyl and pentyl parahydroxybenzoates from gelatin and vacant capsules for medicinal use [11]. Recently, liquid chromatography time-of-fight mass spectrometry (HPLC/TOF-MS) was developed to identification and quantification of 18 synthetic preservatives in beverages [12].

Gas chromatography (GC), with or without derivatization is also employed for the selective determination of food preservatives [13, 14] in beverages [15], soft drinks, yogurts and sauces [16]. Capillary electrophoresis method was developed to determine simultaneously artificial sweeteners, preservatives and dyes used as additives in carbonated soft drinks [17, 18]. A microemulsion electrokinetic chromatographic (MEEKC) method was used to separate seven preservatives (four parabens -methyl, ethyl, propyl and butyl, sorbic acid, benzoic acid, and dehydroacetic acid) which are commonly used as additives in various food products such as drinks, soy sauces and wines [19]. This method was successfully applied also for separation and determination of parabens (methyl, ethyl, propyl, and butyl *p* -hydroxybenzoate) in cosmetic products [20, 21].

The determination of preservatives using conventional methods like HPLC, GC and capillary electrophoresis (CE), some time can be difficult because of high-cost instruments and time-consuming pretreatment technique separations. Besides, equipments for these techniques are not available for small laboratories due to their high cost.

Thin-layer chromatographic procedure (TLC) was successfully used for separation of preservatives in cosmetics [22-24], in foods and beverages [25-27] and minimal sample preparation is necessary.

The purpose of this work was to investigate potential use of TLC (on different stationary phases) for rapid separation and identification of preservatives from carbonated soft drinks.

RESULTS AND DISCUSSION

The obtained R_f values of studied preservatives and mobile phases used for different HPTLC plates are listed in Table 1. As we can see from this table, the sorbic, benzoic, salicylic, ascorbic acids and salts like potassium sorbate and sodium benzoate (preservatives founded usually together in foods) were accurately separated on CN F_{254s} plates and Nano-SIL Diol/UV_{254} plates. The best stationary phases for the separation of potassium sorbate, sodium benzoate and ascorbic acid (found in mixture in majority of soft drinks), are silica gel RP-18wF_{254s} and silica gel CN F_{254s}.

80

Table 1. R_f values of some preservatives on Silica gel HPTLC plates

Compounds	R_f values Silica gel HPTLC plates			
	RP-18F$_{254s}$ Mobile phase MeOH:H$_2$O (6:4, v/v)	RP-18wF$_{254s}$ Mobile phase MeOH:H$_2$O (1:1, v/v)	CN F$_{254s}$ Mobile phase MeOH:H$_2$O (3:7, v/v)	Nano-SIL Diol/UV$_{254}$ Mobile phase MeOH:H$_2$O (4:6, v/v)
1. Sorbic Acid	0.39	0.45	0.40	0.63
2. Potassium Sorbate	0.41	0.44	0.40	0.67
3. Benzoic Acid	0.43	0.47	0.29	0.70
4. Sodium Benzoate	0.48	0.53	0.54	0.73
5. Salicylic Acid	0.37	0.48	0.22	0.58
6. 3-Hydroxybenzoic Acid	0.68	0.61	0.46	0.72
7. 4- Hydroxybenzoic Acid	0.68	0.58	0.44	0.67
8. 4-Aminobenzoic Acid	0.76	0.61	0.41	0.76
9. Sodium Salicylate	0.64	0.67	0.62	0.70
10. Methylparaben	0.44	0.34	0.21	0.45
11. Ethylparaben	0.31	0.25	0.15	0.38
12. Propylparaben	0.20	0.17	0.10	0.27
13. Butylparaben	0.11	0.10	0.05	0.15
14. Ascorbic Acid	0.77	0.82	0.86	0.87
15. Isoascorbic Acid	0.73	0.80	0.86	0.84
16. Gallic Acid	0.81	0.76	0.64	0.72
17. Propyl Gallate	0.55	0.41	0.21	0.44
18. Tert-Buylhydroquinone	0.44	0.33	0.14	0.37

In order to separate and identify preservatives from some commercially available soft drinks, the samples (20 mL) were passed through the C18 column for the solid phase extraction at the rate of approximately 0.5 mL/ minute. The column was conditioned prior to use by washing with methanol (5 mL) and water (5 mL). After retention of the interested compounds from the sample, the column was washed with water (10 mL) and the adsorbed preservatives were eluted with 2 mL methanol. The resulted samples were analyzed by HPTLC using mixtures of methanol:water (1:1 v/v, for RP-18wF$_{254s}$ plates and 3:7 v/v, for CN F$_{254s}$ plates) as mobile phase. The obtained chromatograms are shown in Figure 2.
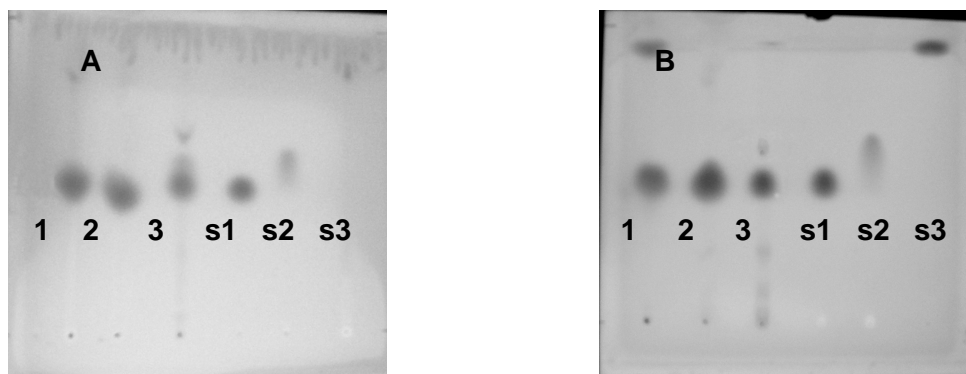
Figure 2. Chromatograms of soft drinks on RP-18wF$_{254s}$ silica gel plates (A) and CN F$_{254s}$ silica gel plates (B) obtained using methanol:water as mobile phase.(1. juice Adria-oranges; 2. juice Giusto natura-tropical and 3. juice Frutti Fresh-pink, s1-standard of potassium sorbate, s2-standard of sodium benzoate, s3-standard of ascorbic acid).

As we can see from chromatograms, using solide-phase extraction on C18 column for sample preparation and TLC method for identification, the preservatives from soft drinks were separated and identified. On RP-18wF$_{254s}$ silica gel plates only potassium sorbate was identified in analysed soft drinks. On CN F$_{254s}$ plates we identified potassium sorbate and ascorbic acid in Adria-orange juice, potassium sorbate in Giusto natura-tropical juice and potassium sorbate and sodium benzoate in Frutti Fresh-pink juice.

CONCLUSIONS

The retention behavior of 18 preservatives has been investigated by TLC on different stationary phases. The best separation was achieved for parabens (which can be found in mixtures in pharmaceuticals and cosmetics) for all types of studied HPTLC plates. The sorbic, benzoic, salicylic, ascorbic acids and salts like potassium sorbate and sodium benzoate (preservatives founded usually together in foods) were accurately separated on CN F$_{254s}$ plates and Nano-SIL Diol/UV$_{254}$ plates.

Ascorbic acid, potassium sorbate and sodium benzoate can be identified from soft drinks using TLC method after sample preparation by solid-phase extraction on C18 column.

EXPERIMENTAL SECTION

The preservatives sorbic acid, potassium sorbate, benzoic acid, sodium benzoate, salicylic acid, 3-hydroxybenzoic acid, 4- hydroxybenzoic acid, 4-aminobenzoic acid, sodium salicylate, methylparaben, ethylparaben,

propylparaben, butylparaben, ascorbic acid, isoascorbic acid, gallic acid, propyl gallate and tert-butylhydroquinone of analytical grade were obtained from Merck or Fluka. The samples analyzed (soft drinks) are commercially available.

Thin-layer chromatography was performed on 10x10 cm glass HPTLC plates coated with silica gel RP-18F$_{254s}$, RP-18wF$_{254s}$, CN F$_{254s}$ and Nano-SIL Diol/UV$_{254}$.

The standard solutions (1 mg mL^{-1}) were prepared in methanol and 2μL of them were applied manually on the plates as spots. Different mixtures of methanol:water (6:4 v/v for RP-18F$_{254s}$ plates, 1:1 v/v for RP-18WF$_{254s}$ plates, 3:7 v/v for CN F$_{254s}$ plates and 4:6 v/v for Nano-SIL Diol/UV$_{254}$ plates) were used as mobile phases. The plates were developed on a distance of 8 cm in a normal chamber (Camag) in all cases. After development the plates were dried in air and inspected under UV illumination at λ=254 nm.

From soft drinks (Adria-oranges, Giusto natura-tropical and Frutti fresh-pink grapefruit) preservatives were isolated using solid-phase extraction on C18 column and identified by RP-TLC on 10x10 cm HPTLC plates coated with silica gel RP-18wF$_{254s}$ and silica gel CN F$_{254s}$.

ACKNOWLEDGMENTS

REFERENCES

1. M. G. Soni, G. A. Burdock, S. L. Taylor, N. A. Greenberg, *Food Chem. Toxicol.*, **2001**, *39,* 513.
2. M.G. Soni, S.L. Taylor, N.A. Greenberg, G. A. Burdock, *Food Chem. Toxicol.*, **2002**, *40*, 1335.
3. J. Ring, K. Brockow, H. Behrendt, *J. Chromatogr. B*, **2001**, *756*, 3.
4. M. Moors, C. R. R. Teixeira, M. Jimidar, D. L. Massart, *Anal. Chimica Acta*, **1991**, *255*, 177.
5. S. A. V. Tfouni, M. C. F. Toledo, *Food Control*, **2002**, *13*, 117.
6. B. Saad, Md. F. Bari, M. I. Saleh, K. Ahmad, Mohd. K. Mohd. Talib, *J. Chromatogr. A,* **2005**, *1073*, 393.
7. F. J. M. Mota, I. M. P. L. V. O. Ferreira, S. C. Cunha, M. Beatriz, P. P. Oliveira, *Food Chemistry,* **2003**, *82*, 469.
8. I. M. P. L. V. O. Ferreira, E. Mendes, P. Brito, M. A. Ferreira, *Food Research International,* **2000**, *33*, 113.

9. E. Mikami, T. Goto, T. Ohno, H. Matsumoto, M. Nishida, *J. Pharm. Biomed. Analysis,* **2002**, *28*, 261.
10. Q. C. Chen, J. Wang, *J. Chromatogr. A*, **2001**, *937*, 57.
11. H. Lian, D. Li, X. Wu, L. Tian, *J. Pharm. Biomed. Analysis*, **2005**, *37*, 369.
12. X. Q. L. F. Zhang, Y. Y. Sun, W. Yong, X. G. Chu, Y. Y. Fang, J. Zweigenbaum, *Anal. Chim. Acta*, **2008**, *608*,165.
13. C. De-Luca, S. Passi, E. Quattrucci, *Food Addit. Contam.,* **1995**,*12*, 1.
14. M. Gonzalez, M. Valcarcel, *J. Chromatogr. A*, **1998**, *823*, 321.
15. C. Dong, W. Wang, *Anal. Chim. Acta*, **2006**, *562*, 23.
16. L. Wang, X. Zhang, Y. Wang, W Wang, *Anal. Chim. Acta*, **2006**, *577*, 62.
17. R.A. Fraizer, E L. Inns, N. Dossi, J. M. Ames, Harry E. Nursten, *J. Chromatogr. A*, **2000**, *876*, 213.
18. M. C. Boyce, *J. Chromatogr. A*, **1999**, *847*, 369.
19. H. Y. Huang, C. L. Chaung, C. W. Chiu, J. M. Yeh, *Food Chemistry*, **2005**, *89*, 315.
20. F. Han, Y. Z. He, C. Z. Yu, *Talanta*, **2008**, *74*, 1371.
21. S. He,Y. Zhao, Z. Zhu, H.Liu, M. Li, Y. Shao, Q. Zhuang, *Talanta,* **2006**, *69*, 166.
22. N. De Kruijf, M. A. H. Rijk, L. A. Pranoto-Soetardhi, A. Schouten, *J. Chromatogr. A*, **1987**, *470*, 395.
23. N. Dimov and K. Filcheva,*J. Planar Chromatogr.*, **1996**, *9*, 197.
24. M. Thomassin, E. Cavalli, Y. Guillaume, C.Guinchard *J. Pharm. Biomed. Anal*., **1997,** *15,* 831.
25. A. Mirzaie, A. Jamshidi, S. W.Husain, *J. Planar Chromatogr.*, **2007**, *20*, 141.
26. S. H. Khan, M. P. Murawski, J. Sherma, *J. Liq. Chromatogr.*, **1994**, *17*, 855.
27. M. C. Smith, J. Sherma, *J. Planar Chromatogr.*, **1995**, *8*, 103.

DIMENSIONLESS ANALYSIS OF THE FREE DROP MOVEMENT AT LOW REYNOLDS NUMBER

MARIA TOMOAIA-COTISEL[a*], AURELIA STAN[b], IOAN-RADUCAN STAN[c]

ABSTRACT. We report on the movement of a free drop at low Reynolds number, initially at rest, by methods of similarity theory and non-dimensional analysis. Because the drop is motionless, we have introduced as scale velocity, a characteristic velocity, U_c, and a new dimensionless number, Ch, which is related to Reynolds number. This permits us to evaluate the Marangoni force in the dimensionless form, as well as the deformation, the translational motion and even the break up of a free drop, under surfactants adsorption.

Keywords: *drop deformation, drop break up, surfactant adsorption, dimensionless number, Marangoni force.*

INTRODUCTION

Numerous problems in surface science deal with molecular motions [1-11] and relaxation phenomena [12-18] at fluid interfaces containing surface active substances (in short surfactants).

Under given conditions, tangential forces may exert in the interface of two liquids, together with the normal pressure. If the surface tension, σ, of the liquid interface changes from point to point, a tangential force will be exerted in addition to the pressure normal to the surface and its magnitude is determined by the surface tension gradient [1], which per unit area is $\vec{p}_t = grad\ \sigma$. The plus sign preceding the gradient indicates that this force tends to move the surface of the liquid in a direction from lower to higher surface tension.

There are many examples where the presence of a surfactant has an important role. Probably the best known is the effect of a surfactant on a liquid drop, immersed in a bulk liquid, initially at rest [2, 3]. The force acting on the unit volume of the drop (with density ρ') immersed in a bulk liquid (of

[a*] *Babes-Bolyai University, Department of Physical Chemistry, Arany Janos Str., Nr. 11, 400028 Cluj-Napoca, Romania; mcotisel@chem.ubbcluj.ro*
[b] *Augustin Maior Technical College, Calea Motilor Str., Nr. 78, 400370 Cluj-Napoca, Romania*
[c] *Babes-Bolyai University, Department of Mechanics and Astronomy, Kogalniceanu Str., Nr. 1, 400084 Cluj-Napoca, Romania*

density ρ), will be cancelled $(\rho-\rho')\ \vec{g}=0$ either when the densities of the two liquids are equal (ρ'=ρ) or in the absence of gravity $\vec{g}=0$ (zero gravity). Such a drop is called "free" and is motionless.

Recently, we have presented both experimental data and theoretical approach [7, 8] on the motion of non-deformed and deformable free drops in a continuous medium. However, to provide accurate description for the movement of a free drop, including the deformation, the translation as well as the breaking up of the drop, the present study explores the drop shapes using dimensionless analysis and a new dimensionless number, which is related to the Reynolds number. Consequently, the Marangoni force in the dimensionless form acting on the drop is calculated.

HYDRODYNAMIC EQUATIONS

We shall consider a viscous liquid drop L' (density ρ') immersed in an immiscible bulk liquid L, (density ρ). If the two liquids have the same density, ρ' = ρ, the drop is called free and is motionless or at zero gravity. The two liquids outside and inside the drop (see Fig.1) are considered Newtonians, incompressible and viscous having the viscosities μ and μ', respectively. The surface between the two liquids is characterized by an interfacial tension, noted σ_0.
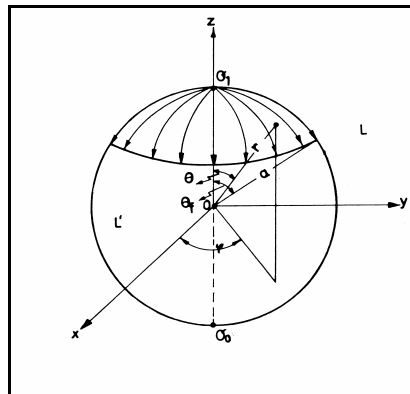
Figure 1. The spreading of a surfactant on a free drop surface

A small quantity of a surfactant (e.g., a droplet of 10^{-3}-10^{-2} cm^3, which is very small compared with the volume of the initial drop) is introduced in a point (called injection point) on the drop surface. The surfactant, because of its molecular structure, is spread and simultaneously adsorbed at the liquid-liquid interface and it is continuously swept along the meridians of the drop, by the convective transport. In the injection point the interfacial tension is

instantaneously lowered to σ_1 ($\sigma_1 < \sigma_0$) value. Since the interfacial tension is a function of the surfactant concentration, a gradient of interfacial tension is established over the surface of the drop. Consequently, the Marangoni spreading of the surfactant takes place from low surface tension to high surface tension.

The equations governing the flow considered quasi steady and axisymmetric [4] are the continuity equations for an incompressible fluid

$$\nabla \cdot \vec{v} = 0 , \tag{1}$$

$$\nabla \cdot \vec{v}' = 0 , \tag{2}$$

where $\vec{v}$ and $\vec{v}'$ are the velocities of the bulk liquid L, respectively, of the liquid L' within the drop, and the Navier- Stokes equations, for a steady flow

$$(\vec{v} \cdot \nabla)\, \vec{v} = -\frac{1}{\rho} \nabla\, p + \nu\, \Delta \vec{v} , \tag{3}$$

$$(\vec{v}' \cdot \nabla)\, \vec{v}' = -\frac{1}{\rho} \nabla\, p' + \nu'\, \Delta \vec{v}', \tag{4}$$

where p, p' are the pressures, outside and inside the drop and $\nu = \dfrac{\mu}{\rho}$,

$\nu' = \dfrac{\mu'}{\rho}$ are the kinematic viscosities of continuous liquid and drop liquid, respectively.

The equation of the interfacial flow [5, 6] is given by

$$\Gamma \left(\vec{w} \cdot \nabla_S \right) \vec{w} = \vec{F} + \nabla_S \sigma + \left(\kappa + \varepsilon \right) \nabla_S \left(\nabla_S \cdot \vec{w} \right), \tag{5}$$

where $\vec{w} = \vec{v}_s$ is the interface velocity, $\vec{F} = \Gamma\, \vec{g} + \vec{T} - \vec{T}'$ is the external force acting on the drop surface, $\vec{T}$ and $\vec{T}'$ are the tractions exerted by the outer and inner liquid on the drop interface, Γ is the surface density, κ and ε are the surface dilatational and shear viscosity, respectively, and ∇_S is the surface gradient operator. Because the surface density is very small ($\Gamma \approx 10^{-7}$g cm^{-2}) the inertial term in (5) can be neglected against the remainder terms.

In order to find the distributions of the velocities $\vec{v}, \vec{v}'$ and of the pressures p, p', the system of Eqs (1)-(5) must be solved taking into account some appropriate boundary conditions [4]. Some details are recently given by our group [7, 8].

The symmetry of the problem suggests a system of spherical coordinates (r, θ, φ) with the origin placed in the drop center and with the Oz axis passing through the sphere, (see fig. 1) in the point of the minimum interfacial tension, i. e., the injection point of the surfactant.

We underline that the surfactant injection point at the drop surface may be taken anywhere, the drop being initially at rest. In the following, we shall take it like shown in Fig. 1. The surfactant front position, in this radial flow, is noted by the angle θ_f.

The interfacial tension, σ, is considered a unique function of the angle θ. Within the surfactant invaded region, $(0 \leq \theta \leq \theta_f)$, for the variation of the interfacial tension with θ, we take [9]

$$\sigma(\theta) = \frac{\sigma_0 - \sigma_1}{1 - \cos \theta_f} (1 - \cos \theta) + \sigma_1 , \tag{6}$$

where $\quad \sigma_0 = \sigma(\theta_f) \quad$ and $\quad \sigma_1 = \sigma(0)$.

Derivation of Eq. (6) gives the interfacial tension gradient in the invaded drop region with surfactant

$$\frac{d\sigma}{d\theta} = \frac{\sigma_0 - \sigma_1}{1 - \cos \theta_f} \sin \theta , \tag{7}$$

where, the interfacial tension, σ_0, is constant in any point of the uncovered surface, while the interfacial tension difference, Π, also called surface pressure is

$$\Pi = \sigma_0 - \sigma_1 , \tag{8a}$$

or

$$\Pi = \sigma_0 (1 - \beta), \tag{8b}$$

where β is the interfacial tensions ratio

$$\beta = \frac{\sigma_1}{\sigma_0} , \tag{9}$$

and arises only in the invaded region. It is clear that only σ_1 and σ_0, i. e. the minimum and the maximum values of the interfacial tension, can be experimentally measured.

The surface flow leads to a stream of liquid directed to the drop along the Oz axis. This stream arises as a consequence of the continual replacement of that liquid layer which has been displayed by the surface flow, like a ventilation effect [3]. We immediately find that as the flow occurs with the driving by viscosity of the outer liquid L, forces of hydrodynamic pressure will act on the drop L'. The resultant of the forces exerted by the fluid on the drop ,F_M, due to the symmetry of the Marangoni flow is oriented along the Oz axis and may be calculated from the general expression of force [4] by integration on the covered drop surface:

$$F_M = \iint_S [(p_{rr})_{r=a} \cos\theta - (p_{r\theta})_{r=a} \sin\theta] \, ds , \tag{10}$$

where S is the surface covered with surfactant, ds is the surface element, and p_{rr} , $p_{r\theta}$ are the normal and tangential components, of the viscous stress tensor [4] on the surface.

88

DIMENSIONLESS ANALYSIS

In dimensionless analysis, a dimensionless quantity (or more precisely, a quantity with the dimensions of 1) is a quantity without any physical units and thus is a pure number. Such a number is typically defined as a product or ratio of quantities which do have units, in such a way that all the units cancel out. For the dimensionless analysis of a mathematical model of a physicochemical phenomenon, the equations that describe the phenomena must be expressed in dimensionless form and therefore all dimensional variables that appear in the hydrodynamics equations must be expressed in terms of characteristic factors of these variables, named the scaling process. In our case the radius (a) of the drop is a characteristic length.

All linear dimensions can therefore be dimensionless ratios, of the form $\bar{r} = \dfrac{r}{a}$. In the same manner, the initial interface tension σ_0 may be considered as the characteristic dimension of the interfacial tension so that we have the dimensionless surface tension $\bar{\sigma} = \dfrac{\sigma}{\sigma_0}$.

Because the drop is initially at rest, we don't possess a characteristic velocity, U_c, so that we shall introduce one, expressed with the aid of some characteristic data of our problem. With these scale references we have the following dimensionless variables:

$$\bar{r} = \frac{r}{a}, \quad \bar{v} = \frac{v}{U_c}, \quad \bar{p} = \frac{p}{\rho U_c^2}, \quad \bar{\sigma} = \frac{\sigma}{\sigma_0}, \quad \bar{F} = \frac{F}{\rho a^2 U_c^2}, \tag{11}$$

where $\bar{v}$ is the dimensionless velocity, $\bar{p}$ represents the dimensionless pressure, $\bar{\sigma}$ is the dimensionless interface tension and $\bar{F}$ stands for the dimensionless force.

The substitute of the dimensionless variables (11) in equations (1, 2) gives

$$\nabla \cdot \vec{\bar{v}} = 0 \tag{12}$$

$$\nabla \cdot \vec{\bar{v}}' = 0 \tag{13}$$

the dimensionless continuity equations. In the same manner from (3, 4) we have

$$(\vec{\bar{v}} \cdot \nabla)\vec{\bar{v}} = -\nabla \bar{p} + \frac{1}{Re}\Delta \vec{\bar{v}} \tag{14}$$

$$(\vec{\bar{v}}' \cdot \nabla)\vec{\bar{v}}' = -\nabla \bar{p}' + \frac{1}{Re'}\Delta \vec{\bar{v}}' \tag{15}$$

89

for the Navier-Stokes dimensionless equations. Here, $\mathrm{Re} = \dfrac{\rho a U_c}{\mu}$ and

Re'=$\dfrac{\rho a U_c}{\mu'}$ are the Reynolds numbers for the outside and inside flows.

If we consider the outer flows with Reynolds number equal to unity, Re = 1 we have

$$U_c = \frac{\mu}{\rho a} \tag{16}$$

This characteristic velocity, U_c, is called sometimes the viscous velocity.

For the flow inside the drop we'll obtain for the Reynolds number

$$\text{Re'}=\frac{\mu}{\mu'}. \tag{17}$$

With the values of the viscosities taken from [3, 8], the Reynolds number corresponding to the drop phase ranges between 1/80 and 1/2; this means that the Reynolds number is less than unity Re'<1. Introducing the ratio of the bulk viscosities [10], $\lambda = \mu'/\mu$, we have also

$$\text{Re'} = 1/\lambda. \tag{18}$$

The velocities of the inner and outer liquid of the drop must satisfy the following kinematic conditions:

- the outer velocity must be zero far from the drop surface,
  $\vec{v}=0$ for $\overline{r} \to \infty$;
- the normal component of the outer and the inner velocities must be zero on the surface of the drop
  $\vec{v}_n = \vec{v}'_n = 0$, at $\overline{r} = 1$
- the tangential velocity components of the two liquids at the interface must be continuous:
  $\vec{v}_t = \vec{v}'_t$ at $\overline{r} = 1$
- the velocity $\vec{v}$' within the drop must remain finite at all points, particularly at the centre of the drop ($\overline{r} = 0$ the origin of the coordinates).
- In addition to these kinematic conditions, a dynamic condition must be fulfilled at the interface, given by (5) in dimensionless form.

Eqs. [12-15] with these appropriate boundary conditions lead to the distribution of the velocity $\vec{v}$ and of the pressures $\overline{p}$, outside the drop:

$$\overline{v}_r = \frac{Ch\,A}{(1-\cos\theta_f)}\left(\frac{1}{\overline{r}^3}-\frac{1}{\overline{r}}\right)\cos\theta\,, \tag{19}$$

$$\overline{v}_\theta = \frac{Ch\,A}{(1-\cos\theta_f)}\left(\frac{1}{2\overline{r}^3}+\frac{1}{2\overline{r}}\right)\sin\theta\,, \tag{20}$$

$$\overline{p} = -\frac{Ch\,A}{(1-\cos\theta_f)}\frac{1}{\overline{r}^2}\cos\theta\,, \tag{21}$$

where A is a dimensionless constant of the following form:

$$A = \frac{(1-\beta)}{3(1+\lambda)}\,. \tag{22}$$

Here, we have introduced a new dimensionless number, Ch, given by:

$$Ch = \frac{\sigma_0\rho\,a}{\mu^2}\,. \tag{23}$$

We named this new dimensionless number, Ch, Chifu's number, as recognition of Chifu's excellent scientific contributions to the examination and characterization of the behavior of liquids under the action of surface tension gradients caused by various surfactants or by differences in temperature, under the normal conditions or in conditions of microgravity [19- 21].

We have to observe that for the proposed characteristic velocity, U_c, we have for the Ch number the following connections with well-known dimensionless numbers, such as capillary number, Ca, Ohnesorge number, Oh, and Weber number, We. So, we have $Ch = \dfrac{1}{Ca}$ where, $Ca = \dfrac{\mu U_c}{\sigma_0}$ is the capillary number, $Ch = \dfrac{1}{Oh^2}$, for $Oh = \dfrac{\mu}{\sqrt{\sigma_0 a\rho}}$ being the Ohnesorge number and $Ch = \dfrac{1}{We}$, where $We = \dfrac{\rho U_c^2\,a}{\sigma_0}$ is the Weber number.

Further, we mention here, that the surface tension σ usually depends on the scalar fields, applied to the system (e.g., the temperature field and the electrical field) as well as on the concentration of foreign materials on the surface (so named surfactants). In the present paper, we focus on the variation due to surfactants (foreign materials) given by σ(θ), which deepens not only on θ but also on σ_0, σ_1, μ and μ', all being concentrate in constant A.

The Marangoni force acting on the drop in dimensionless form is

$$\overline{F}_M(\theta_f) = \frac{2\pi\,Ch\,(1-\beta)}{3(1+\lambda)}(1-2\cos\theta_f - 2\cos^2\theta_f)\,. \tag{24}$$

Eq. (24) represents the dimensionless Marangoni force acting on the drop surface along the Oz axis. It can be seen that this force depends on the θ_f angle, namely, on the extent to which the drop surface is covered by the surfactant, the interfacial tension ratio, β, the ratio of the viscosities, λ, and the dimensionless number Ch.

From (24) it is observed that the force acting on the drop depends direct proportionally on the number Ch.

For further discussions of the dimensionless Marangoni force, it is useful to introduce the function

$$f(\theta_f) = 1 - 2\cos\theta_f - 2\cos^2\theta_f \ . \tag{25}$$

The value of θ_f, for which $f(\theta_f) = 0$, is noted by θ_0, and its value is $\theta_0 \approx 68.53^0$. This θ_0 is the value of θ_f for which the resultant force cancels. Also, we note that for $\theta_f \in [0, \theta_0)$, this function is negative $f(\theta_f) < 0$, and for $\theta_f \in (\theta_0, 180^0]$ the function is positive $f(\theta_f) > 0$, having the greatest value for $\theta_m = 120^0$.

From Eq. (24) it is found that for a coverage degree $\theta_f < \theta_0$ of the drop with surfactant, as a result of the appearance of interfacial tension gradient, the pressure force $\overline{F}_M$ exerted by the external liquid upon the drop is oriented toward the negative direction of the Oz axis (Fig. 1). This is similar with the application of a "hammer" knock on the drop in the injecting point of the surfactant. For a coverage degree θ_f greater than θ_0, the force $\overline{F}_M$ is oriented towards the positive direction of the Oz axis. This is the propulsive (lifting) resultant force $\overline{F}_M > 0$, responsible for the upward movement of the drop.

The action of the Marangoni force $\overline{F}_M$ on the drop is maximum at the injection point of the surfactant, for which $\theta_f = 0$

$$\overline{F}_M(0) = \frac{2\pi Ch(1-\beta)}{1+\lambda} \ , \tag{26}$$

where for physical meanings, we have taken its absolute value. The Marangoni force, noted also $\overline{F}(0)$, produces the hammer effect, identified earlier by us [7, 8]. It depends on Ch number, viscosities ratio, λ, and surface tension ratio, β.

RESULTS AND DISCUSSION

In the following, we present the physical and chemical characteristics of the six investigated experimental systems (Table 1). Each system contains a free drop, initially at rest. Upon the surfactant injection in a particular point on the drop surface, we have experimentally observed the shape modifications and the movement of the drops in time [8].

Table 1. Composition and physical characteristics of the liquid/liquid systems. The drop radius (a) is 1.19 cm for systems 1 and 2 and 0.46 cm for systems 3 to 6.

Sys-tem No.	Density g/cm^3	Continuous Phase (L)			Drop Phase (L')		Surfactant Solution (S)	
		Compo-sition (% vol)	μ(cP)	σ_0(L/L') (dyn/cm)	Compo-sition (% vol)	μ'(cP)	Compo-sition (% vol)	σ_1 (L'/S) (dyn/cm)
1	0.863	Ethanol 78.6 Water 21.4	2.26	7.9	Paraffin oil	80	Propanol 77.3 Water 22.7	3.5
2	0.863	Methanol 78 Water 22	1.33	10.2	Paraffin oil	80	Propanol 77.3 Water 22.7	3.5
3	1.068	NaNO$_3$ 15.1 Water 84.9	1.1	28.7	Chlor benzene 40 Silicon oil 60	8.04	Benzylic alcohol 89 CCl$_4$ 11	3.6
4	1.068	NaNO$_3$ 15.1 Water 84.9	1.1	28.2	Chlor benzene 50 Silicon oil 50	5.46	Benzylic alcohol 89 CCl$_4$ 11	3.6
5	1.066	NaNO$_3$ 15 Water 85	1.1	25.6	Chlor benzene 85 Silicon oil 15	1.40	Benzylic alcohol 89 CCl$_4$ 11	3.5
6	1.064	NaNO$_3$ 14.9 Water 85.1	1.1	22.8	Chlor benzene 92 Silicon oil 8	1.03	Benzylic alcohol 89 CCl$_4$ 11	3.6

Further, we examine the shapes, positions and movements of the six freely suspended drops at zero density difference between the drop and the suspending (continuous) medium. Each free drop is under a different interfacial tension gradient acting on the drop surface. The drop dynamics is investigated as a function of the drop to medium viscosity ratio, λ, the surface tension ratio, β, and the surface pressure, Π.

Furthermore, the experimental data are explored using non-dimensional analysis, and consequently, the dimensionless values of Ch number and of Marangoni hammer force, $\bar{F}(0)$, are calculated and are also given in Table 2.

The surfactant film, spread and adsorbed on the drop surface, exerts a certain surface pressure, Π, which is given by the difference between the interfacial tension σ_0, which is constant in any point of the uncovered surface, and the interfacial tension σ_1 at the injection point with surfactant at the drop surface (Fig. 1). The experimental observations are given in Table 2 for the six investigated systems.

Table 2. Surface pressure, Π, the viscosities ratio, λ, the ratio of surface tensions, β, non-dimensional number, Ch (Eq. (23)), and the Marangoni hammer force, $\bar{F}(0)$ (Eq. (26)), in its non-dimensional form, for the six chosen systems, given in Table 1.

System No.	Π (dyn/cm)	λ	β	Ch x 10^{-4}	$\bar{F}(0)$ x 10^{-4}	Experimental Observations
1	4.4 ± 0.3	35.39	0.44	1.5884	0.1535	The drop remains practically undeformable and motionless. Experimental work is given in [8].
2	6.7 ± 0.3	60.15	0.34	5.9218	0.4014	
3	25.1± 0.3	7.31	0.12	11.6527	7.7494	The drop shows deformations but after 0.6-0.8 sec., it returns to its initial form. A translation motion is also observed [8].
4	24.6±0.3	4.96	0.13	11.4497	10.4961	
5	22.1±0.3	1.27	0.14	10.3746	24.6833	The drop, after 0.3-0.4 sec., breaks up into two droplets. The resulted droplets have translation motion [8].
6	19.2±0.3	0.94	0.16	9.2225	25.0776	

Analyzing the data from Table 2, it is to be noticed that the low values of Marangoni hammer force corresponding to low Ch numbers will not have a strong effect on the drop (see, cases 1 and 2).

At medium values of both Ch and $\bar{F}(0)$, the drops are deformable but they will reach a steady state shape with a small translational movement (see, cases 3 and 4, given in Table 2).

At very high values of the Marangoni hammer force $\bar{F}(0)$ and still high Ch numbers the deformations and particularly the elongations of the drop are high resulting in the breaking up of the drop (cases 5 and 6, given in Table 2).

For chosen λ and Π values, and for an initial drop position, drops show increasingly pronounced deformations with increasing Ch number (cases 3 and 4, Table 2). For very high λ (cases 1 and 2, Table 2) the drops are nondeformable.

94

At λ approximately 1, for high Ch numbers, the drops show increasingly pronounced deformations. Then, a continued drop elongation brings the possible onset of drop break up. The last effect is observed for sufficiently large Ch numbers and Π values and for low λ values (cases 5 and 6, Table 2).

As shown above, the movements of free drops depend on Ch number, viscosities ratio, λ, the surface pressure, Π, and the Marangoni hammer force, $\overline{F}(0)$. From theory and experimental work it is clear that λ ratio has a critical role for drop deformations and translation movement.

Thus, by using the dimensionless analysis, the dimensionless values of Ch number and of Marangoni force $\overline{F}(0)$ were calculated and consequently, the deformations and the movement were accurately described for free drops, at low Reynolds numbers.

CONCLUSIONS

The movement of free drops, such as deformations, translation motion and break up of the free drops, was explored using dimensionless analysis, a new dimensionless number, Ch, which is related with Reynolds numbers, and the Marangoni hammer force, $\overline{F}(0)$ in its dimensionless form.

We found that the movement of free drops suspended in a continuous medium depends on the viscosity ratio, λ, the surface pressure, Π, and dimensionless values of Ch number and of the Marangoni hammer force, $\overline{F}(0)$.

For very viscous drops and not so high values of Π, Ch number and of $\overline{F}(0)$, the drops remain undeformable and a very small translational motion is observed (cases 1 and 2, given in Table 2).

At medium values of $\overline{F}(0)$ and λ, and high values of both surface pressure, Π, and Ch number, the drops are deformable but they will reach a steady state shape with a small translational movement (cases 3 and 4, given in Table 2).

At very high values of the Marangoni hammer force $\overline{F}(0)$ and still high values of Ch numbers and of surface pressure, Π, but for low values of λ, the deformations and particularly the elongations of the drops are high resulting in the braking up of the drops (cases 5 and 6, given in Table 2).

Certainly, the obtained results can be attributed to a complex mechanism including the surface dilution and tip-stretching of the surface tension, as well as capillary forces.

In our opinion, the real flow at the drop interface causes the motion of the neighbouring liquids by viscous traction and generates the Marangoni force, which is the principal factor that develops the deformation and the translational motion of the free drops.

The results of our theoretical hydrodynamic model are in a substantial agreement with the observed experimental data.

EXPERIMENTAL SECTION

The experimental work on the drop dynamics was performed in liquid-liquid systems of equal densities and recently published by us [8].

The mixtures, making up the continuous L phase, were placed in a thermostated vessel of 1 dm^3, made of transparent glass. The drop (L') was made of various radii between 0.46 and 1.19 cm, by using the mixtures described in Table 1.

After the system was stabilized, a small quantity (10^{-3}-10^{-2} cm^3) of the surfactant solution (S) was injected with a micrometric syringe, in a point on the drop surface (injection point in Fig. 1).

The interfacial tension for the liquid/liquid systems, e.g. L/L' and L'/S, was determined by a method based on capillarity [3] and its value is given in Table 1 at constant temperature (20 ± 0.1^{o}C) as described in [8]. The position of the surfactant front and the sequences of the drop dynamics for the six investigated systems are also presented elsewhere [8].

REFERENCES

1. V. G. Levich, "*Physicochemical Hydrodynamics*", Prentice-Hall, Englewood Cliffs, New Jersey, **1962**.

2. R. S. Valentine, W. J. Heideger, *Ind. Eng. Chem. Fund.*, **1963**, *2*, 24.

3. E.Chifu, I. Stan**,** Z. Finta, E. Gavrila*, J .Colloid Interface Sci.,* **1983**, *93*, 140.

4. L. Landau, E. Lifschitz, "*Mecanique des fluides",* Ed. Mir, Moscou, **1971**.

5. L. E. Scriven, *Chem. Eng. Sci.,* **1960**, *12*, 98.

6. R. Aris, "*Vectors, Tensors and the Basic Equations of Fluid Mechanics"*, Prentice-Hall, Englewood Cliffs, New Jersey, **1962**.

7. I. R. Stan, M. Tomoaia-Cotisel, A. Stan, *Bull. Transilvania Univ. Brasov*, **2006,** *13*(48), 357.

8. M. Tomoaia-Cotisel, E. Gavrila, I. Albu, I.-R. Stan, *Studia, Univ. Babes-Bolyai, Chem*., **2007**, *52*(3), 7.

9. I. Stan**,** C.I. Gheorghiu, Z. Kása, *Studia Univ. Babes- Bolyai, Math.,* **1993**, *38*(2), 113.

10. Y. T. Hu, A. Lips, *Phys. Rev. Lett.*, **2003**, *91*, 1.

11. E. Chifu, I. Stan, M. Tomoaia-Cotisel, *Rev. Roum. Chim.,* **2005**, *50* (4), 297.

12. M. Tomoaia-Cotisel, P. Joos, *Rev. Roum. Chim.,* **2004**, *49*(6), 539.

13. P. Joos, A. Tomoaia-Cotisel, A. J. Sellers, M. Tomoaia-Cotisel, *Colloids and Surfaces. B. Biointerfaces*, **2004**, *37*, 83.

14. M. Tomoaia-Cotisel, J. Zsakó, E. Chifu, D. A. Cadenhead, *Langmuir*, **1990**, *6*(1), 191.

15. E. Chifu, M. Tomoaia-Cotisel, M. Sălăjan, A. Chifu, J. Zsakó, *Stud. Univ. Babes-Bolyai, Chem.*, **1989**, *34* (2), 28.

16. M. Tomoaia-Cotisel, J. Zsakó, E. Chifu, D. A. Cadenhead, H. E. Ries, Jr., in "*Progress in Photosynthesis Research*", (J. Biggins, Ed.), *Vol.II*, Martinus Nijhoff Publ., Dordrecht, **1987**, p. 333.

17. F. Monroy, F. Ortega, R. G. Rubio, M. G. Velarde, *Adv. Colloid Interface Sci.*, **2007**, *134-135,* 175.

18. Gh. Tomoaia, A. Tomoaia-Cotisel, M. Tomoaia-Cotisel**,** A. Mocanu, *Cent. Eur. J. Chem.,* **2005**, *3*(2), 347.

19. M. Tomoaia-Cotisel, D. A. Cadenhead, *J. Colloid Interface Sci.,* **1997**, *195*, 271.

20. M. Tomoaia-Cotisel, J. Zsako, *Studia Univ. Babes-Bolyai, Chem.,* **1998**, *43*(1-2), 3.

21. M. Tomoaia-Cotisel, *Studia, Univ. Babes-Bolyai, Chem.*, **2007,** *52*(3), 1.

MORPHOLOGY OF COLLAGEN AND ANTI-CANCER DRUGS ASSEMBLIES ON MICA

LIVIU-DOREL BOBOS[a], GHEORGHE TOMOAIA[b], CSABA RACZ[a], AURORA MOCANU[a], OSSI HOROVITZ[a], IOAN PETEAN[a] AND MARIA TOMOAIA-COTISEL[a*]

ABSTRACT. Self-assemblies of type I collagen (COL) from bovine Achilles tendon and an anti-cancer drug, such as 5-fluorouracil (FLU) or doxorubicin (DOX), on mica substrate are investigated by atomic force microscopy (AFM). The AFM technique allows visualisation of these assemblies and determination of their morphology and surface roughness. The AFM images show different morphology of self assemblies made of COL, COL-FLU and COL-DOX. The data suggest that the anti-cancer drugs guide to the formation of collagen self assemblies with a notable level of stability, reflecting a high level of nanometer scale order within the adsorbed layers on mica surface. These systems might be well appropriate as biological surfaces for biomedical, drug delivery and sensing applications.

Keywords: collagen, fluorouracil, doxorubicin, mica surface, self-assemblies, morphology, atomic force microscopy

INTRODUCTION

The formation of protein self-assemblies from aqueous solutions onto various surfaces is of increasing importance [1-18] with a wide range of applications, including implant biocompatibility, cell adhesion and growth, [10, 11] and biomaterials design [9,10]. Such applications require a controlled morphology of the self-assembled dried layers of biomolecules at various surfaces, as in the case of biosensor devices, for which the distribution of proteins can influence the signal transduction [14] and the cellular response [14, 15]. Several factors drive the nanometer scale organization of protein layers, such as distribution of charged groups in the protein interfacial layer [6,7, 26] and the characteristics of the substrate surface [6,7,21-26].

[a] *Babes-Bolyai University of Cluj-Napoca, Faculty of Chemistry and Chemical Engineering, Department of Physical Chemistry, 11 Arany Janos Str., 400028 Cluj-Napoca, Romania*
[b] *Iuliu Hatieganu University of Medicine and Pharmacy, Department of Orthopedic Surgery and Traumatology, 47 Mosoiu Str., 400132 Cluj-Napoca, Romania*

Type I collagen represents one of the most common form of structural proteins in vertebrates, comprising up to 90% of the skeletons of the mammals. In addition to bones, it is also widespread all over the body, in skin, tendons, ligaments, cornea, intervertebral disks, dentine, arteries and granulation tissues [1,2]. The stability of collagen and its importance for biological processes [26-31] make the collagen an ideal compound for the investigation of protein adsorption onto solid surfaces.

The structure of adsorbed collagen layers on solid substrates [21-27] is essential if the collagen surfaces are to be used as sensing or healing surfaces or as anchorage of biomolecules for drug delivery systems [28-31]. On the other hand, the self-assembly formation of type I collagen is important for biomedical research, the collagen nanostructures being generally involved in many human diseases, including cancer, osteoporosis, atherosclerosis. However, the nanostructure formation of collagen layers is not yet completely understood.

The type I collagen molecule comprises three polypeptide chains (α-chains) which form a unique triple-helical structure composed of two α_1 and one α_2 chains. Chemically, each chain is constructed from repeating amino acid sequences of glycine–X-Y, where X and Y positions may be occupied by any amino acid. Frequently, proline is in the X position and hydroxyproline is in the Y position [2,23]. The type I collagen molecule contains a triple helix of 1.5 nm in diameter flanked by short nonhelical telopeptides. The telopeptides count up for 2% of the collagen molecule and are essential for self-assembly formation [3].

The previous studies concerning the organization of collagen onto solid surfaces [21-27] showed that the collagen presents different morphologies according to the sample history. For example, homogeneous layers of collagen molecules are observed after adsorption or layer by layer deposition on solid substrates (e.g., glass) from diluted acidic collagen aqueous solutions [22]. In contrast, fibrillar structures were obtained depending on the collagen concentrations and the time elapsed for assembly formation in aqueous solutions kept at high temperature of 37 $^{\circ}$C [21]. It was also indicated that the morphology of collagen films can be changed upon drying process, [5,24] or depending on the solid surface characteristics, [21,24-26] like roughness, hydrophilicity as well as the charged surface.

The purpose of this work is to characterize the influence of experimental conditions on the self-assemblies formation of the type I collagen from bovine Achilles tendon (COL) in adsorbed layers on mica, in order to get a deeper insight into the various collagen nanostructures.

The self-assemblies of collagen are examined using three parameters able to affect the nanostructure formation, namely, the chosen period of time for self assembly process in collagen solutions kept at high temperature,

the adsorption time on the mica substrate, and the presence of two anti-cancer drugs in collagen solutions. Among the anti-cancer drugs, we have used 5-fluorouracil (FLU) and doxorubicin (DOX). The self assemblies of COL, COL and FLU and COL and DOX were obtained by adsorption from bulk solutions and drying on mica surface. The nanometer scale organization of collagen both in the absence and in the presence of anti-cancer drugs is followed by atomic force microscopy (AFM).

AFM was specifically chosen to explore the nanostructure of these layers since it is a nondestructive experimental technique under the actual working conditions. In addition, during the last decade, it was recognized that AFM observations [2,5-7,15,18,21,22,26] allow a better understanding of biomolecule layer organization. The AFM has received considerably attention due to its potentiality to analyze in situ a broad range of biological objects. It can be therefore expected that the AFM serves to gain deeper insights into the morphology of collagen layers and into the collagen auto-associative properties. An advantage of AFM observations, particularly when AFM is used in the tapping mode (alternative contact), is offered by topographic and phase images, which are obtained simultaneously. The latter ones present better contrast and resolution than topographic images, and moreover, they furnish further systematic information upon the different phases present in collagen layers. In the following, it is worthwhile to note that the term layer is used interchangeable with film adsorbed on mica surface.

Previously, we studied the nanostructured organization of collagen and anti-cancer compounds on glass surface by using AFM [21,22]. Glass substrates are negatively charged and present a roughness, indicated by root mean square (RMS) values, of about 7 Å obtained by AFM, while the mica surface is atomically flat and more negatively charged than glass. It is therefore of a major interest to investigate these systems on mica support, in order to evidence the effect of a different substrate on the morphology of various collagen nanostructures. The resulted multifunctional bionanostructures are formed by molecular self-assembly of these biocompounds on mica surface during their adsorption from bulk solutions.

RESULTS AND DISCUSSION

A systematic study using atomic force microscopy for collagen self-assemblies adsorbed on mica surface was carried out, trying to evidence the morphology of these layers. We have also investigated the mixtures of type I collagen and an anti-cancer drug (e.g. 5-fluorouracil: FLU or doxorubicin: DOX) as described in experimental section.

The representative AFM images for the pure COL film assembled on mica from its aqueous saline solution are given for a scanned area of 1 μm x 1 μm (Fig. 1) and of 500 nm x 500 nm (Fig. 2).
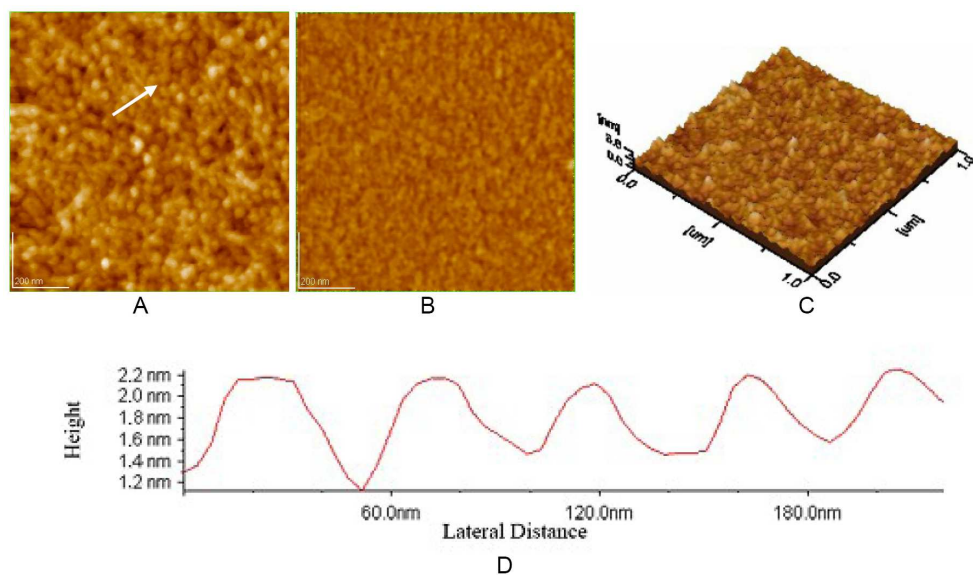
Figure 1. Collagen film on mica. A) 2D – topography; B) phase image; C) 3D-topography; D) profile of the cross section along the arrow in Fig. 1A. Scanned area: 1 µm x 1 µm.
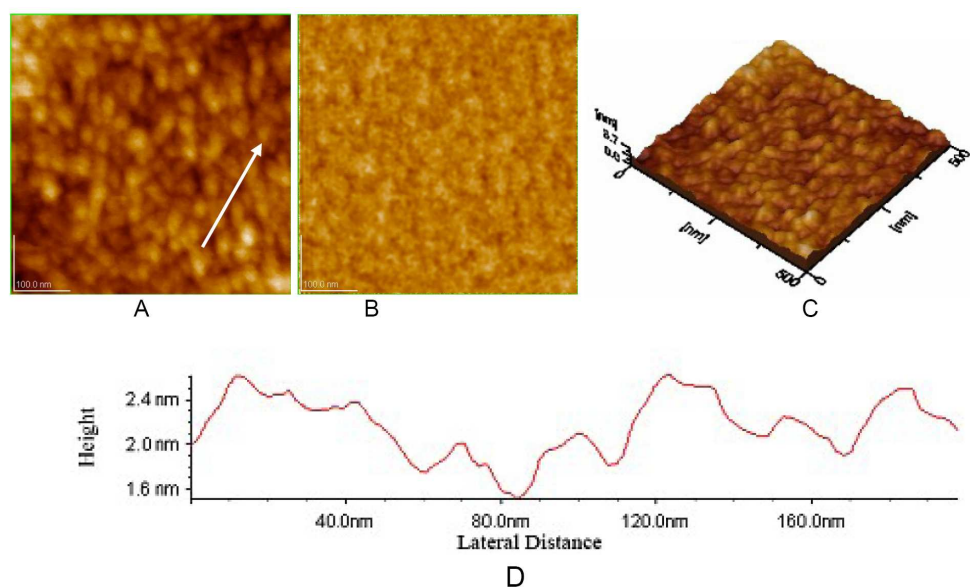
Figure 2. Collagen film on mica. A) 2D – topography; B) phase image; C) 3D-topography; D) profile of the cross section along the arrow in Fig. 2A. Scanned area: 0.5 µm x 0.5 µm.

From these images the self-organisation of collagen molecules can be observed, both in the topographic (Figs. 1A and 2A) and in the phase images (Figs. 1B and 2B), as well as in the three-dimensional (3D) topographies (Figs. 1C and 2C). The phase images present a very good contrast and high resolution. The AFM images indicate the association of collagen molecules in a globular structure. The height of the collagen film on mica, estimated from the cross section profiles (Figs. 1D and 2D), is in the range 2 to 2.2 nm. The thickness of the collagen film on mica is comparable with that corresponding to the collagen film on glass (comprised between 1.4 nm and 1.6 nm [22]) or with the 1.5 nm value reported for the diameter of the collagen molecule [1,2,17].

The surface roughness of the COL film on mica, measured by the RMS values on the film surface (0.4 nm, Figs. 1A and 2A, Table 1) and on the cross section profile (0.2 nm, Figs. 1D and 2D, Table 1) is much lower then for the similar films on glass (e.g., RMS of 1.0-1.8 nm on film area and RMS of 0.4-0.6 nm on cross profile) [22]. These observations indicate the formation of nearly homogeneous layers of collagen molecules by their adsorption on the mica surface. Obviously, a flattening of the collagen films is observed, caused at least in part by the strong interaction of films with the mica surface. Therefore the physical and chemical properties of the hydrophilic surface (e.g., mica or glass) affect the nanostructure of collagen self-assemblies. Accordingly, the mica surface structure mediates the interactions between the solid surface and the collagen molecules adsorbed onto that surface.

Table 1. RMS values for collagen, anti-cancer drugs, and collagen mixtures with an anti-cancer drug as adsorbed layers on mica surface, obtained from AFM observations. RMS roughness measurements are given for the scanned areas or on the cross section profiles of these layers

Fig.	Sample	RMS on area, nm	RMS on profile, nm
1	Collagen, scanned area: 1 µm x 1 µm	0.4	0.2
2	Collagen: 0.5 µm x 0.5 µm	0.4	0.2
-	5-Fluorouracil: 1 µm x 1 µm	0.7	0.5
-	Doxorubicin: 1 µm x 1 µm	0.8	0.4
-	Collagen and 5-fluorouracil: 1 µm x 1 µm	0.3	0.2
3	Collagen and 5-fluorouracil: 0.5 µm x 0.5 µm	0.3	0.3
-	Collagen and doxorubicin: 1 µm x 1 µm	0.9	0.6
4	Collagen and doxorubicin: 0.5 µm x 0.5 µm	1.1	0.4

Because mica is a hydrophilic, negatively charged substrate, while collagen is positively charged in acid aqueous solutions (pH about 3), it is apparent that electrostatic interactions might contribute, at least in part, to a relatively high stability of these assembled layers. These observations made on type I collagen from bovine Achilles tendon are quite similar to those made on dried samples of type I collagen from calf skin on hydrophilic substrate, such as plasma oxidized polystyrene [3] in suitable experimental conditions. On the other hand, random drying patterns of COL assemblies were also reported due to the drying process of COL solutions on mica [34].

Due to its structure, [1,23,29] collagen is not expected to undergo conformational changes [24] upon adsorption, except in the telopeptide zones. The driving force for adsorption is expected to be a gain of entropy due to the release of water molecules, [24] along with the role of electrostatic interactions that can not be ruled out under the working conditions.

The AFM images for the mixed films of collagen and an anti-cancer drug assembled on mica surface are given in Figs. 3 and 4.
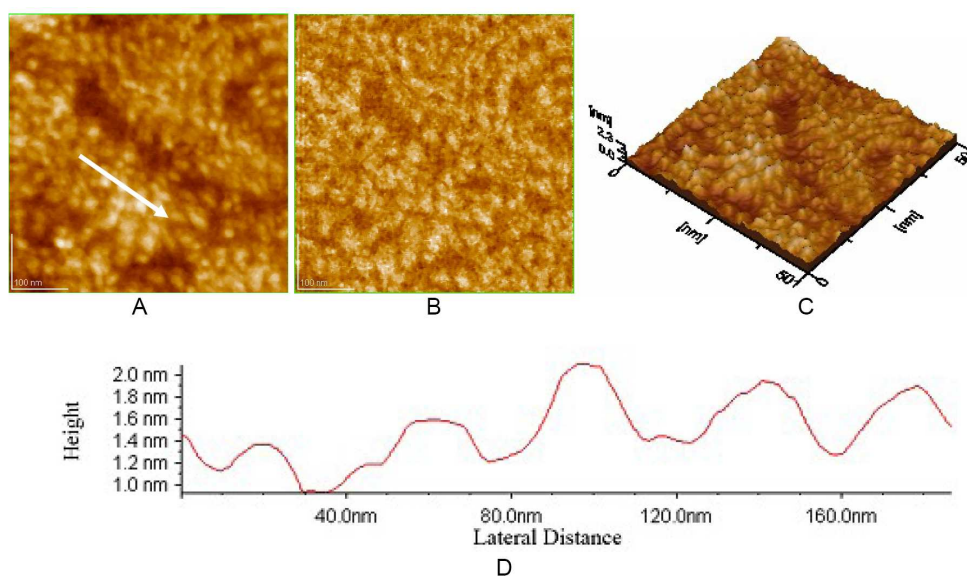
Figure 3. Collagen with 5-fluorouracil film on mica. A) 2D – topography; B) phase image; C) 3D-topography; D) profile of the cross section along the arrow in Fig. 3A. Scanned area: 0.5 μm x 0.5 μm.

For the mixed COL and FLU films, AFM images are given for a scanned area of 0.5 μm x 0.5 μm (Fig. 3). In Fig. 3 (A, B, C) a nanostructured mixed COL and FLU assembly is observed. The structure of COL and FLU film is rendered by rows arranged approximately parallel. Film thickness is about

104

2 nm (Fig. 3D). The RMS roughness of mixed COL and FLU films is of 0.3 nm for scanned areas (Fig. 3A) and 0.3 nm for profile given in Fig. 3D. It is to be noted that the roughness of mixed COL and FLU films shows almost the same RMS values as for pure COL films (Table 1). These findings indicate that FLU seems to penetrate and be entrapped within the COL matrix in a substantial agreement with data reported for the mixed hydrogel [28] made of collagen and poly(hydroxyethyl methacrylate) containing FLU. The FLU appears to stabilize the COL film and generate stable 2D- and 3D-nanostructures with a low roughness in comparison with its corresponding films on glass [22].
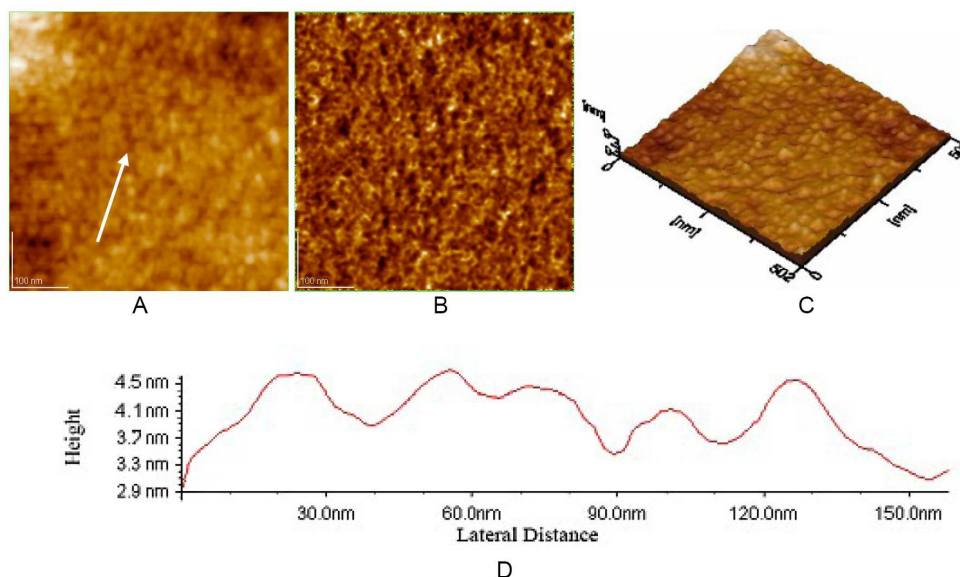
Figure 4. Collagen with doxorubicin film on mica. A) 2D – topography; B) phase image; C) 3D-topography; D) profile of the cross section along the arrow in Fig. 4A. Scanned area: 0.5 μm x 0.5 μm.

The AFM images for the COL and DOX films assembled on mica from mixed aqueous solutions are given for a scanned area of 0.5 μm x 0.5 μm in Fig. 4. The mixed COL and DOX films present a homogeneous nanostructure (Figs. 4A-4C), similar those formed on glass [22], but morphologically on mica surface these formations are much smaller. The film thickness is about 4.6 nm (Fig. 4D) very close to the values corresponding for pure DOX films on mica [35]. Because the DOX molecule is large, its binding to COL molecules leads to thicker mixed COL and DOX films when compared with pure COL layers (Figs 1D and 2D). Moreover, the RMS roughness (Table 1) is close to that of pure DOX film on mica [35]. For example, RMS value for mixed COL and

DOX film is of about 1.1 nm for scanned area of 0.5 µm x 0.5 µm rather close to RMS values for pure DOX film (of 0.8 nm) [35]. For cross section profiles, RMS roughness is about 0.4 nm (Fig. 4D) and coincides with 0.4 nm for pure DOX films [35]. The roughness of COL and DOX films is also increased in comparison with pure COL layers on mica (Table 1). However, the RMS roughness for COL and DOX films on mica is smaller than its corresponding value for the mixed COL and DOX layers on glass [22].

From this investigation, we suggest that the anti-cancer drugs as FLU or DOX can be incorporated into collagen layers by specific lateral interactions between components, such as hydrogen bonding, or simply by entrapment. The binding between collagen and anti-cancer drug might take place through molecular recognition between the less ordered zone of collagen, named telopeptides, and anti-cancer drug leading to more ordered mixed self assemblies. The mixed COL and FLU or COL and DOX layers present a good adhesion on mica surface, which in turn gives a high stability of these nanostructured self assemblies.

The morphology of the collagen assemblies is also modified depending on the characteristics of the solid surface, such as roughness and surface charge. As mentioned above, mica surface is atomically flat and has a more negative charge than glass. On the hydrophilic mica support, smooth collagen layers are formed, presenting a globular structure (Figs. 1 and 2). În the presence of anti-cancer drugs, the structure of collagen on mica presents characteristic features particularly for COL and FLU (Fig. 3). As compared with the corresponding layers on glass [22], it is clear that the interaction of these layers with the mica surface is stronger and generally the self assemblies are better organized showing low roughness in all these cases.

The advanced assembly of collagen both in absence and in presence of anti-cancer drugs are stable and may be used to cover the implants needed in nanomedicine, due to their biocompatibility with natural structures.

CONCLUSIONS

The nanostructured self assembly of type I collagen, in the absence and in the presence of two anti-cancer drugs (FLU or DOX) was investigated by adsorption from bulk solutions on mica surface by AFM, operated in tapping mode. The AFM observations enabled the examination of morphology, thickness and surface roughness of these layers at the nanometer scale and confirmed that these biomolecules form supramolecular associations on mica surface.

This work shows that the interaction of these self assemblies of COL, COL : FLU or COL : DOX with mica surface is strong and generally the layers are better organized than those adsorbed on glass substrate. The difference in the nanostructured organization of these layers is attributed, at

least in part, to the electrostatic interaction with the mica surface, which is more negatively charged than glass. In addition, the specific interactions between these molecules within the self assembled layers could be explained by hydrogen bonds, but the simple entrapment of drug molecules into the collagen matrix can not be rulled out.

Our findings could offer a strong promise for nanometer scale engineering of collagen self-assembling systems focused on the design and production of novel biomaterials with applications in nanoscience and nanobiotechnology.

On the other hand, a direct incorporation of small molecules, such as anti-cancer drugs, into the collagen assemblies represents a step toward rational design of nanostructured materials for potential applications in industry, medicine and synthetic biology, for drug delivery systems and nanobiotechnology.

In our laboratories the efforts to develop new drug delivery systems continue, because no anti-cancer drug kills selectively the cancer cells, without toxicity to normal cells.

EXPERIMENTAL SECTION

Materials and solutions. Type I collagen (COL, from bovine Achilles tendon) was purchased from Sigma-Aldrich Chemical, Corp., Milwaukee, WI. It was dissolved in 0.167 M acetic acid solution at 4 ^{o}C and an aqueous acidic solution of collagen concentration of 0.5 mg/mL was obtained (pH $\approx$ 3). After sonication for 30 min, the collagen solution was filtered through a 0.45 µm Millipore filter to remove pre-aggregated collagen oligomers. From this initial collagen solution, two series of stock solutions were prepared, one in the absence and the other in the presence of an anti-cancer drug. The stock collagen solution was obtained starting from the initial collagen solution mixed at 37 ^{o}C with an equal volume of 0.3 M NaCl solution. Similarly, the stock mixed collagen solutions containing an anti-cancer drug were prepared, but the aqueous saline solution contained also 0.1 mM anti-cancer drug.

The used anti-cancer drugs are doxorubicin hydrochloride (DOX, of purity >98% by TLC) and 5-fluorouracil (FLU, minimum 99% by TLC), both purchased from Sigma-Aldrich Chemical. The aqueous solutions of DOX (in 0.3 M NaCl) and FLU in ethanol and water mixture (1:1 v/v, containing 0.3 M NaCl), of the initial concentration in anti-cancer drug of about 0.1 mM, were obtained. Ultra pure deionised water [32,33] was used (pH 5.6) in all experiments. In the resulted final solutions of collagen or of collagen and anti-cancer drugs, the collagen concentration of about 250 µg/mL was obtained.

The final collagen solutions both in the absence and in the presence of anti-cancer drugs were allowed to stand at high temperature of 37 ^{o}C, for 1, 10 h or even 48 h, to let the auto-association of collagen in solutions with the view of the formation of supramolecular assemblies. For comparison

with our previous work, [22] we will present our results for 48 h elapsed time at high temperature for assembly formation in bulk aqueous solutions. After the heating period, the final solutions of collagen were further used to prepare self assemblies adsorbed on mica surface at room temperature. By using the above experimental strategy, the aggregation of collagen in bulk solution might be induced by increasing the ionic strength and the temperature of the initial cold collagen solution, in substantial agreement with findings on type I collagen from calf skin [2,5,15].

Mica substrate and self assembled layers. The used hydrophilic substrates are mica plates of 1 cm x 1 cm surface area. The mica surface was freshly cleaved before adsorption of collagen with or without anti-cancer drugs. At room temperature, the final solution (about 2 mL), both in the absence or in the presence of anti-cancer drugs, was added to each horizontal mica substrate. The samples were incubated at room temperature, for the chosen periods of time. For the sake of comparison with our previous studies, [22] for all samples presented here, the adsorption time lasted 30 min. This chosen period of time enabled the collagen, as well as the collagen with anti-cancer drug, to adsorb and assemble on mica surface.

After the adsorption time, the samples were rinsed with deionised water. For each sample, there were made two identical preparations, because two different washing modes were applied to the samples. A washing procedure was used by adding 3 mL of deionised water, directly to the sample being in contact with the bulk solution, stirring gently, pumping 3 mL of solution, adding 3 mL of water, and repeating these last steps five times, in order to eliminate the salt and other solution ingredients adsorbed on the sample.

For the other series of preparations, after the adsorption time, the samples were gently taken out from bulk solutions and another washing procedure was applied by adding water (about 20 mL) on slightly tilted substrates, with adsorbed layers on them.

Afterwards, all rinsed samples were dried slowly in air, being dust protected, and used for AFM examination. No significant differences were observed for the two different washing procedures indicating that the adsorbed layers have good adhesion and are rather stable on mica surface.

Atomic force microscopy (AFM). The AFM investigations were executed on collagen samples, without and with anti-cancer drugs, using a commercial AFM JEOL 4210, operating in tapping (noted *ac*) mode. Standard cantilevers, non-contact conical shaped of silicon nitride, coated with aluminium were used. The tip was on a cantilever with a resonant frequency in the range of 200 - 330 kHz and with a spring constant between 17.5 and 50 N/m. AFM observations were repeated on different areas from 20 μm x 20 μm to 0.5 μm x 0.5 μm of the same sample.

The images were obtained from at least ten macroscopically separated areas on each sample. All AFM experiments were carried out under ambient laboratory conditions (about 20 ^{o}C) as previously reported [6,7,21,22]. All images were processed using the standard procedures for AFM.

ACKNOWLEDGEMENT:

REFERENCES

1. C.C. Dupont-Gillain, I. Jacquemart and P.G. Rouxhet, *Colloid and Surfaces. B: Biointerfaces*, **2005**, *43*, 178.

2. E. Gurdak, P. G. Rouxhet and Ch. C. Dupont-Gillain, *Colloid and Surfaces. B: Biointerfaces*, **2006**, *52*, 76.

3. K.E. Kadler, D.F. Holmes, J.A. Trotter and J.A. Chapman, *Biochem. J,* **1996**, *316,* 1.

4. J.P. Orgel, T.J. Wess and A. Miller, *Structure*, **2000**, *8,* 137.

5. V.M. De Cupere and P.G. Rouxhet, *Surface Sci.*, **2001**, *491*, 395.

6. M. Tomoaia-Cotisel, "The nanostructure formation of the globular seed storage protein on different solid surfaces studied by atomic force microscopy", In *Convergence of Micro-Nano-Biotechnologies*, Series in *Micro and Nanoengineering*, *Vol.* 9, Editors: Maria Zaharescu, Emil Burzo, Lucia Dumitru, Irina Kleps and Dan Dascalu, Roumanian Academy Press, Bucharest, 2006, p. 147.

7. M. Tomoaia-Cotisel, A. Tomoaia-Cotisel, T. Yupsanis, Gh. Tomoaia, I. Balea, A. Mocanu and Cs. Racz, *Rev. Roum. Chim.,* **2006**, *51*,1181.

8. O. Horovitz, Gh. Tomoaia, A. Mocanu, T. Yupsanis and M. Tomoaia-Cotisel, *Gold Bull.*, **2007,** *40*, 213.

9. J. T. Elliott, J. T. Woodward, A. Umarji , Y. Mei and A. Tona, *Biomaterials*, **2007**, *28*, 576.

10. M. Brama, N. Rhodes, J. Hunt, A. Ricci , R. Teghil, S. Migliaccio, C. Della Rocca, S. Leccisotti, A. Lioi, M. Scandurra, G. De Maria, D. Ferro, F. Pu, G. Panzini, L. Politi and R. Scandurra, *Biomaterials*, **2007**, *28*, 595.

11. S. Rammelt, T. Illert, S. Bierbaum, D. Scharnweber, H. Zwipp and W. Schneiders, *Biomaterials*, **2006***, 27*, 5561.

12. I.J.E. Pamula, V.M. De Cupere, P.G. Rouxhet and C.C. Dupont-Gillain, *J. Colloid Interface Sci.*, **2004**, *278*, 63.

13. I.J.E. Pamula, V.M. De Cupere, Y. F. Dufrene and P.G. Rouxhet, *J. Colloid Interface Sci.*, **2004**, *271*, 80.

14. F.A. Denis, P. Hanarp, D.S. Sutherland, J. Gold, C. Mustin, P.G. Rouxhet and Y.F. Dufrene, *Langmuir*, **2002**, *18*, 819.

15. K. Kato, G. Bar and H.-J. Cantow, *Eur. Phys. J.*, **2001**, *E6*, 7.

16. R. Usha, R. Maheshwari, A. Dhathathreyan and T. Ramasami, *Colloid and Surfaces. B: Biointerfaces*, **2006**, *48*, 101.

17. K. Poole, K. Khairy, J. Friedrichs, C. Franz, D. A. Cisneros, J. Howard and D. Mueller, *J. Mol. Biol.*, **2005,** *349*, 380.

18. Y.F. Dufrene, T.G. Marchal and P.G. Rouxhet, *Langmuir*, **1999**, *15*, 2871.

19. I. Bratu**,** M. Tomoaia–Cotisel**,** G. Damian and A. Mocanu, *J. Optoelectron. Adv. Mat.*, **2007**, *9*, 672.

20. M. Tomoaia-Cotisel, A. Mocanu, N. Leopold, M. Vasilescu, V. Chiş and O. Cozar, *J. Optoelectron. Adv. Mat.,* **2007**, *9*, 637.

21. Gh. Tomoaia, M. Tomoaia-Cotisel, A. Mocanu, O. Horovitz, L.D. Bobos, M. Crisan and I. Petean, *J. Optoelectron. Adv. Mat.,* **2008**, *10,* 961*.*

22. Gh. Tomoaia, V.D. Pop-Toader, A. Mocanu, O. Horovitz, D. L. Bobos and M. Tomoaia-Cotisel, *Studia Univ. Babes-Bolyai, Chem.*, **2007**, *52* (4), 137.

23. E. Gurdak, J. Booth, C. J. Roberts, P. G. Rouxhet and Ch. C. Dupont-Gillain, *J. Colloid Interface Sci.*, **2006**, *302*, 475.

24. I. Jacquemart, E. Pamula, V.M. De Cupere, P. G. Rouxhet and Ch. C. Dupont-Gillain, *J. Colloid Interface Sci.*, **2004**, *278*, 63.

25. S. E. Woodcock, W. C. Johnson and Z. Chen, *J. Colloid Interface Sci.*, **2005**, *292*, 99.

26. J. Friedrichs, A. Taubenberger, C. M. Franz and D. J. Muller, *J. Mol. Biol.*, **2007**, *372*, 594.

27. P. Arpornmaeklong, N. Suwatwirote, P. Pripatnanont and K. Oungbho, *Int. J. Oral Maxillofac. Surg.*, **2007**, *36*, 328.

28. R. Jeyanthi and K. Panduranga Rao, *J. Controlled Release*, **1990**, *13*, 91.

29. W. Friess, *Eur. J. Pharmaceutics Biopharmaceutics*, **1998**, *45*, 113.

30. C. H. Lee, A. Singla and Y. Lee, *Int. J. Pharmaceutics*, **2001**, *221*, 1.

31. T. Takezawa, T. Takeuchi, A. Nitani, Y. Takayama, M. Kino-oka, M. Taya and S. Enosawa, *J. Biotech.*, **2007**, *131*, 76.

32. P. Joos, A. Tomoaia-Cotisel, A. J. Sellers and M. Tomoaia-Cotisel, *Colloids and Surfaces. B: Biointerfaces*, **2004**, *37*, 83.

33. Gh. Tomoaia, A. Tomoaia-Cotisel, M. Tomoaia-Cotisel and A. Mocanu, *Centr. Eur. J. Chem.,* **2005**, *3*, 347.

34. M. Mertig, U. Thiele, J. Bradt, G. Leibiger, W. Pompe and H. Wendrock, *Surface and Interface Analysis*, **1997**, *25*, 514.

35. Gh. Tomoaia, C. Borzan, M. Crisan, A. Mocanu, O. Horovitz, L.-D. Bobos and M. Tomoaia-Cotisel, *Rev. Roum. Chim.,* **2009** (in press).

DISTANCE MATRIX AND WIENER INDEX OF ARMCHAIR POLYHEX NANOTUBES

SHAHRAM YOUSEFI[a], ALI REZA ASHRAFI[a,*]

ABSTRACT. The Wiener index of a molecular graph G is defined as the sum of all distances between distinct vertices of G, where the distance between two atoms is the minimum number of bonds connecting them in G. In this paper an algorithm for computing distance matrix of an armchair polyhex nanotube is introduced. As a consequence, the Wiener index of this type of nanotubes is computed.

Keywords: Armchair polyhex nanotube, distance matrix, Wiener index.

INTRODUCTION

A large number of chemical and physical properties of various small molecules are closely related to the topological nature of their skeletal structure. Thus, some quantitative measures reflecting the essential features of a given topological structure have been introduced for the prediction of their properties. Such measures are called topological indices [1,2]. Topological indices are graph invariants and are used for Quantitative Structure-Activity Relationship (QSAR) and Quantitative Structure-Property Relationship (QSPR) studies. The QSAR and QSPR studies are the active areas of chemical research that focus structure-dependent chemical behavior of molecules, [3].

Among topological indices, the Wiener index [4] is probably the most important one. This index was introduced by the chemist H. Wiener to demonstrate correlations between physicochemical properties of organic compounds and the topological structure of their molecular graphs. He defined his index as the sum of distances between any two carbon atoms in the molecules, in terms of carbon-carbon bonds. Next Hosoya named such a graph invariant, topological index, [5]. We encourage the reader to consult papers [6,7] and references therein, for further study on the topic.

The problem of computing topological indices of nanostructures raised by Diudea and his co-authors, [8-14]. The presented authors computed the distance matrix of a polyhex and $TUC_4C_8(R/S)$ nanotori as well as zig-zag

---

[a] *Institute for Nanoscience and Nanotechnology, University of Kashan, Kashan, Iran*
[*] *Author to whom correspondence should be addressed. (E-mail: ashrafi@kashanu.ac.ir)*

polyhex nanotube, [15-19]. In this paper we continue this program to find an algorithm for computing distance matrix of an armchair polyhex nanotube, Figure 1. As an immediate consequence, the Wiener index of this type of nanotubes is computed.

Throughout this paper our notation is standard and taken mainly from [20].
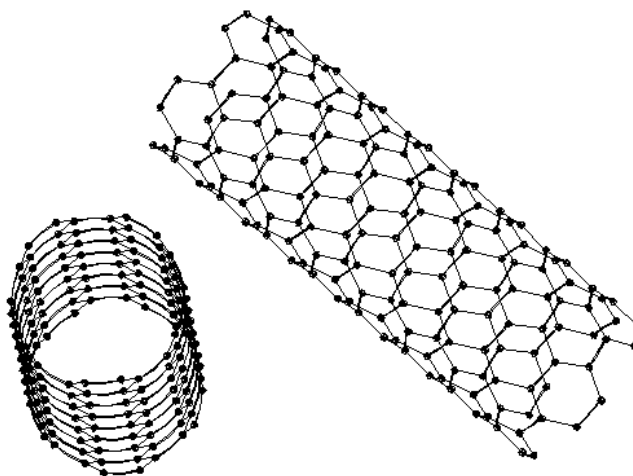
Figure 1. An Armchair Polyhex Nanotube.

RESULTS AND DISCUSSION

Carbon nanotubes form an interesting class of carbon nanomaterials. These can be imagined as rolled sheets of graphite about different axes. There are three types of nanotubes: armchair, chiral and zigzag structures. Further nanotubes can be categorized as single-walled and multi-walled nanotubes and it is very difficult to produce the former.

Diudea, Stefu, Pârv and John [9] computed the Wiener index of an armchair polyhex nanotube $T = TUVC_6[n,m]$, for the first times. Here n is twice the number of vertical crenels and m is the number of rows, see Figure 2. It is obvious that n is even and $|V(T)| = mn$. In this section, distance matrices of these nanotubes are computed.

We first choose a base vertex b from the 2–dimensional lattice of $T = TUVC_6[m,n]$, Figure 2 and assume that $x_{i,j}^{(1,1)}$ is distance between (1,1) and (i,j). This defines a matrix

$$X_{m \times n}^{(1,1)} = [x_{i,j}^{(1,1)}], \text{ where } x_{1,1}^{(1,1)} = 0, \quad x_{1,2}^{(1,1)} = x_{2,1}^{(1,1)} = 1. \tag{1}$$

It is clear that by choosing different base vertices, we find different distance matrices of T. Suppose $s_k^{(p,q)}$ is the sum of kth row of $X_{m \times n}^{(p,q)}$, where (p,q) is the base vertex. Then $s_k^{(p,1)} = s_k^{(p,q)}$, $1 \leq k \leq m$, $1 \leq p \leq m$ and $1 \leq q \leq n$. On the other hand, by Eq. (1) and choosing a fixed column, we have:

$$s_k^{(i,j)} = \begin{cases} s_{i-k+1}^{(1,1)} & 1 \leq k \leq i \leq m, \ 1 \leq j \leq n \\ s_{k-i+1}^{(1,1)} & 1 \leq i \leq k \leq m, \ 1 \leq j \leq n \end{cases}. \tag{2}$$
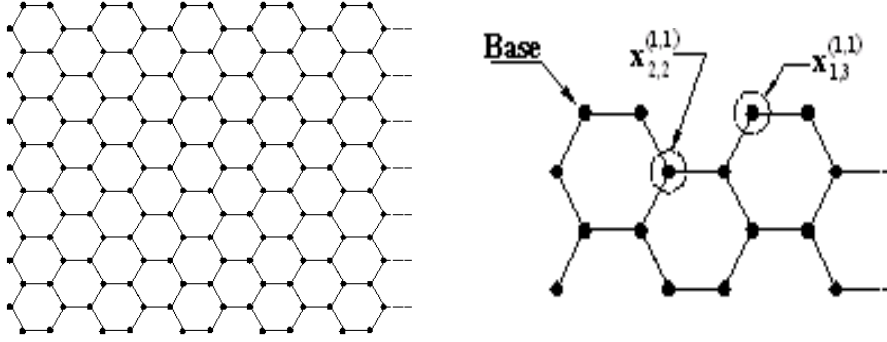
Figure 2. The 2–Dimensional Fragments of an Armchair Polyhex Nanotube.

We now define two matrices $A_{(n/2+1) \times n}$ and $B_{(n/2+1) \times n}$ by the following equations:

$$a_{1,j} = \begin{cases} a_{1,j-1}+1 & j \leq (n/2)+1 \\ a_{1,j-1}-1 & j > (n/2)+1 \end{cases}; \quad a_{2,j} = \begin{cases} a_{1,j}+1 & j \leq (n/2)+1 \\ a_{1,j}-1 & j > (n/2)+1 \end{cases} \quad 2 \mid j,$$

$$a_{2,j} = \begin{cases} a_{2,j-1}+1 & j \leq (n/2)+1 \\ a_{2,j-1}-1 & j > (n/2)+1 \end{cases}; \quad a_{1,j} = \begin{cases} a_{2,j}+1 & j \leq (n/2)+1 \\ a_{2,j}-1 & j > (n/2)+1 \end{cases} \quad 2 \nmid j,$$

$$a_{i,j} = \begin{cases} a_{1,j} & 2 \nmid i \\ a_{2,j} & 2 \mid i \end{cases}; \ a_{1,1}=0; \ a_{2,1}=1, \tag{3}$$

$$b_{n/2+1,j} = \begin{cases} n/2+j-1 & j \leq n/2+1 \\ 3n/2-j+1 & j > n/2+1 \end{cases}; \ b_{i,j} = b_{i+1,j}-1, i < n/2+1.$$

113

By Eqs. 1-3, one can prove:

$$x_{i,j}^{(1,1)} = \begin{cases} c_{i,j} & i \le (n/2)+1 \\ x_{i-1,j}^{(1,1)}+1 & i > (n/2)+1 \end{cases}, \quad c_{i,j} = \text{Max}\{a_{i,j}, b_{i,j}\}. \qquad (4)$$

We now apply Eqs. 2-4 to compute the distance matrix $X_{m \times n}^{(p,q)}$ related to vertex (p,q) is computed. Suppose $s_i^{(p,q)}$ is the sum of ith row of $X_{m \times n}^{(p,q)}$. Then, we have:

$$s_i^{(1,q)} = \begin{cases} (n^2/2)+i^2-2i+(1/2)\left(1-(-1)^{\left(\frac{n}{2}-1\right)}\right) & i \le n/2+1 \\ (n^2/4)+n(i-1) & i > n/2+1 \end{cases}, 1 \le i \le m; 1 \le q \le n. \quad (5)$$

Suppose S_p is the sum of all entries of distance matrix $X_{m \times n}^{(p,q)}$. Then

$$S_1 = \sum_{i=1}^{m} s_i^{(1,q)} \qquad \text{and} \qquad S_p = S_1 + \sum_{i=2}^{p} s_i^{(1,q)} - \sum_{i=m-p+2}^{m} s_i^{(1,q)}. \qquad \text{Thus}$$

$$S_1 = \begin{cases} (m/6)(3n^2+2m^2-3m-2)+\left[(-1)^{(n/2)}/4\right]\left[1-(-1)^m\right] & m \le n/2+1 \\ (n/24)(n^2+12m^2+6mn+3n-12m-4)+(1/4)\left[(-1)^{(n/2)}-1\right] & m > n/2+1 \end{cases}. \qquad (6)$$

If $m \le n/2+1$ then a direct calculation shows that

$$S_p = (m/6)(3n^2+2m^2+3m-2)-mp(m-p+1)-(1/4)\left[(-1)^{\left(\frac{n}{2}+p\right)}\right]\left[1-(-1)^m\right]. \qquad (7)$$

Hence it is enough to consider case that m > n/2 + 1. To complete this case, we consider three sub cases as follows:

I) $p \le n/2+1$, $p \le m-n/2+1$. In this case, we have:
$$S_p = (n/24)(n^2+12m^2+6mn-3n+12m-4)+(p^2/2)(n-1)+(p/12)(3n^2-6n-12mn-4)$$
$$+(p^3/3)+(1/4)\left[1-(-1)^{\left(\frac{n}{2}+p\right)}\right].$$

II) $m-n/2+1 < p \le n/2+1$. In this case, we have: $\qquad (8)$
$$S_p = (m/6)(3n^2+2m^2+3m-2)-mp(m+1)+mp^2-(1/4)\left[(-1)^{\left(\frac{n}{2}+p\right)}\right]\left[1-(-1)^m\right].$$

III) $p > n/2+1$. In this case, $S_p = (n^3/12)-(n/3)+(mn/4)(n+2m+2)-np(m+1)+np^2$.

We now apply Eqs. 5-8 to compute Wiener index of this nanotube. Therefore,

$$W_{m \times n} = \begin{cases} n\left(\sum_{i=1}^{(m-1)/2} S_i + (1/2)S_{(m+1)/2} \right) & 2 \mid m \\ n\sum_{i=1}^{m/2} S_i & 2 \nmid m \end{cases}$$

$$= \begin{cases} (m^2 n / 12)\left(3n^2 + m^2 - 4\right) + (n/8)(-1)^{(n/2)}\left[1 - (-1)^m\right] & m \le n/2 + 1 \\ (mn^2 / 24)\left(n^2 + 4m^2 + 3mn - 8\right) - (n^3/192)\left(n^2 - 16\right) + (n/8)\left[(-1)^{(n/2)} - 1\right] & m > n/2 + 1 \end{cases}$$

This completes our arguments.

CONCLUSIONS

Our method for computing distance matrix of armchair polyhex nanotube is general and can be extended to every regular or near to regular graph. Here, a near to regular graph is a graph with exactly two distinct numbers as the degree of vertices. In such graphs, it is possible to consider a base vertex and then compute the distance matrix as a function of base matrix.

ACKNOWLEDGMENTS

REFERENCES

1. N. Trinajstic, "Chemical graph theory", 2nd edn, CRC Press, Boca Raton, FL, **1992**.

2. I. Gutman, O. E. Polansky, "Mathematical Concepts in Organic Chemistry", Springer-Verlag, New York, **1986**.

3. A. T. Balaban, Eds, "Topological Indices and Related Descriptors in QSAR and QSPR", Gordon and Breach Science Publishers, Amsterdam, **1999**.

4. H. Wiener, *J. Am. Chem. Soc.*, **1947**, *69*, 17.

5. H. Hosoya, *Bull. Chem. Soc. Japan*, **1971**, *44*, 2332.

6. 7. A. A. Dobrynin, R. Entringer, I. Gutman, *Acta Appl. Math.*, **2001**, *66*, 211.

7. A. A. Dobrynin, I. Gutman, S. Klavžar, P. Zigert, *Acta Appl. Math.*, **2002**, *72*, 247.

8. P. E. John, M. V. Diudea, *Croat. Chem. Acta*, **2004**, *77*, 127.

9. M. V. Diudea, M. Stefu, B. Pârv, P. E. John, *Croat. Chem. Acta*, **2004**, *77*, 111.

10. M. V. Diudea, *J. Chem. Inf. Model.*, **2005**, *45*, 1002.

11. M. V. Diudea, *J. Chem. Inf. Comput. Sci.*, **1996**, *36*, 833.

12. M. V. Diudea, A. Graovac, *MATCH Commun. Math. Comput. Chem.*, **2001**, *44*, 93.

13. M. V. Diudea, I. Silaghi-Dumitrescu, B. Parv, *MATCH Commun. Math. Comput. Chem.*, **2001**, *44*, 117.

14. M. V. Diudea, P. E. John, *MATCH Commun. Math. Comput. Chem.*, **2001**, *44*, 103.

15. S. Yousefi, A. R. Ashrafi, *MATCH Commun. Math. Comput. Chem.*, **2006**, *56*, 169.

16. S. Yousefi, A. R. Ashrafi, *J. Math. Chem.*, **2007**, *42*, 1031.

17. A. R. Ashrafi, S. Yousefi, *MATCH Commun. Math. Comput. Chem.*, **2007**, *57*, 403.

18. S. Yousefi, A. R. Ashrafi, *Current Nanoscience*, **2008**, *4*, 161.

19. A. R. Ashrafi, S. Yousefi, *Nanoscale Res. Lett.*, **2008**, *2*, 202.

20. P. J. Cameron, "Combinatorics: Topics, Techniques, Algorithms", Cambridge University Press, Cambridge, **1994**.

THE IODINE CONTENT OF MINERAL WATERS

GEORGETA HAZI AND MIRCEA DIUDEA[a]

ABSTRACT. Iodine plays an important biochemical role in the synthesis of thyroid hormones, the iodine deficiency producing the increase of thyroid gland volume and the presence of goiter. The daily iodine intake need can be provided by drinking water and food. The aim of this study is to determine the iodine level in mineral waters and tap water. The iodine in mineral waters was quantitatively determined by Sandell-Kolthoff method. The concentration of iodine in the studied mineral waters shows a panel of values, being of particular interest for physicians and population as well.

Keywords: iodine, mineral waters

INTRODUCTION

The iodine, a non-metal of the VII-th group of Periodic Table, has been discovered by Courtois, in 1811, in the ashes of marine algae. It is spread in the earth crust as sodium and calcium iodate in the Chile's salpeter deposits, reprezenting 1-3 x 10^{-5} % of earth crust, as iodides in marine algae and in iodided mineral water sources [1].

Iodine has an essential biochemical role in the synthesis of two hormones produces by thyroid gland, triiodotironine and tetraiodotironine, which play an important role in the regulation of body cells' metabolism. The iodine deficiency determines the hypertrophy of thyroid gland called goiter. An increased volume of the thyroid gland, with the ostensible maintenance of the secretor function, with prevalence of more than 10%, within a community of a geographic region, defines the endemic goiter. Because of a large area spread, it can affect hundreds of millions people around the world, and because of the consequences and complications that can occur, it represent a matter of public health [2, 3].

Currently, in over than 118 countries, the iodine deficiency is considered a matter of public health. It is estimated that 1571 millions of people around the world (representing 28.9% of the world population) live in areas with

[a] *Faculty of Chemistry and Chemical Engineering, Babeş-Bolyai University, Arany Janos 11, RO-400084, Cluj-Napoca, Romania*

iodine deficiency, exposed to the risk of thyroid dystrophies, 656 millions have goiter and over 20 millions of them suffer from mental retardation [4, 5, 6]. The world and national experience show that prophylaxis can lead to the goiter eradication. These are based on actions meant to improve the iodine intake (the usage of iodinated salts in public consumption) and the social-economical conditions.

The daily iodine intake need by the adult human body, according to the standards of the World Health Organization, is rated to 100-200 µg/day, and even more for the pregnant women [7]. It can be suplyed by daily drinking water and food. Water is an important source of minerals for the human nutrition. The composition of water reveals various substances: macro-elements (calcium, magnesium, sodium, potasium salts, clorides) and micro-elements (iodine, fluor, cobalt, zinc, selenium, lithium, copper). The intake of these minerals is ensured by food, which contains a much bigger concentration than water, about 90 per cent of the mineral comes from food and about 10 per cent of the daily intake of them is provided by the drinking water [8].

RESULTS AND DISCUSSION

In order to determine the amount of the iodine in waters, twenty types of mineral waters present in Romanian market were tested: A_1-A_{14} – sparkling mineral waters, A_{15}-A_{19} –non-gaseous mineral water and A_{20}-tap water (see Experimental section).

The results of the sample analyzed waters are presented in Table 1 and displayed in Figure 1:

Tabel 1 Average values of iodine concentration in studied waters.

Conc.	A_1	A_2	A_3	A_4	A_5	A_6	A_7	A_8	A_9	A_{10}
Iodine (µg/L)	14,53 ± 1,91	4,16 ± 0,95	5,43 ± 1,28	23,56 ± 0,86	5,66 ± 0,76	23,86 ± 1,62	6,56 ± 1,45	13,02 ± 2,02	62,06 ± 3,12	26,23 ± 1,25
	A_{11}	A_{12}	A_{13}	A_{14}	A_{15}	A_{16}	A_{17}	A_{18}	A_{19}	A_{20}
Iodine (µg/L)	15,33 ± 1,25	156,3 ± 2,74	3,76 ± 0,25	4,93 ± 0,51	12,66 ± 2,41	23,06 ± 2,20	57,83 ± 4,01	13,22 ± 1,5	10,16 ± 0,95	15,7 ± 1,30
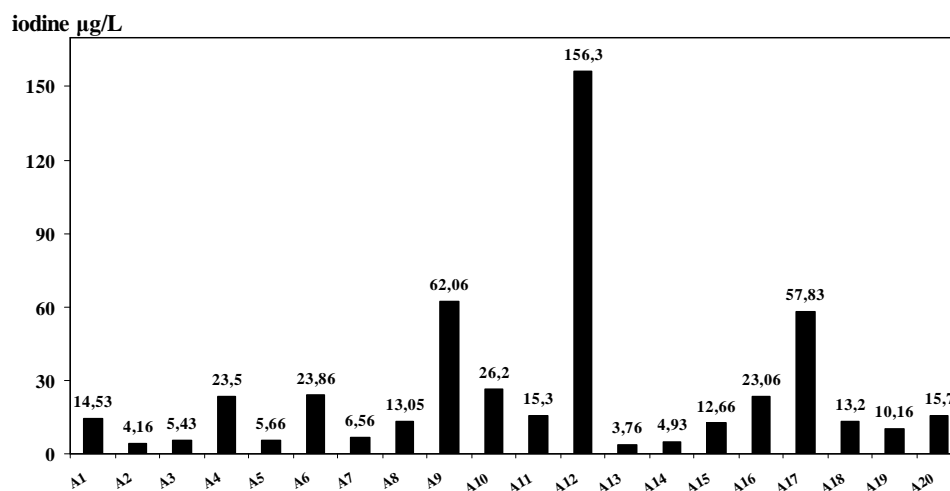
Figure 1: The iodine concentration in the studied waters

The daily iodine intake from water can vary very much, depending on water. The critical value of iodine concentration in water that can induce goiter is 2 – 3 µg/L iodine. Recent studies remark that, in the areas with goiter prevalence, the iodine concentration in water is at most 0.3 µg/L, while in other areas it is higher than 25 µg/L [9, 10].

The performed study shows that the iodine level in waters can vary much. The data show a high iodine level in the sparkling mineral water A_{12} (156.3 µg/); if it would like to provide the daily iodine intake by this water, it would be enough to consume 1L/day of it. A pretty good concentration show the mineral waters A_9 (62.06 µg/L) and A_{17} (57.83 µg/L). The samples A_4, A_6, A_{10} and A_{16} have an average iodine level of 23 µg/L, while some other waters have a lower concentration (4.1 – 6.5 µg/L). Tap water shows a concentration of 15.7 µg/L iodine. All the analyzed waters show a satisfactory level of iodine, higher than the level causing the goiter.

In the endemic areas, the level of iodine in soil, water and food (vegetables, plants) is low and is strictly correlated with the endemic goiter. Out of the low iodine level, the soil and water can contain significant quantities of organic, inorganic, bacterial substances and pollutants which represent a potential goitrous factor. For example, the consumption of water with high nitrates concentration (over 50 mg/L) causes thyroid hypertrophy, but without affecting the urinary iodine levels [11, 12].

Studies performed on the Black Sea shore areas and in central Dobrogea on the phreatic water characteristics, show waters having normal levels of iodine, but highly mineralized, especially by calcium salts, and containing organic residues [13].

Romanian mineral waters show a large hydro-chemical variety, caused by the complex geological structure of our country. The majority of the waters studied by us originates in Eastern Carpathian Mountains, and shows a panel of values of iodine concentration, predominating lower iodine concentrations (below 10 µg/L). We observed that the waters coming from volcanoes mountains show a higher iodine concentration (sparkling mineral water A_{12} and non-gaseous mineral water A_{17}).

Other studies made in our country concerning the levels of iodine in phreatic waters, show different values, depending on the geographical region. In some areas the level of iodine decreased by 70% in a period of 15 years, probably because of non-ecological agriculture and the increase of polluting substances [14].

Other studies show various levels of iodine in waters. In Israel the concentration of iodine measured by using the same dosing method (Kolthoff) was 22.8 µg/L in tap water and 7 µg/L in mineral water [15].

Waters analyzed in China show concentrations of 0.6 – 84.8 µg/L, with lower levels in the mountains areas. The iodine level in tap water was 4.3 ± 2.43 µg/L, water from source 23.59 ± 27.74 µg/L and in water from other natural sources 12,72 ± 10,72 µg/L. The concentration of iodine soil was found 0.11 – 2.93 mg/kg, without statistical differences between soils from different districts. The data show that soil and water iodine levels are not high, which implies the consumption of iodized salt [16].

Studies performed in Denmark, regarding the level of iodine in drinking water of 55 different cities, show values between less than 1 up to 139 µg/L, with higher levels in the samples taken from islands or in the coast areas. It has been determined a significant statistical correlation between the iodine in drinking water and the levels of urinary iodine [17, 18, 19].

In Greenland, the iodine level in drinking water is lower than 3.3 µg/L for all the samples examined [20].

The data presented show that the iodine levels in drinking water and other sources (springs, mineral waters, juices) may significantly differ by geographical region, soil composition, influencing the daily iodine intake.

EXPERIMENTAL SECTION

Measuring the iodine concentrations in waters was done by using the Sandell-Kolthoff method. Iodide was measured by its catalytic action on the reduction of the ceric ion (Ce^{4+}) to the cerous ion (Ce^{3+}) coupled to the oxidation of As^{3+} to As^{5+}, in oxido-reducing reaction between Ceric ammonium sulphate and Arsenious acid. This reaction, called the Sandell-Kolthoff reaction, is written as follows:

$$2\ Ce^{4+} + 2\ I^- \rightarrow 2\ Ce^{3+} + I_2$$
$$I_2 + As^{3+} \rightarrow As^{5+} + 2I^-$$
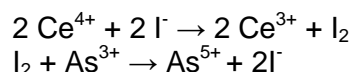
The reaction is slow, but could be accelerated by the iodide ion. The ceric ion (Ce^{4+}) has a yellow color, while the cerous (Ce^{3+}) is colorless. Thus, the course of reaction can be followed by the disappearance of yellow color as the ceric ion is reduced. The speed of this color disappearance is directly proportional to the amount of iodide catalyzing it and is measured by a spectrophotometer, after an exact time, at 405 nm [21,22].

CONCLUSIONS

The various brands of mineral waters studied by us show variable values of iodine concentration. However, the mineral water consumption cannot provide the whole need of the daily intake of this oligo-mineral, essential for the human body, but can contribute to the daily iodine supply.

REFERENCES

1. C. D. Nenițescu, "Chimie generală", Ed. Didactică și Pedagogică, București, **1972**, 862.
2. F. Delange, *Thyroid*, **1994**, *4,* 107.
3. L. Gozariu, "Endocrinologie", Litografia U.M.F, Cluj-Napoca, **1987**, 115.
4. F. Delange, H. Burgi, Z. P. Chen J. T. Dunn, *Thyroid*, **2002**, *12***,** 915.
5. P. Vitti, F. Delange, A. Pinchera, M. Zimmermann, J. T. Dunn, *The Lancet*, **2003**, *361*, 1126.
6. *** WHO, UNICEF, ICCIDD, Bull. WHO, Geneva, **2001**, *1*, 1.
7. *** WHO, UNICEF, ICCIDD, Bull. WHO, Geneva**, 1994**, *8*, 1.
8. M. Vlad In: "Magneziul în biologia și patologia umană", N. Miu, G. Dragotoiu, Ed Casa Cărții de Știință, Cluj, **2000**, 52.
9. G. Buia, M Rădulescu, "Geologie Medicală", Ed. Universitas, București, **1999**, 67.
10. M Vernescu, "Apele minerale. Captare, transport prin conducte, condiționare, înmagazinare, distribuție", Ed. Tehnică, București, **1988**, 16.
11. A. G. Ubom, *Sci. Tot. Envir.*, **1991**, *107*, 1.
12. J. M. S. van Maanen, A. van Dijk, K. Mulder, M. H. Baets, P. Menheere, D. van der Heide, P. Merents, J. Kleinjans, *Toxicol. Lett.*, **1994**, *72*, 365.
13. E. Circo, *Acta Endocrinol.*, **2005**, *1*, 73.
14. C. Dumitrache, M. Popa, Al IX-lea Congres al Societății Române de Endocrinologie, Cluj-Napoca, 13-15 sept. **2001**, vol. rez, 141.
15. C. Benbassat, G. Tsvetov, B. Schindel, M. Hod, Y. Blonder, B. A. Sela, *Isr. Med. Assoc. J*, **2004**, *6,* 97.

16. Y. L. Lu, N. J. Wang, L. Zhu, G. X. Wang, H. Wu, L. Kuang, W. M. Zhu, *J. Zhejiang Univ. Sci. B*, **2005**, *6*, 1200.
17. S. Andersen, K. M. Pedersen, F. Iversen, S. Terpling, P. Gustenhoff, S. B. Petersen, P. Laurberg**,** *Br. J. Nutr*, **2007**, *8*, 1.
18. L. B. Rasmussen, E. H. Larsen, L. Ovesen, *Eur. J. Clin. Nutr*, **2000**, *54,* 57.
19. S. Andersen, S. B. Petersen, P. Laurberg, *Eur. J. Endocrinol*, **2002**, *147*, 663.
20. S. Andersen, B. Hvingel, P. Laurberg, *Int. J. Circumpolar Health*, **2002**, *61*, 332.
21. Sandell EB, Kolthoff IM. *Mikrochimica Acta*, 1**937***, 1*, 9.
22. J. T. Dunn, H. E. Crutchfield, R. Gutekunst, *WHO, UNICEF, ICCIDD*, Netherlands, **1993**, 7.

OPTIMIZATION OF OPERATING PARAMETER OF A QUADRUPOLE INDUCTIVELY COUPLED PLASMA MASS SPECTROMETER USED IN THE DETERMINATION OF LEAD ISOTOPIC RATIO

CLAUDIU TĂNĂSELIA[a], MIRELA MICLEAN[a], CECILIA ROMAN[a], EMIL CORDOŞ[a], LEONTIN DAVID[b]

ABSTRACT. Due to small (but random) plasma variations while the quadrupole scans multiple masses, the single detector of a commercially available ICP-MS instrument will sequentially receive data that is affected by the non constant plasma power. Present study focuses on DRC's RPq parameter and quadrupole's sweeps optimization, for a quadrupole based ICP-MS instrument. The proposed method is used for lead isotopic ratio in vegetables, soils, concentrated mining ores and leaded gasoline, offering a RSD between 0.12% and 0.91%. Measured isotopic ratio for ^{207}Pb / ^{206}Pb varied from 0.829 (mining ore) to 0.890 (leaded gasoline) respectively 2.048 (mining ore) to 2.155 (leaded gasoline) for ^{208}Pb / ^{206}Pb.

Keywords: mass spectrometry, isotopic ratio, instrument optimization

INTRODUCTION

Lead, as a heavy metal, it is known to be a toxic pollutant and total world production has increased continuously beginning from Roman Empire to present days [1]. The natural level of lead present in the atmosphere today is 1-2 levels of magnitude greater than the natural sources [2]. Lead is present in nature in 4 stable isotopes among which only ^{204}Pb (1.4%) is primordial lead, thus being distributed almost homogeneous in Earth's crust, all the other three are final stages of heavier nuclei decay processes, with their distribution varying accordingly with the uranium and thorium deposits nearby. ^{238}U is responsible for ^{206}Pb isotope (24.1%), ^{235}U for ^{207}Pb (22.1) and ^{232}Th finally decays in ^{208}Pb (52.4%). [3]

Isotopic ratio from one sample does not change, no matter the chemical or conventional physical phenomena suffered, thus one can trace the origin for a specific sample.

[a] *INCDO-INOE 2000, Research Institute for Analytical Instrumentation, Donath 67, Cluj-Napoca, Romania*
[b] *Babeş-Bolyai University, Faculty of Physics, M. Kogălniceanu 1, Cluj-Napoca, Romania*

Historically, thermo-ionization mass spectrometry was the technique mainly used for isotopic ratio. A major drawback of TIMS is the lengthy process of sample preparation and reading time so that when ICP-MS start emerging on the market, new alternatives appeared. Multi-collector ICP-MS counter-balance the plasma fluctuation by adding multiple detectors and in this way doing simultaneous mass detection, as opposed to single-collector ICP-MS where the detector sequentially reads the ion coming from the mass filter, on which little plasma fluctuation have a unwanted effect [4]. In this paper we tried to minimize those effects by carefully optimizing two parameters (sweeps and Rpq) and using a single detector, commercially available ICP-MS instrument for precise isotope ratio determination. The proposed method offers cost effective and fast lead isotopic ratio measurements with minimal sample preparation with good accuracy, using a standard quadrupole ICP-MS instrument.

RESULTS AND DISCUSSION

Instrument was carefully optimized daily, using a solution of 1 ppb In, Mg, Ce, Th, U and 10 ppb Ba. Oxides and double ionization levels were monitored and kept under 3% during all analysis. Also a mass tuning was performed periodically. Lens voltages were optimized specifically for optimum passage of Pb ions.

Isotope ^{204}Pb was excluded from all measurements due to its low natural abundance that causes errors on all other ratios involving this isotopes and increases analysis time needed to read it. Furthermore, ^{204}Pb can be affected by interference caused by ^{204}Hg [8] and the focus of this study was to provide a method with DRC used in rf-only mode, without any pressurized gas (which could remove the unwanted interference).

For all optimization measurements, a solution prepared from NIST 981 standard reference material (SRM) was used. The standard is shipped in wire form and it was cut, weighted and used to prepare a concentrated stock solution from which, by multiple dilutions, we've created a 20 ppb solution, used daily for all measurements. This concentration was chosen to avoid any pulse pile-up phenomenon that can occur if lead concentration is to high in the ion beam [9].

Sweeps are number of times during one reading when the specified mass range is scanned from the lowest to the highest mass. Higher value for sweeps translates into better statistics and lower RSD, but if the sweeps value got to high, then plasma variation over longer time period affects the results and overcome the statistical positive factor. NIST 981 SRM solution prepared in-lab as described above and 100, 200, 400, 600 and 800 sweeps values were chosen and the prepared solution was read 5 times. An isotopic ratio average was calculated from the obtained results and calibration was performed at the start of each batch of 5 samples. Calibration was performed after each batch and software's correction coefficients were used each time. Averages and RSDs for sweep optimization are plotted on Figure 1.
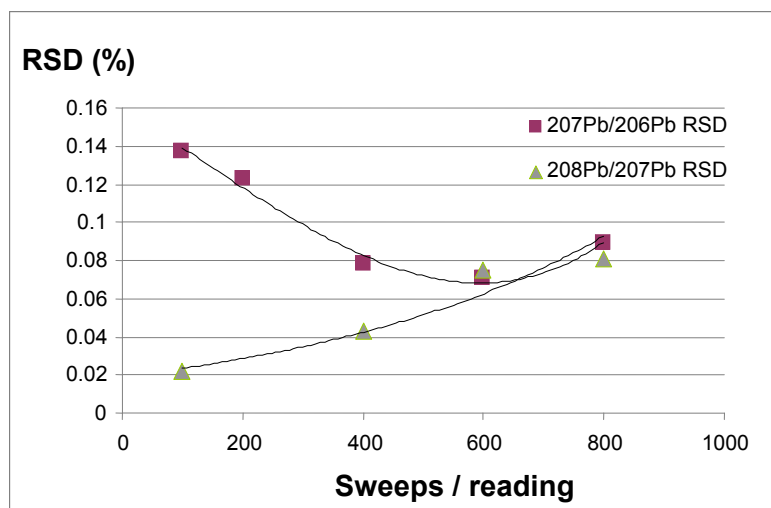
Figure 1. Sweeps /reading vs. obtained RSD

400 sweeps is an intermediary value that offers satisfactory RSD for both ^{207}Pb / ^{206}Pb and ^{208}Pb / ^{207}Pb ratio. While it is not the optimum value for both ratios, it's a good compromise between the two of them, offering satisfactory results while having a decent analysis time.
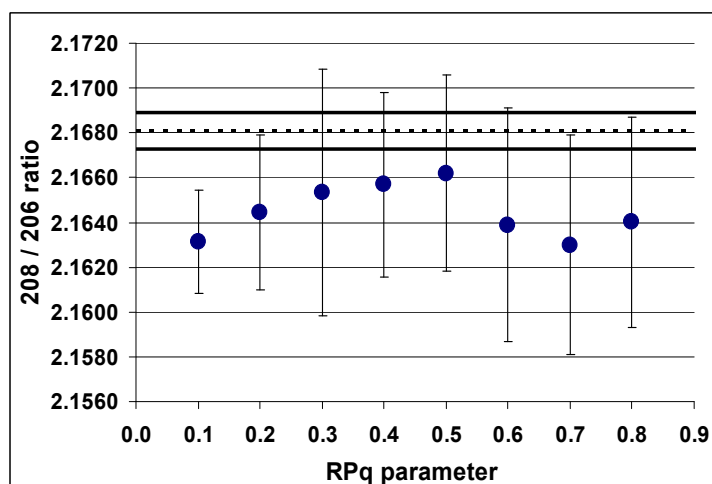
Figure 2a. RPq optimization of ^{208}Pb / ^{206}Pb ratio. The dotted line represents the NIST 981 certified value together with standard deviation (thick continuous lines)
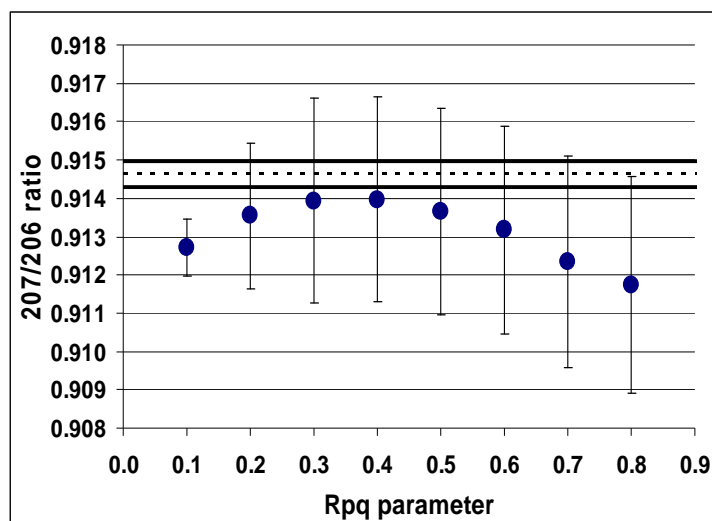
Figure 2b. RPq optimization of ^{207}Pb/^{206}Pb ratio. The dotted line represents the NIST 981 certified value together with standard deviation (thick continuous line)

RPq parameter optimization was done in a similar manner. After five readings, an average was considered, and then a calibration was performed and reading of the sample with the next RPq value (values were chosen from 0.1 to 0.8, with an increasing step of 0.1).

While a lower RSD value gives better precision, best accuracy for both ratios is obtained when using a Rpq value of 0.45 (compared to NIST 981 standard reference material's certified value). The certified NIST samples have better RSD values (0.036% - 0.063%), due to different techniques used, than the values obtained in this study (0.12% - 0.91%). However, those values of RSD are better enough to differentiate between mining ore samples, vegetables and leaded gasoline respectively, which fits the purpose of this study. Results of the study are listed in Table 1.

Table 1. Results range for lead isotopic ratio for mining ore, vegetables, soil and leaded gasoline samples

Sample type	^{207}Pb/^{206}Pb ratio	^{208}Pb/^{206}Pb ratio
Mining ore	0.829 – 0.866	2.048 – 2.100
Vegetables	0.846 – 0.849	2.095 – 2.100
Soil	0.834 – 0.842	2.110 – 2.126
Leaded gasoline	0.890	2.155

EXPERIMENTAL SECTION

For all the measurements, a SCIEX Elan DRC II (Toronto, Canada) ICP-MS was used. This model is a quadrupole based mass spectrometer, with only one detector, that does not offer the advantages of multicollector ICP-MS instruments. It is also equipped with a Dynamic Reaction Cell which consists on an enclosed second quadrupole placed after the interface part and before the main quadrupole. The quadrupole's chamber can be pressurized with a reaction (He) or reaction (NH_3, CH_4, O_2) gas for eliminating various interferences. However, only the rf-only capability of the DRC quadrupole was used (no gas), since no interferences are expected to form at the masses we are watching (206, 207, 208).

Dwell time was chosen 30 ms for ^{208}Pb and 60 ms for ^{206}Pb and ^{207}Pb. According to isotope distribution, this settings is optimum for analysis time and signal quality. Other ICP-MS settings are listed in Table 2.

Table 2. ICP-MS running parameters

Parameter	Value
Plasma	
Power / W	1300
Plasma gas flow / l min^{-1}	12.00
Auxiliary gas flow / l min^{-1}	1.20
Nebuliser gas flow / l min^{-1}	0.92
Sample/Skimmer cone	Platinum
Quadrupole	
Quadruple rod offset (QRO) / V	0.00
Cell rod offset (CRO)/V	- 8.00
Cell path voltage (CPV)/V	- 20.00
Measurement mode	Peak hopping
Dwell time / ms	30 / 60
Integration time / ms	Varying
Reading per replicate	1
Replicate measurements	5
DRC	
Reaction Gas	None
Lens voltage / V	10.00

Vegetables (VG) and were collected from resident's gardens and were washed with ultrapure water then oven-dried at 80-90°C for 30 minutes and at 65°C for 12-24h. Samples were ground and 5g of every sample were

digested with concentrated HNO_3 and $HClO_4$. Gasoline (Pb-GS) was extracted with concentrated HCl at reflux conditions and then the acid layer was separated. Soils (SO) were collected from the same gardens as vegetables and were prepared according to ISO 11466:1995. Mining ores (MO) were digested in microwave oven (O-I Analytical), in a three steps program with total running time of 24 minutes, using a mixture of HNO_3, HCl, H_2O and HF and the obtained solution was diluted several times until the concentration was in range of 20 – 80 ppb of Pb.

CONCLUSIONS

This paper has shown that quadrupole ICP-MS can be used for isotopic ratio measurements, being capable of discrimate samples from various origins. For achieving this, RPq and sweeps number optimization for Pb were performed, along with standard daily procedures. The ease of sample preparation, analysis time and relatively small running costs points to quadrupole-based ICP-MS as a serious alternative to more historically used isotope ratio measurements techniques. Although the RSD values of multicollector ICP-MS are superior [17], the quadrupole offers a much more cost-effective approach. Our optimized method was successfully applied on vegetable, soil, concentrated mining ore and leaded gasoline samples from Western Romania.

REFERENCES

1. J. O. Nigrau, A history of global metal pollution, *Science*, **1996**, 272, 223
2. M. Komarek, V. Chrastny, V. Ettler, P. Tlustos, *Environment International*, **2007**, 33, 677
3. I. Planner, Modern Isotope Ratio Mass Spectrometry, John Wiley and sons, Wiley, **1997**, Appendix I
4. Y. Yip, J. Lam, W. Tong, *Trends in Analytical Chemistry*, **2008**, 27, 460
5. S. Tanner, V. Baranov, *Atomic Spectroscopy*, **1999**, 20, 45
6. D. Bandura, V. Baranov, S. Tanner, *Journal of Analytical Atomic Spectrometry*, **2000**, 15, 921
7. S. Tanner, V. Baranov, *Journal of American Society for Mass Spectrometry*, **1999**, 19, 1083
8. T. May, R. Wiedmeyer, *Atomic Spectroscopy*, **1998**, 16, 150
9. F. Monna, J. Loizeau, A. Thomas, C. Guenguen, Y. Favarger, *Spectrochimica Acta Part B*, **1998**, 53, 1317
10. I. Renberg, M-L. Brannvall, R. Binder, O. Emteryd, *Ambio*, **2000**, 29, 150

11. A. Dolgopova, D.J. Weiss, R. Seltmann, B. Kober, T.F.D. Mason, B. Coles, C.J. Stanley, *Applied Geochemistry*, **2006**, 21, 563
12. M. Barbaste, L. Halicz, A. Galy, B. Medina, H. Emteborg, F. Adams, R. Lobinski, *Talanta*, **2001**, 54, 307
13. M. Mihaljevic, V. Ettler, O. Sebek, L. Strnad, V. Chrastny, *Journal of Geochemical Exploration*, **2006**, 88, 130
14. E. Margui, Iglesias, I. Queralt, M. Hidalgo, *Science of Total Environment*, **2006**, 367, 988
15. T. Shimamura, S. Iijima, M. Iwashita, M. Hattori, Y. Takaku, *Atmospheric Environment*, **2007**, 41, 2797
16. J. Baker, D. Peate, T. Waight, C. Meyzen, *Chemical Geology*, **2004**, 21, 275
17. F. Monna, J. Lancelot, I. Croudace, A. Cundy, J. Lewis, *Environmental. Science and Technology*, **1997**, 31, 2277